PREPARATION, CHARACTERIZATION AND CATALYTIC PROPERTIES OF COBALT PHTHALOCYANINE ENCAPSULATED IN ZEOLITE EMT AND ZEOLITE BEA

NANTAPHOL KLANSORN

A THESIS SUMMITTED IN PARTIAL FULFILLMENT

OF THE REQUIREMENT FOR THE DEGREE OF

MASTER OF SCIENCE IN PETROCHEMICALS AND HYDROCABON CHEMISTRY

SCHOOL OF GRADUATE STUDIES

KING MONGKUT'S INSTITUTE OF TECHNOLOGY LADKRABANG

2003

ISBN 974-324-693-2

หัวข้อวิทยานิพนธ์	การสังเคราะห์และการศึกษาสมบัติการเป็นตัวเร่งปฏิกิริยาของสารประกอบเชิงซ้อนโคบอลท์พทาโลไซยานินในรูพรุนจุลภาคของซีโอไลต์ EMT และซีโอไลต์BEA
นักศึกษา	นายณันฐพล กลั่นสอน
รหัสประจำตัว	41065111
ปริญญา	วิทยาศาสตร์มหาบัณฑิต
สาขาวิชา	ปิโตรเคมีและเคมีไอโครคาร์บอน
พ.ศ.	2546
อาจารย์ผู้ควบคุมวิทยานิพนธ์	ผศ.ดร.ตะวัน สุขน้อย

บทคัดย่อ

สารประกอบเชิงซ้อนโคบอลท์พทาโลไซยานิน (CoPc) ถูกสังเคราะห์ในรูพรุนจุลภาคของซีโอไลท์ EMT และ BEA ด้วยเทคนิค Ship in the bottle โดยการบรรจุโคบอลท์ไอออนสามารถทำได้โดยวิธีการแลกเปลี่ยนไอออนและวิธีการฝังตัว สารประกอบเชิงซ้อนโคบอลท์พทาโลไซยานินที่ถูกสังเคราะห์ในรูพรุนจุลภาคของซีโอไลท์สามารถตรวจสอบได้โดยเทคนิค X-ray Powder Diffraction (XRD) Fourier Transform Infrared Spectroscopy (FTIR) Thermogravimetric Analysis (TGA) UV/Visible Spectrophotometry (UV/VIS) Scanning Electron Microscopy (SEM) และ Gas Adsorption Analysis จากนั้นนำไปศึกษาสมบัติการเป็นตัวเร่งปฏิกิริยาในปฏิกิริยาออกซิเดชัน (liquid phase) ของเอทิลเบนซีนและไซโคลเฮกเซน โดยทำปฏิกิริยาแบบครั้ง (Batch reaction) ภายใต้ความดันของก๊าซออกซิเจนที่อุณหภูมิ 136 และ 70 องศาเซลเซียสตามลำดับ สารผลิตภัณฑ์ที่เกิดขึ้นสามารถตรวจสอบได้โดยเทคนิค Gas Chromatography (GC)

จากการศึกษาพบว่าสารประกอบเชิงซ้อนที่อยู่ภายในรูพรุนของซีโอไลต์ BEA มีความว่องไวกว่าสารประกอบเชิงซ้อนที่อยู่ภายในรูพรุนของซีโอไลต์ EMT ในปฏิกิริยาออกซิเดชันของเอทิลเบนซีนพบว่าการเปลี่ยนแปลงของเอทิลเบนซีนไปเป็นสารผลิตภัณฑ์จะมีค่ามากขึ้นเมื่อเพิ่มอัตราการไหลของก๊าซออกซิเจน แต่การเปลี่ยนแปลงของเอทิลเบนซีนไปเป็นสารผลิตภัณฑ์จะมีค่าลดลงเมื่อใช้อัตราการไหลของก๊าซออกซิเจน สูงถึง 80 มิลลิลิตรต่อนาที ทั้งนี้เนื่องจากตำแหน่งว่องไว (Active site) บางส่วนถูกออกซิไดซ์ขณะเกิดปฏิกิริยา และจากปฏิกิริยาออกซิเดชันของไซโคลเฮกเซนพบว่าความเป็นขั้วของสารละลายที่มีอิทธิพลต่อการเปลี่ยนแปลงของไซโคลเฮกเซนไปเป็นสารผลิตภัณฑ์ โดยพบว่าเมื่อใช้กรดแอซิติกเป็นสารละลายทำให้ได้การเปลี่ยนแปลงของไซโคลเฮกเซนไปเป็นสารผลิตภัณฑ์ที่สูงสุดนอกจากนี้ยังพบว่าปฏิกิริยาออกซิเดชันของไซโคลเฮกเซนเกิดผ่านสารมัธยันตร์ (Intermediate) อนุมูลอิสระ (Free radical) และการเกิดสารเชิงซ้อน

(Complexation) ระหว่างออกซิเจนกับตำแหน่งว่องไวของตัวเร่งปฏิกิริยามีบทบาทสำคัญที่ทำให้เกิดปฏิกิริยา

.

Thesis Title	Preparation, Characterization and Catalytic Properties of Cobalt Phthalocyanine Encapsulated in Zeolite EMT and Zeolite BEA
Student	Nantaphol Klansorn
Student ID.	41065111
Degree	Master of Science
Program	Petrochemicals and Hydrocarbon Chemistry
Year	2003
Thesis Advisor	Assit.Prof.Dr. Tawan Sooknoi

ABSTRACT

Cobalt Phthalocyanine (CoPc) encapsulated into cavities of zeolites EMT and BEA are synthesized using "ship in the bottle" strategy. Cobalt (II) ion can be loaded in the cavities of zeolite by ion exchange and impregnation. Cobalt Phthalocyanine encapsulated in zeolite were characterized by X-ray Powder Diffraction (XRD), Fourier Transform Infrared Spectroscopy (FTIR), Thermogravimetric Analysis (TGA), UV/Visible Spectrophotometry (UV/VIS), Scanning Electron Microscopy (SEM) and Gas Adsorption Analysis. The catalytic property of the catalysts was studied in the oxidation of ethylbenzene and cyclohexane. The liquid phase oxidation of ethybenzene was carried out in a batch reactor with flow of oxygen at 138 °C, while a Parr reactor under the pressure of oxygen was used for the oxidation of cyclohexane at 70 °C. Products were analyzed by Gas Chromatography (GC).

It was found that CoPc encaged in zeolite BEA (CoPcBEA) appeared to be more active than CoPc in zeolite EMT (CoPcEMT). In contrast, CoPcEMT was relatively more stable as compared to CoPcBEA. The ethylbenzene conversion increased with an increased in oxygen flow rate. The ethylbenzene conversion, however, decreased when oxygen flow rate exceeds to 80 ml/min due to the destruction of the active sites via the oxidation process. Cyclohexane conversion was influenced by the polarity of solvent used in the reaction and acetic acid was found to be efficient for this reaction. Accordingly, it is suggested that the oxidation of cyclohexane proceed via a free radical intermediate and the complexation of oxygen with active site plays an important role on oxidation activity.

ACKNOWLEDGEMENTS

The author would like to express his profound gratitude to his advisor, Assist. Prof. Dr. Tawan Sooknoi for helpful suggestions and encouragements throughout this thesis. He is also grateful to Dr. Patchanee Charoenying, Assoc.Prof. Dr. Sakda Trisak, and Assist. Prof. Kornvalai Panpae for serving as the chairperson and the committee, and their valuable comments.

The author would like to extend his sincere appreciation to all of his friends for their support and encouragement.

Finally, the author dedicated his work to his above parents and brother for the constant love and encouragement.

Nantaphol Klansorn

CONTENTS

CONTENTS (Continued)

CONTENTS (Continued)

LIST OF TABLES

LIST OF FIGURES

LIST OF FIGURES (Continued)

LIST OF FIGURES (Continued)

LIST OF FIGURES (Continued)

LIST OF FIGURES (Continued)

Chapter 1

Introduction

1.1 Motivation

Zeolites, both natural and synthetic, have been demonstrated to have catalytic properties for various types of hydrocarbon conversion [1-3]. From these outstanding properties of this catalyst, there are many attempts to develop their use in reactions with high product selectivity.

In nature, microorganism can transform substrate into the product without wasting reagents and energy. This is achieved by enzyme [4] having definite and complicated structures and a metal is a part of the active center. The metal active sites possess a well-defined coordination and are surrounded by polymeric segments giving a precise shape to the cavity. Therefore the desire to mimic enzymatic systems has prompted an extensive area of research and many attempts have been made to simulate natural enzyme by encapsulating a coordinate compound into the network porous solid. Synthesizing transition metal phthalocyanine complex immobilized into the cavities of zeolite is a choice of intimating such excellent property [5]. This approach can be rationalized by imaging that the complex encapsulated into zeolites will provide the best arrangement for the catalytic site and will direct the substrate towards these centers [6]. Fig. 1.1 illustrates this concept.

In this study, BEA and EMT are used as host material. EMT is a cage structure zeolite. It is expected that cobalt phthalocyanines are located in the cage. While BEA is a channel structure zeolite. The structures of zeolites EMT have many features like the structure of faujasite [7]. Both of them possess large cavities (diameter about 1.3 nm). However, there are four 12-membered ring opening to each supercage in the faujasite structure, while the large cage of zeolite EMT (so-called hypercages) can be reached through five windows. According to this feature, reactant molecule can reach through the large cage better. In contrast, BEA is a channel structure zeolite and it is expected that cobalt phthalocyanines are located in the intersection of each channel. Therefore phthalocyanine complex encapsulated in zeolite BEA are also synthesized to compare with those in zeolites EMT. The resulting inclusion compounds will be characterized by selected physicochemical techniques and the oxidation of cyclohexane with molecular oxygen is used as catalytic testing.

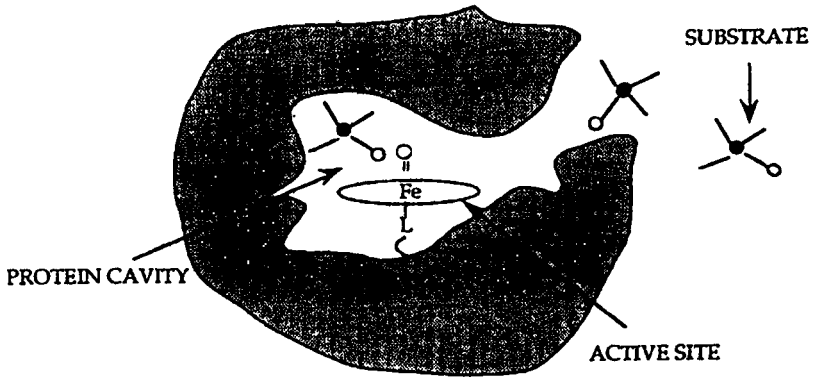

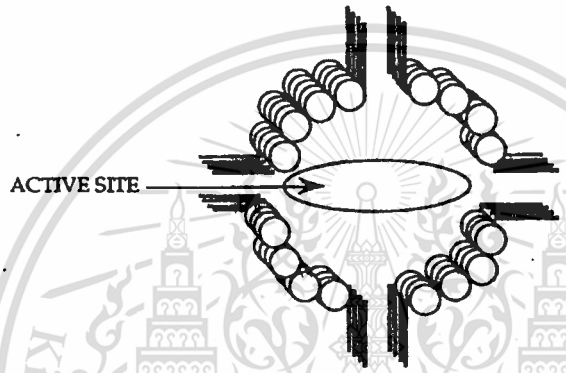

Figure 1.1 Conceptual approaches for mimicking the protein of natural enzyme

1.2 Objective

1. To obtain cobalt phthalocyanine encapsulated in channel structure zeolite.
2. To understand the catalytic properties of cobalt phthalocyanine encapsulated in zeolite EMT and zeolite BEA in the oxidation of cyclohexane
3. To understand the influence of oxygen flow rate on cyclohexane conversion.
4. To understand the influence of solvent using in the reaction on cyclohexane conversion.

1.3 Scope of this study

There is difference between silica to alumina ratio of EMT and BEA. EMT can be crystallized from alumino-silica gel containing silica to alumina ratio 4-5 while BEA can be synthesized with variation of framework silica to alumina ratio, from 5-100. Accordingly, in this thesis, BEA is synthesized with silica to alumina ratio within a range similar to those of zeolite EMT for a better comparison in catalytic behavior. It is because the properties of zeolites can be influence by changing the structural silica to alumina ratio.

For a preparation of cobalt phthalocyanine encapsulated in zeolite, the Ship-in-the-bottle method is employed. There are 2 methods to loading metal ion into the cavities of zeolite.

The first one is ion exchanging of Co^{2+} with Na form zeolites.

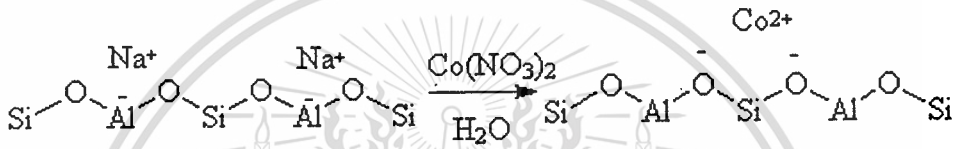

Another one is impregnation of Co^{2+} salt directly into zeolites.

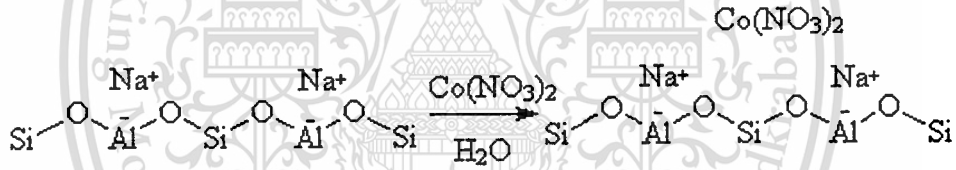

Co^{2+} loaded by ion exchange method would act as charges balancing cationwhile cobalts cationloaded by impregnation method would be present as ion cluster within the zelites pore.

Atomic Absorption Spectroscopy (AAS), X-ray Powder Diffraction (XRD), Fourier Transform Infrared Spectroscopy (FTIR), Thermogravimetric Analysis (TGA), UV/Visible Spectrophotometry (UV/VIS) and Scanning Electron Microscopy (SEM) are used to characterize the cobalt phthalocynine encapsulated in zeolite. The catalysts will then be tested in the oxidation of cyclohexane with molecular oxygen. Products from this reaction are analyzed by gas chromatography (GC).

1.4 Expected result

1. Catalysts that have better catalytic properties (cobalt phthalocyanine encapsulated in channel zeolite) are obtained from this research.
2. The appropriate reaction condition such as solvent and oxygen flow rate can be obtained from this research.
3. This research would provide alternative procedure for production of cyclohexanol and cyclohexanone.

Chapter 2

Literature Review and Theory

2.1 Literature Review

At the moment, more than 10^6 tons of cyclohexanol and cyclohexanone are made worldwide per year for the production of Nylon-6 and Nylon-6-6. Industrially, cyclohexane is oxidized at 423-433 K and 0.9 MPa air in the presence of cobalt naphthenate or metaboric acid to form a mixture of cyclohexanol and cyclohexanone [8]. However, in living organisms selective oxidation are achieved under mild condition by enzymes. Enzymes, cytochrome P-450, are capable of oxidizing cyclohexane to cyclohexanol and cyclohexanone at room temperature with high selectivity [6]. The ability of cytochrome P-450 to activate oxygen to hydrocarbon oxidation has motivated many studies involving metalloporphyrin catalyst.

In the Gif system of Barton et al. [9], which saturated hydrocarbons were oxidized at ambient condition, the hydrocarbon in pyridine-acetic acid solvent is oxidized in the presence of iron-based catalyst and an electron source. Gif systems were designed to emulate the non-heme enzymatic oxidations of alkanes. A major drawback of Gif system is that during the oxidation, radical reactions become more important causing over-oxidation and coupling of the products with pyridine. Parton et al. [10] found that iron phthalocyanine encapsulated in Y zeolite catalysts are more active and regenerable than the homogeneous complexes which are oxidatively destroyed under reaction conditions and are therefore not regenerable.

Synthesis of metal phthalocyanine complex encapsulated the cavities of zeolite by ship-in-the-bottle method was firstly reported by the group of Romanovsky [11]. Their ship-in-the-bottle synthesis involved the introduction of the metal via ion exchange or preadsorption of labile metal complex, e.g., carbonyl or a metallocene, followed by reaction with 1,2-dicyanobenzene (DCB) at temperature 250 °C to 350 °C. Such intrazeolite complexes were physically trapped in the zeolite pores.

Metal phthalocyanine encapsulated in zeolite pores can also be prepared by the in-situ method [12-13]. This method involves encapsulation of complex during crystallization of the host zeolites. Prerequisites for the use of in-situ method are (i) the stability of the complexes under the condition of zeolite synthesis (pH, temperature, hydrothermal condition) and (ii) a sufficient solubility

in the synthesis medium in order to enable random distribution of the complex in the synthesis mixture as well as in the finally obtained host/guest compound.

Kenneth J. Balkus et al. found that either the ship-in-the-bottle synthesis or the in-situ synthesis method can use to prepare cobalt and copper perfluorophthalocyanine encapsulated in both NaX and NaY [14]. However, in the case of in-situ method, the portion of the gel with the high concentration of metal complex become more hydrophobic and float on the top of the reaction mixture. It makes the gel be a non-homogeneous gel.

Furthermore, from report of S. Ernst et al., cobalt phthalocyanine encapsulated in zeolite EMT was synthesized by using ship-in-the-bottle strategy [12]. Zeolite EMT and faujasite have many features in common. Although, there are four 12-membered ring opening to each supercage in faujasite structure, the large cages in zeolite EMT (so-called hypercages) can be reached through five windows. In the catalytic point of view, this feature could be resulted in a better accessibility to the encapsulated complexes of reactant molecules. It was found that cobalt phthalocyanine encapsulated in zeolite EMT is able to catalyze ethylbenzene oxidation with molecular oxygen giving 1-phenylethanol and acetophenone as major products.

Metallophthalocyanine immobilized in mesoporous MCM-41 molecular sieve can also be synthesized [15-16]. However, metallophthalocyanine immobilized in mesoporous MCM-41 molecular sieve formed in relax planar would be less active as oxidation catalyst than a constraint saddle conformation of metal phthalocyanine encapsulated in faujasite type zeolite where the metal sites shifted out of the macrocycle and more accessible to coordinate the oxidizing agent. Therefore, the suitable template should be selected to prepare MCM-41 where would be well fit with molecular size of metallophthalocyanine. If the pore windows were bigger than metallophthalocyanine, it would leach from a catalyst.

In addition, metal phthalocyanine encaged in ZSM-5, channel structure zeolite, can be prepared by in-situ method. It can be able to catalyze phenol hydroxylation [17]. A. Gedeon [18] found that the host material would be good crystallinity if the amount of complex trapped is much lower than the number of channel intersections. This is the only place where the complex can be located without too much distortion. Accordingly, in-situ- method is not suitable for synthesis metal phthalocyanine encaged in channel structure zeolite.

Parton et al. use metal phthalocyanine encapsulated in Y zeolite synthesized by ship-in-the-bottle method as catalyst in oxidation of cyclohexane with tertiary-butylhydroperoxide. Sorption measurements of Parton et al. show a high preference of the catalyst for polar reagent

and products like acetone, cyclohexanol, cyclohexanone and tertiarybutylhydroperoxide. Therefore, addition of peroxide and the use of solvent have a strong influence on the reaction rate.

Robert R. et al. [19] found that the molecular cross-section of oxidizing agent (alkyl hydroperoxide) influence on the reaction rate of oxidation of cyclohexane. The rate of oxidation decrease when increase the molecular cross section of alkyl hydroperoxide. Moreover they also show that the higher conversion is gained by using cobalt perchlorophthalocyanine encapsulated in zeolite X as compared to those using copper perchlorophthalocyanine encapsulated in zeolite X.

2.2 Zeolites

The word "zeolite" is Greek in origin, derived from the words "zein" and lithos" meaning to boil and rock. It was first used by the Swedish chemist who found that upon heating, the zeolite sample evolved steam [20]. There was little interest in zeolites until the late 1930's when the modern founder of zeolite chemistry, Barrer began the characterization of zeolite structure and chemistry. His initial work studying zeolites confirmed the molecular sieving properties of the microporous solids and was reported in a paper titled "the sorption of polar by zeolites" and published in the Proceeding of the Royal Society [21]. These discoveries sparked huge interest in the synthesis of shape selective zeolite catalysts in companies such as Union Carbide and Mobil in the late 1950's. Today, one of the most industrially important uses of zeolites as chemical catalysis, most notably in the petrochemical industry where zeolites are used in oil refining as cracking catalysts and the Methanol to Gasoline (MTG) catalytic conversion process [22].

2.2.1 Zeolites 's structure

Zeolites are crystalline aluminosilicates. Zeolites 's structure is open framework constructed from SiO_4 and AlO_4 tetrahedral linked through oxygen bridges [2] Two silicon or aluminum atoms share each oxygen atom. The large variety of zeolite structure types is a consequence of the flexibility of the Al-O-Si linkage, which depend on the conditions of their hydrothermal synthesis. The tetrahedral coordination of Si-O and Al-O permits a variety of ringed structures containing 4, 5, 6, 10 or 12 Si or Al. These rings are jointed to form prisms and more complex cages and the cages are jointed to give three-, two- or one-dimensional. Figure 2.1 illustrates this model and some examples of zeolite are shown in Figure 2.2. There are two types of zeolite 's structure, one provides an internal pore system comprised of interconnected cage like

voids; the second provides a system of uniform channels which, in some instances, are one-dimensional and in the others intersect with similar channels provide two- or three-dimensional channel systems.

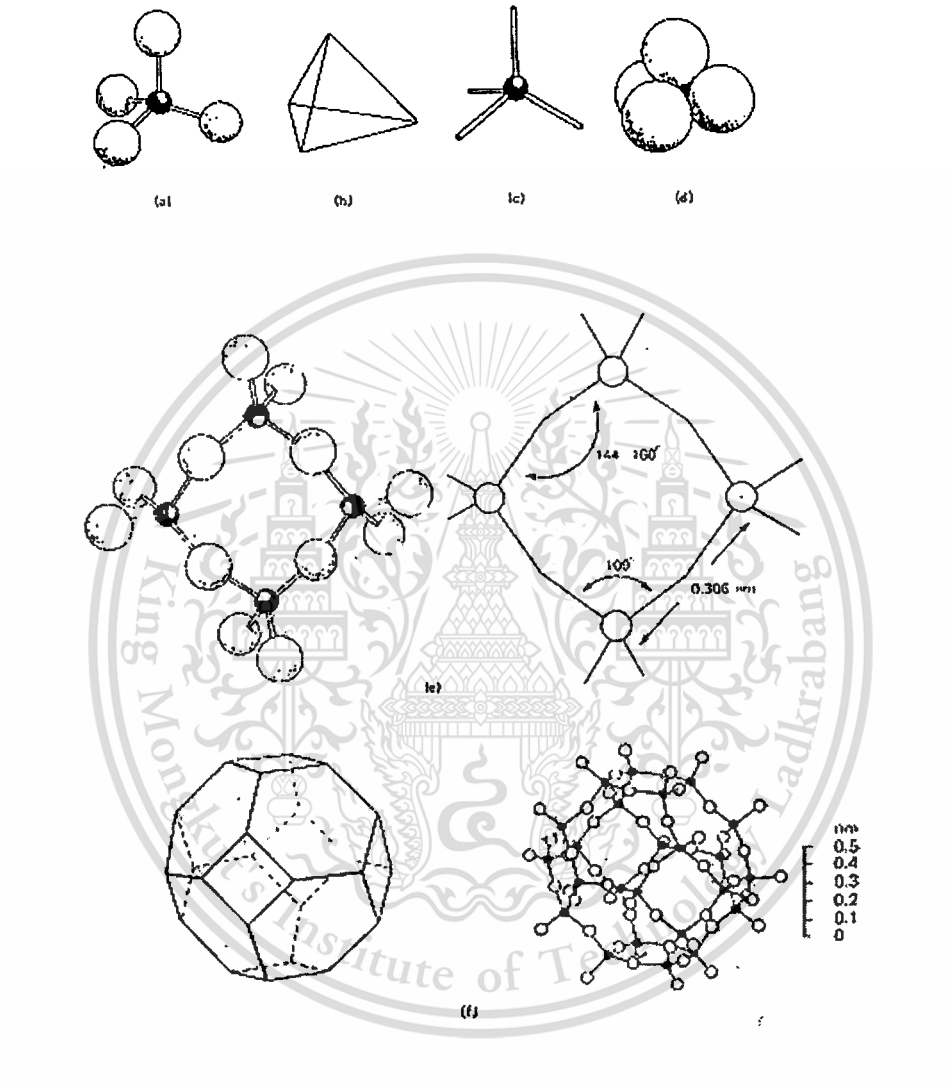

Figure 2.1 (a-d) Methods for responding SiO_4 and AlO_4 tetrahedral by means of ball-and –stick model, solid tetrahedron, skeletal tetrahedron, and space filling of packed spheres species. (e) Linking of four tetrahedra in a four-memberd ring. (f) Secondary buiding unit called truncated octahedron as represented by a solid model, left, and ball-and-stick model, right.

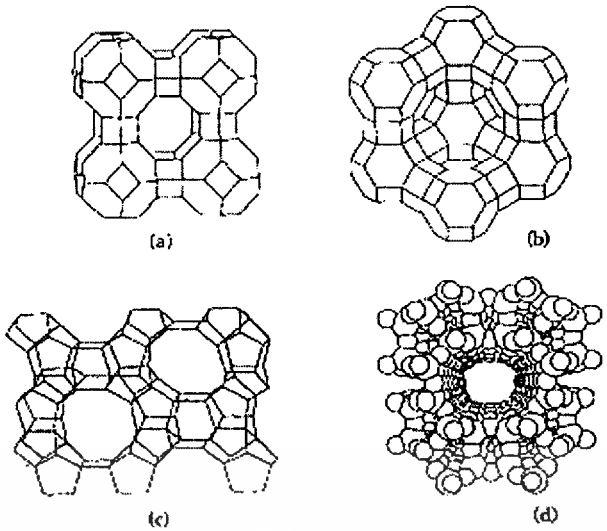

Figure 2.2 Representative zeolite structures: (a) zeolite A: (b) zeolite Y: (c) zeolite ZSM-5 (d) zeolite mordenite

2.2.2 Zeolite minerals

Zeolite minerals are formed over much of the earth's surface, including the sea bottom [20]. Until about twenty years ago, zeolite minerals are considered as typically occurring in cavities of basaltic and valcanic rock. During the last 20 – 25 years, however, the use of X-ray diffraction for the examination of very fine-grained sedimentary rocks has led to the identification of several zeolite minerals which were formed by the natural alteration of volcanic ash in alkaline environments. Zeolites formed naturally always perform in low crystalline, low purity and are used without any benefit.

However, of 40 known zeolite minerals, chabasite, erionite, mordenite, and clinoptiolite occurred in quantity and reasonably high purity, high crystalline and are available as commercial products and the important natural zeolites are listed in Table 2.1. In general, these zeolites occur in two types of deposits:

Closed-system deposits, where volcanic ash was deposited in the Cenozoic lakes of the western United State, for example, and over long periods of time converted to zeolites. Owing to hydrolysis of the alkaline constituents of the volcanic ash, the water became salty and alkaline and the ash crystallized to zeolites. The pH may have reached 9.5. The resulting zeolites were produced as readily accessible flat-lying beds.

The open-system type refers to the deposition of sedimentation on land thick beds and subsequent conversion to zeolite by the downward percolation. The city of Naples is underlain by a zeolitic deposit some 200 km^2 (77 mi^2) in area which is only 5 of 10 thousand years old.

Table 2.1 Zeolite composition

Zeolite	Typical Formula
Natural	
Chabasite	$Ca_2[(AlO_2)_4(SiO_2)_8].13H_2O$
Mordenite	$Na_8[(AlO_2)_8(SiO_2)_{40}].24H_2O$
Erionite	$(Ca,Mg,Na_2,K_2)4.5[(AlO_2)_9(SiO_2)_{27}].27H2O$
Synthetic	
Zeolite A	$Na_{12}[(AlO_{12})_9(SiO_2)_{12}].27H_2O$
Zeolite X	$Na_{86}[(AlO_2)_{86}(SiO_2)_{106}].264H_2O$

2.2.3 Synthetic zeolites

Now more than 150 synthtic zeolites have been reported and some of examples of important synthetic zeolites are shown in Table 2.1. These include zelites A, X, Y, and Zeolite H, a synthetic form of mordenite. In addition high silica synthetic zeolitez are also known such as ZSM-5 and ZSM-11 [3].

The conditions generally used in synthesis are reactive starting materials such as freshly co-precipitated gels or amorphous solids, relatively high pH introduced in the form of alkaline metal hydroxides, low temperature hydrothermal condition with concurrent low autogeneous pressure at saturated water vapor pressure and high degree of supersaturation of the gel components leading to the nucleation of a large number of crystals. The gel is defined as a hydrous metal aluminosilicate prepared from either aqueous solution, reactive solids, colloidal solutions, or reactive aluminosilicates such as the residue structure of meta-kaolin and glasses.

The gels are crystalline in a closed hydrothermal system at temperature varying from room temperature to about 200 °C. The time required for the crystallization varies from a few hours to several days. When the reaction mixtures are prepared from colloidal solution or amorphous silica, additional zeolites may form which do not readily crystallize from the homogeneous sodium silicate-aluminosilicate gels.

The temperature strongly influences the crystallization time of even the most reactive gels; for example, zeolite X crystallizes in 800 h at 25 °C and 6 h at 100 °C.

Synthesis mechanisms of the typical low silica zeolites, such as A, X, or Y are apparently different from the high silica zeolites, such as ZSM-5. In the low silica zeolites, nuclei are formed consisting of alkali metal-ion complexes of the aluminosilicate species. Structural units consisting of 4-membered ring, 6-membered ring, and cages coordinated with cations are involved in the nucleation and crystallization. In high silica zeolites, the mechanism appears to be a templating type where alkylammonium cation complexes with silica by hydrogen bonding. These complexes cause the structures to replicate by hydrogen bonding of the organic cation with framework oxygen atoms.

2.2.4 Zeolite 's Properties and Application

I. Adsorption

Zeolites are highly selective adsorbents because they separate molecules based upon the size and configuration of the molecules relative to the size and geometry of the main apertures of the structures. Moreover, they adsorb molecules, in particular those with a permanent dipolemoment, which show other interaction effect, with a selectivity that is not found in other solid adsorbents. Separation may be based upon the molecular-sieve effect or involve the preferential or selective adsorption of one molecular species over another. These separations are governed by several factors discussed below;

- The basic framework structure, or topology, of the zeolite determines the pore size and the void volume.
- The cations, depending upon their locations, size and contribute electric field effects, which interact with the adsorbate molecules.
- The effect of the temperature of the adsorbents is pronounced in case involving activated diffusion.

At the present, there are many commercial processes utilizing this property of zeolite. In this case, the purposes of each process are purification or bulk separation. Purification refers to separation wherein the feed stream is upgraded by the removal of a few percent or even traces of contaminant. A heated purge gas is usually employed for this purpose.

-***Water***. The dehydration of natural gas and air were the first gas-purification applications for zeolite molecular-sieves. Because of their high adsorptive selectivity for water and high

capacity at low partial pressure, zeolite molecular-sieves were an obvious choice for water removal from natural gas and air. Zeolite molecular-sieves have had increasing use in the dehydration of cracked gases in ethylene plants before low temperature fractionation for olefin production. Type 3A molecular-sieve is size selective for water molecules and dose not co-adsorb the olefin molecules. Zeolite molecular-sieves are also used widely in the dehydration of liquid streams. Both batch-type and continuous processes have been developed for drying a variety of hydrocarbon and chemical liquids.

-***Carbon Dioxide***. Zeolite molecular-sieves are used to purify gas stream containing carbon dioxide in cryogenic application where freeze-out of CO_2 would cause fouling of low temperature equipment. Moreover, commercial processes are available for the removal of CO_2 from air, natural gas, ethylene, ethylene-propane mix, and synthesis gases.

-***Separation of normal and isoparaffins***. the recovery of normal paraffins from mixed refinary streams was one the first commercial application of molecular-sieves, using Type 5A. The normal paeraffins are the raw material for the manufacture of biodegradable detergents, plasticizers, alcohols, and synthetic proteins. Removal of the normal paraffins upgrade gasoline, improve the octane number of the branch fraction.

-***Xylene sparation***. *p*-xylene is separate from mixed xylene and ethylbenzene by means of Universal Oil Products Company's Parex process. High purity *p*-xylene is produced.

-***Olefin separation***. Olefin-containing streams are separated either by Union Carbide Corporation's OlefinSiv process (n-butenes from isobutenes in vapor phase) or Universal Oil Products Company's Orex process (liquid phase).

II. Catalytic properties [23-24]

In zeolites, catalysis takes place within the intracrystalline voids. The aperture size and the channel system affect catalytic reactions caused by diffusion of reactants and products. Activity and selectivity are achieved or altered by modifying the zeolite in several ways. In hydrocarbon reactions in particular, the zeolites with the largest pore size are preferred. Theses include mordenite and zeolites Y, L, and omega. Modification techniques include ion exchange, composition in term of Si/Al ratio (silica to alumina ratio), hydrothermal dealumination or stabilization which produces Lewis acidity, introduction of acidic groups such as OH which impart Bronsted acidity and loading dispersed metal phases such as noble metals.

Acid sites. Acidic zeolite have outstanding catalytic activity. Acidic is introduced by the decomposition of the NH_4^+ ion exchanged form, by hydrogen ion exchange, or by hydrolysis of a zeolite containing multivalent cations during dehydration. For example:

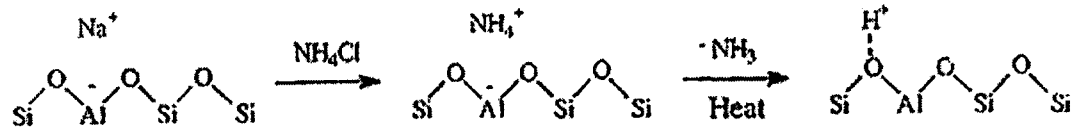

Basic sites. Basic sites in zeolites are always formed in high aluminium zeolite and basic sites forming are shown below

Dispersed metal. Bifunctional zeolite catalysts, primarily zeolite Y, are used in commercial processes such as hydrocraking. These are acidic containing dispersed metals such as platinum or palladium. The metals are introduced by cation exchange of the amine complexes, followed by a reductive decomposition (shown below)

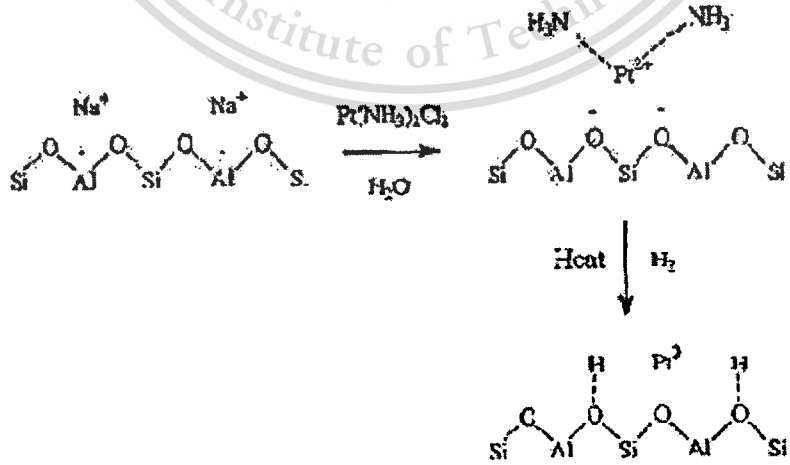

Although it was originally conceived that the platinum was atomically dispersed, it now appear that a bi-disperse system involving agglomerated in the supercages and some crystallites at the external surface is present.

Other transition metal ions such as Cd, Zn, Ni, and Ag are introduced by ion exchange followed by reduction with hydrogen. Agglomeration and migration to the external surface can also occur with these metals.

Stabilized zeolites. Thermal and hydrothermal stability of certain zeolites, in particular zeolite Y, is necessary in many catalytic applications. The stability increases with Si/Al ratio and by exchange with polyvalence cations such as rare earth. Mixed rare earth exchanged zeolite Y is used in cracking catalysts. Increased stability is achieved by hydrothermal treatment of the ammonium or rare earth exchanged form. When heated at high temperature in the present of water vapor, dealumination occurs with the formation of extra-framework Al(OH) species that hydrolyze to $Al(OH)_3$ and the dimeric Al(OH) species located within the framework , imparting additional structural stability. The acidic hydroxyl groups are also maintained. At least one commercial cracking catalyst contains a hydrothermally stabilized zeolite Y as the active component.

In shape selectivity catalysis the pore size of the zeolite is important. For example, the ZSM-5 framework contains 10-memberd ring with 0.6 nm pore size. This material is used in xylene isomerization , ethylbenzene synthesis and the conversion of methanol to liquid hydrocarbon fuels.

The zeolites used are primarily modified forms of zeolite Y, acid forms of synthetic mordenite, silicalite, and ZSM-5. Smaller pore size zeolites such as zeolite T are used in shape-selectivity catalysis.

Some current and possible future zeolite catalyst application are listed below

Alkylation	Dehydration
Cracking	Mathanol to Gasoline
Hydrocracking	Organic Catalysis
Isomerization	Inorganic Reaction
Hydrogenation and Dehydrogenation	H_2S Oxidation
Hydrodealkylation	NH_3 Reduction of NO
Methanation	CO oxidation

III. Ion Exchange [25-27]

The exchange behavior of non-framework cations in zeolites (selectivity and degree of exchange) depends on the nature of the cation (the size and charge of the hydrated cation) and the temperature. Cation exchange may produce considerable changes in other properties such as thermal stability, adsorption behavior, and catalytic properties. The ion exchange process is represented by:

$$z_A B^{z\,+}{}_B(z) + z_B A^{z\,+}{}_A(s) \rightleftharpoons z_A B^{z\,+}{}_B(s) + z_B A^{z\,+}{}_A(z)$$

Where z_A and z_B are the ionic charge of cation A and B and (z) and (s) represent zeolite and solution. The ion exchange isotherm is constructed by plotting A_z versus A_s, where A_z and A_s represent the mole fraction of cation A in zeolite and in solution receptively. Similarly, with B_z and B_s representing the mole fraction of the cation B in the zeolite and in solution, the preference of the zeolite for ion A is given by the separation factor.

Typical exchange isotherm is given in Figure 2.3 for zeolite X. In many case, complete exchange dose not take place, such as for the dipositive and the tripositive ions in zeolite Y because of non-occupancy of cation size type I located in the double six-memberd ring unit. This corresponds to a maximum level of 0.68. Similarly, the level of exchange diminishes with the size and volumes of the cation since the intracrytalline volume available dose not permit full cation site occupancy.

Table 2.2 Ion exchange capacity of various zeolite[a]

Zeolite	Si/Al ratio	Meq/g
Chabazite	2.0	5.0
Mordenite	5.0	2.6
Erionite	3.0	3.8
Clinoptilolite	4.5	2.6
Zeolite A	1.0	7.0
Zeolite X	1.2	6.4
Zeolite Y	2.0	5.0

[a] Anhydrous powder basis

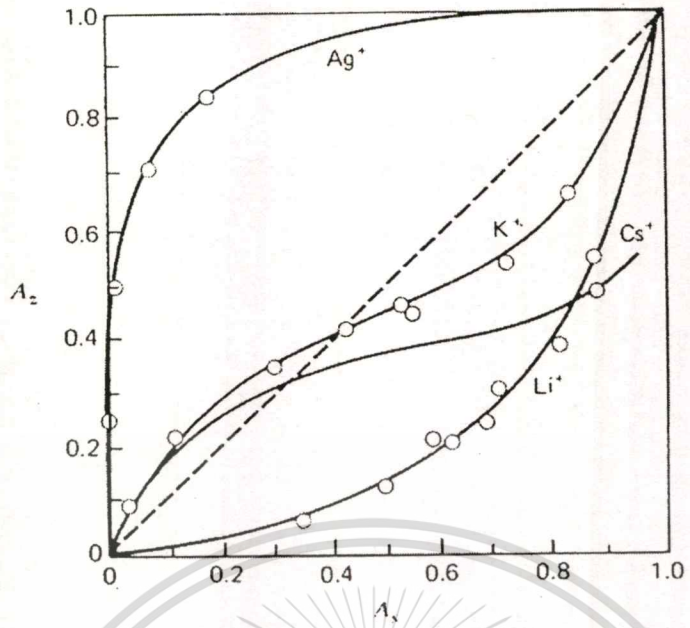

Figure 2.3 Ion exchange isotherm on zeolite X

Now, there are many processes based on this property of zeolite and many provide combination of selectivity, capacity and stability superior to the more common cation exchanger. The utilization of zeolite ion exchangers is shown below;

Cesium and Strontium Radioisotopes. Because their stability in the presence of ionizing radiation and in aqueous solution at high temperature, molecular sieves ion exchangers offer significant advantage in the separation and purification of radioisotopes. Their low solubility over wide pH ranges, together with their rigid framework and dimensional stability and attrition resistance, have endowed zeolites with properties generally surpass those of other inorganic ion exchangers. The high selectivity and capacity of several zeolites for cesium and strontium radioisotopes resulted in the development of processes currently by nuclear processing plant.

Ammonium Ion Removal. A fixed-bed molecular-sieve ion-exchange process has been commercialized for the removal of ammonium ions from secondary wastewater-treatment. This application takes advantage of the superior selectivity of molecular-sieve ion exchangers for the ammonium ion. The first plants employed clinoptilolite because of its availability in natural deposits as a potentially low cost material. The bed is regenerated with a lime-salt solution that can be reused after the ammonia is removed by pH adjustment and air stripping. The ammonium is subsequently removed from the air by acid scrubbing.

2.2.5 Characterization of synthetic zeolite

Each zeolite has a characteristic X-ray powder diffraction pattern that is used for identification and determination of the purity or the quantity of the zeolite present in composite such as catalyst. Generally, powder patterns are determined over a 2θ of 56 to 4 since these materials have large unit cells and correspondingly exhibit the strongest lines at low diffraction angles. However, peak intensities and, to some extent, positions vary with dehydration and/or cation exchange. Other procedures are based on infrared spectroscopy, thermal analysis, and standard chemical analyzes

The BET method (Brunauer-Emmett-Teller) [26], surface area measurement, commonly employed to characterize adsorbents and catalyst that is relevant for zeolite.

Oxygen adsorption at low temperature (-183 °C) is employed as a method for determining zeolite content, utilizing an appropriate reference. Since the structure of the zeolite is known, the void volume and oxygen capacity can be calculated as a reference value. Nitrogen could be used but, because cation-nitrogen interactions would contribute to additional adsorption capacity, oxygen is preferred. Before adsorption, the zeolite sample is outgassed at 350-450 °C under a reduced pressure of 1.3 mPa (10^{-5} mmHg) for 9-16 hours.

2.2.6 Zeolite EMT (Elf Mulhouse Two)

Zeolite EMT can be synthesized by using 18-crown-6-ether as organic template compound. It has many features like FAU (Faujasite). However, the assemblage of secondary building unit is different. From this reason, the difference of pore dimension is observed. In the case of FAU, the diameter of the biggest pore called "supercage" is 1.3 nm. While in the zeolite EMT, there are two important pore, the first one is called "hypocage" (1.3 × 1.3 × 1.4 nm) and the other one is called "hypercage" (0.69 × 1.3 × 1.3 nm). The unit cell composition of zeolite EMT is:

$$Na_{21}(18\text{- crown-6-ether})_n[Al_{21}Si_{75}O_{192}]$$

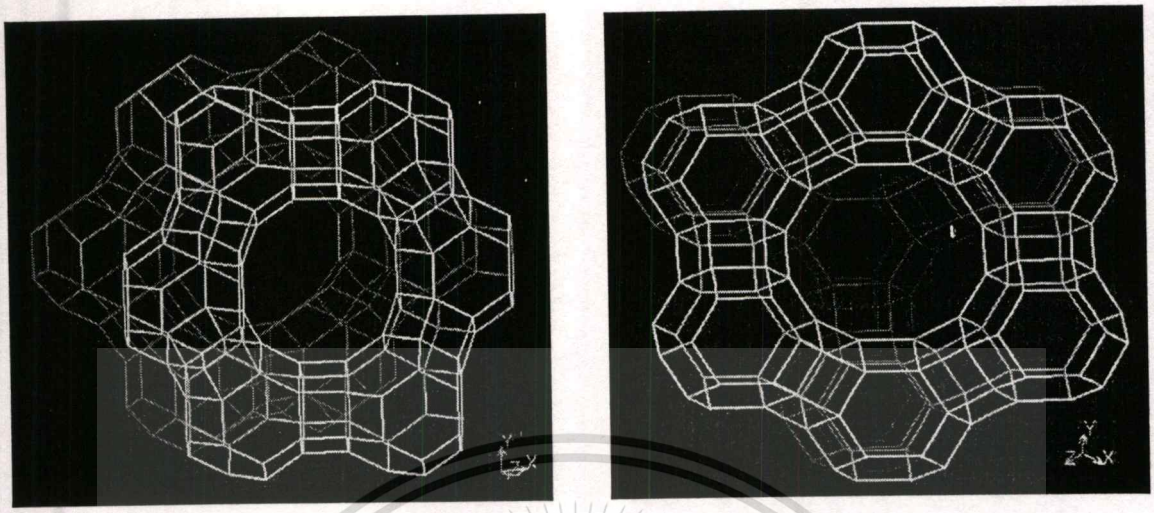

(a) (b)

Figure 2.4 Structure of zeolite (a) FAU along plann 111 and (b) EMT along plane 001

2.2.7 Zeolite BEA

Zeolite BEA was first prepared in 1976 by Wedlinger et al. It can be crystalline in wide range of silica to alumina ratio, $10 < SiO_2/Al_2O_3 < 200$, but the efficiency of crystallization is lower when it crystallize at silica to alumina ratio lower than 19 (6 aluminium atoms per 1 unit cell). Zeolite BEA is a large pore zeolite type. The pore size of zeolite BEA is about 0.7– 0.8 nm, 12-membered ring. The structure of zeolite EMT is illustrated in Figure 2.5

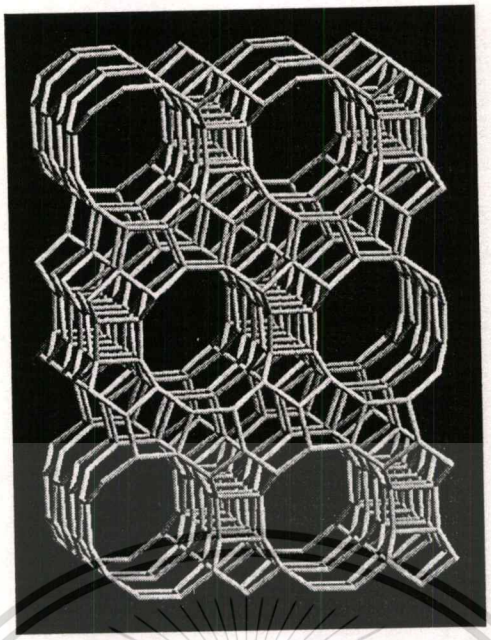

Figure 2.5 Structure of zeolite BEA along plane 100

2.3 Phthalocyanine [27-34]

2.3.1 Discovery of Phthalocyanine

The word phthalocyanine is derived from Greek term for naphtha (rock oil) and for cyanine (dark blue). Phthalocyanine itself is shown in Figure 2.6. The phthalocyanine class of compounds consists of metal derivatives of phthalocyanine. The two hydrogen in the center of molecule can be replaced by metals from every group of periodic table to form the group of compound known as metal phthalocyanines.

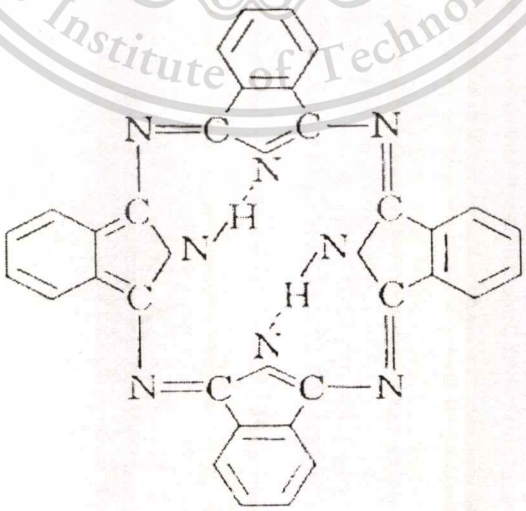

Figure 2.6 Metal free phthalocyanine

Also, from 1 to 16 of the peripheral hydrogen atoms in the 4 benzene rings in the phthalocyanine molecule have been replaced by halogen atoms and by numerous organic and inorganic groups. Now, more than 40 metal phthalocyanine have been prepared and several thousand phthalocyanine compounds have been synthesized.

The phthalocyanines were discovered by accident. In 1907, Braun and Tcheniac at the South Metropolitan Gas Company in London, upon examining the properties of a cyanobenzamide which are made from the reaction phthalamide and acetic anhydride, they have found trace amount of blue substance after heating o-cyanobenzamide, cooling, dissolving in alcohol, and filtration. This substance undoubtedly was phthalocyanine. In 1927 de Diesbach and von der Weid attempted to make the corresponding the nitriles of benzene. However, instead of obtaining nitriles, a blue product was obtained in indicated yield of 23 percent.

In 1928, during the preparation of phthalimide from phthalic anhydride and ammonia in the glass-lined iron kettle at the Grangemounth works of Scottich Dyes Ltd., the formation of a blue impurity in the reaction mass was observed. This impurity, iron phthalocyanine, was formed by the reaction of phthalimide with iron lining in the flaw of the glass of the vessel. Dunworth and Drescher carried out the preliminary examination of the iron compound and remarked on its crystalline form, stability, and the fact that it contained iron which was not remove by sulfuric acid.

In 1929, the first patent was issued with respect to compounds that so called phthalocyanines. Up to 1929, none of the observers of the blue coloring matters attempted to determine its structure. Professor Linstead and his students, at Imperial Chemical Industries, starting in 1929, determined and announced the structure of Phthalocyanine and several metal Phthalocyanine in 1933 and 1934.

Not only are the Phthalocyanine a new class of organic compounds but also they constitute a new class of coloring matter or chromogen. In 1935, the Imperial Chemical Industries began to manufacture copper phthalocyanine. It is named Monastral fast blue and is the first discovery of a blue pigment for over a century. The new pigment is expected to be of especial importance to the printing ink industry.

2.3.2 Feature of Phthalocyanines

The phthalocyanine is macrocyclic compounds containing four pyrole units. The phthalocyanines are closely related in structure to chlorophyll, the pigment of green leaves, and

hemin, the red pigment, which in association with protein is hemoglobin, the coloring matter of mammalian blood. Iron, central atom of Hemin, is an oxygen carrier for blood. Therefore, human lacking iron will have anemia disease. Furthermore the structure of porphin or porphyrin is also like a phthalocyanine. Numerous porphyrins also occur in the animal and vegetable kingdom. The structure of chlorophyll, hemin, and porphin are shown in Figure2.7. The pyrole nuclei in the porphyrin series are joined in the α-carbon position by four methine groups. Phthalocyanine with nuclear hydrogen atoms replaced by other atoms or group are defined according to the positions occupied by the atoms of groups on the available reactive nuclear sites of phthalocyanine molecule.

Roberston determined the structure of phthalocyanine by direct X-ray Fourier analysis of monoclinic crystal. The interatomic distances and bond angle was determined completely (See Figure 2.8). The crystal structures of the phthalocyanines show the presence of approximately square flat molecule having a center of symmetry. This center may be occupied by two hydrogen atoms or by metal.

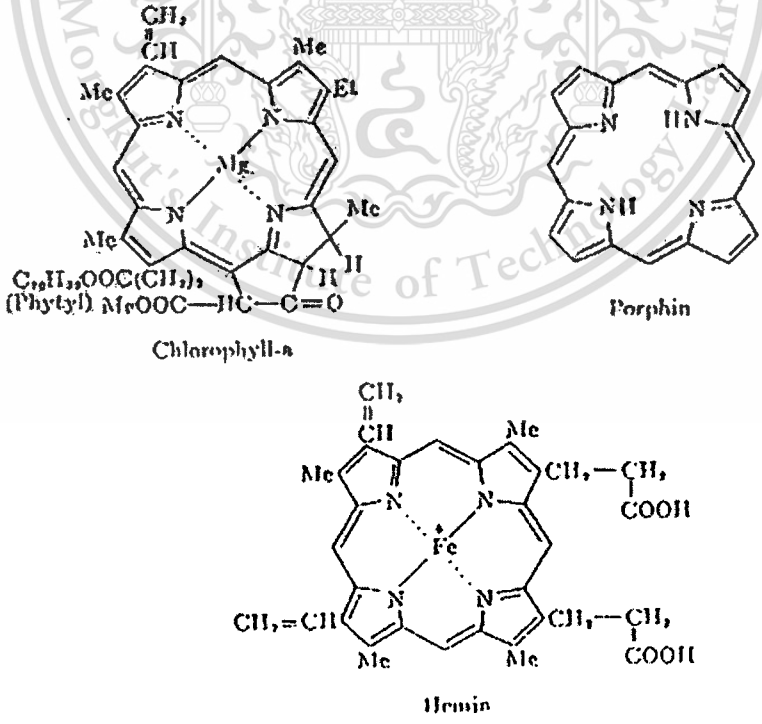

Figure 2.7 Structure of Chlorophyll, Hemin and Porphin

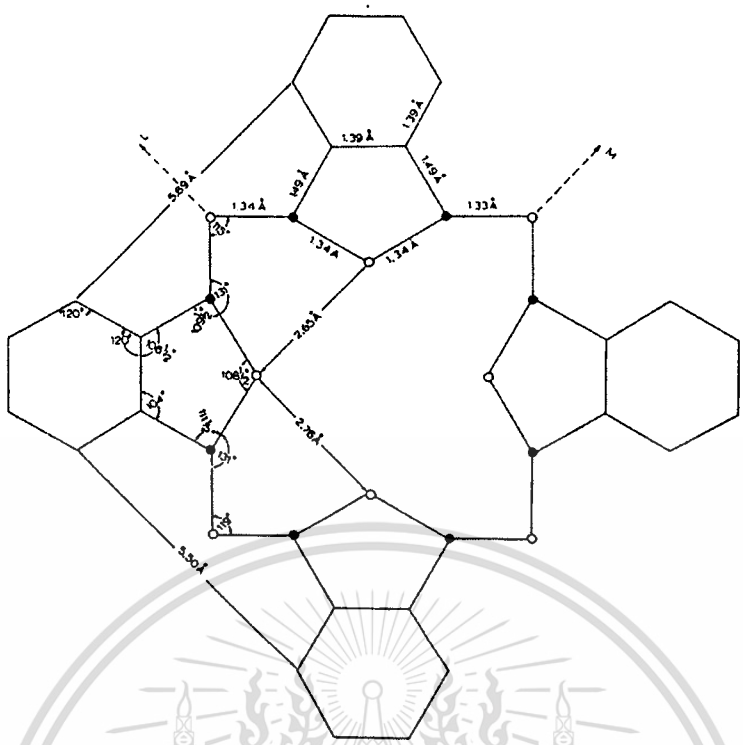

Figure 2.8 Dimension of phthalocyanine molecule

2.3.3 Properties of phthalocyanines

Phthalocyanines and its derivatives are extremely stable compound. Copper phthalocyanine for instance sublimes without decomposition at 550-580 °C, dissolve in concentrated sulfuric acid and is recovered unchanged on dilution. When a concentrated sulfuric acid solution of manganese phthalocyanine is diluted, the metal is removed but the ring system is intact and the product is phthalocyanine itself. An important property of the phthalocyanine is the comparative ease with which they undergo substitutions in the four benzene ring. Thus by direct chlorinating in molten sodium-aluminum chlorine or phthalic anhydride, all the sixteen available positions can be substituted by chlorine atom; the pentadecachloro compound is valuable technical product. The phthalocyanines can also be sulfonated readily, but they are decomposed by nitric acid and can't be nitrated.

Phthalocyanines are stable to atmospheric oxidation up to 100 °C or higher, depending on the metal derivative. In the presence of moisture, strong oxidizing agents oxidize them to phthalimides. In nonaqueous solvent suspension an oxidation product that may be reduced again to the original product is sometimes formed. Vatting procedures reduce many phthalocyanines to products that may be oxidized to the starting material, although copper phthalocyanine is a

notable exception. However, its halogen derivatives may be vatted and subsequently oxidized to the original compound.

An interesting property of the metal phthalocyanine is their ability to catalyze oxidation. Now, phthalocyanines have been used as catalysts for a number of reactions. Benzaldehyde can be oxidized to benzoic acid, and diphenylmethane to benzophenone, by air in the presence of phthalocyanine. Cobalt phthalocyanine has been used to catalyze the oxidation of waste sulfides to sulfate. Iron, cobalt, and vanadium phthalocyanine have been used to oxidized sulfur to a more readily removable in the sweetening process for gasoline. Oxidation of saturated fatty acid esters is catalyzed by nickel phthalocyanine.

2.3.4 Preparation

At the present, there are forty-six metals that have formed known phthalocyanine complexes. However, there is no one method can be used to prepare all metal phthalocyanine, some method can be used to form at least several metal complexes. These methods include (1) the reaction of phthalonitrile with metal or metal salt, (2) the reaction of phthalic anhydride, phthalic acid, or phthalamide, urea, metal salt, and catalyst, (3) the reaction of o-cyanobenzamide with a metal and (4) the reaction of phthalocyanine or replaceable metal phthalocyanine with a metal forming a more stable phthalocyanine.

In method 1, one mole of phthalocyanine is heated with the stoidiometric amount of metal chloride (one-quarter mole) to 180-190 °C for two hours in quinoline or a mixture of a mixture of quinoline and trichlorobenzene. Cobalt, nickel, chromium, iron, vanadyl, choroaluminiuim, lead and titanium phthalocyanines have been made by this method. The reaction may be written:

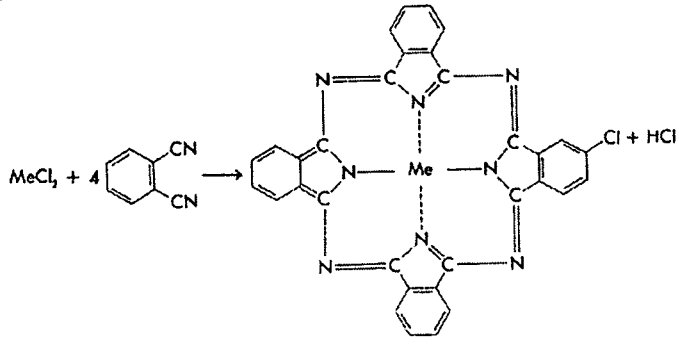

Method 2 uses phthalic anhydride, a metal salt, urea and a catalyst. The reaction is usually complete after four hours heating at 170-200 °C. the higher temperature should be reached at the end of heating period. A reaction medium such as chloronaphthalene may be used. Copper, cobalt, nickel, iron, and tin phthalocyanine have been made by this procedure.

In the third general method o-cyanobenzamide and a metal are heated to 250 °C for 4 to 6 hours. The product is freed of phthalamide and o-cyanobenzamide by heating it with concentrated sodium hydroxide. After filtration, washing, drying and grinding, the products is freed of excess metal by mechanically removing metal, flotation of the pigment in a suitable solvent, or chemical means. Iron, nickel, cobalt, manganese and copper phthalocyanine have been made by this method.

The fourth method involves boiling phthalocyanine and a metal in quinoline or benzophenone. A variation of the last method for the preparation of metal phthalocyanines relates to a double decomposition reaction with a labile metal phthalocyanine and a salt of a less labile metal. Barrett, Frye and Linstaed first used this method to prepare more stable derivatives from dilithium phthalocyanine. This complex is particularly useful because of its solubility in alcohol. Copper phthalocyanine is immediately precipitated when alcoholic solution of dilithium phthalocyanine and anhydrous cupric chloride are mixed. Phthalocyanine derivatives of silver, mercury, calcium, zinc, lead, manganese and cobalt have been similarly prepared. The reaction dose not takes place with metal chlorides subject to alcoholysis, such as those of tin, thorium, bismuth or tungsten oxychloride. A number of rare metal phthalocyanines have been prepared from lithium phthalocyanine by double decomposition with liquid Lewis-base-type organic compounds as the reaction medium, such as dimethyl formamide or methyl sulfoxide. Heavy metal phthalocyanine of uranium, lead, thorium, lanthanum, gadolinium, dysprosium, samarium, holmium, erbium, europium, thulium, lutecium, ytterbium, and hafnium have been made in this manner.

The chemistry of the formation of phthalocyanine, which involves the union of four isoindole units symmetrically about a central atom involving phthalic anhydride, urea, cuprous chloride, and the catalysts in the formation of copper phthalocyanine, the phthalic anhydride is converted to phthalimide, which, in turn, is converted to monoiminophthalimide and di-iminophthalimide. The source of nitrogen may be urea but urea molecule decomposes and polymerizes at the elevated temperature at which copper phthalocyanine and other phthalocyanine

are made. Therefore, the source of nitrogen is probably a mixture of urea, urea decomposition products, and the urea polymers. The stages in which the phthalic residue passes prior to condensation to from phthalocyanine probably are:

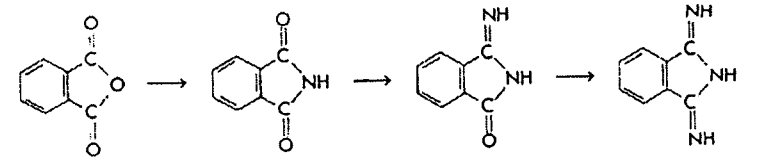

phthalic anhydride phthalimide monoiminophthalimide diiminophthalimide

Either the monodiiminophthalimide molecule or the di-iminophthalimide molecule condenses with itself to form, for example (I)

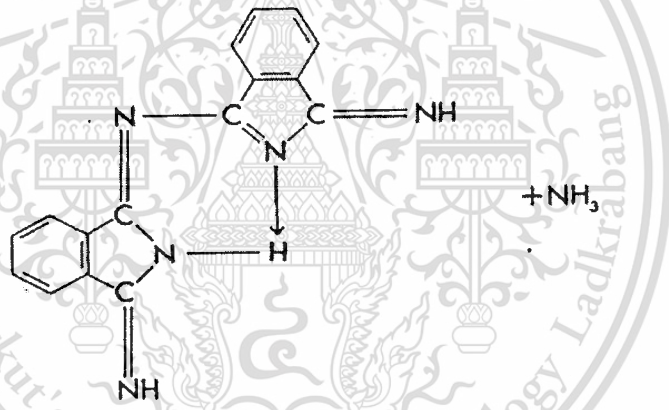

(I)

Followed by reaction with cuprous chloride to form (II)

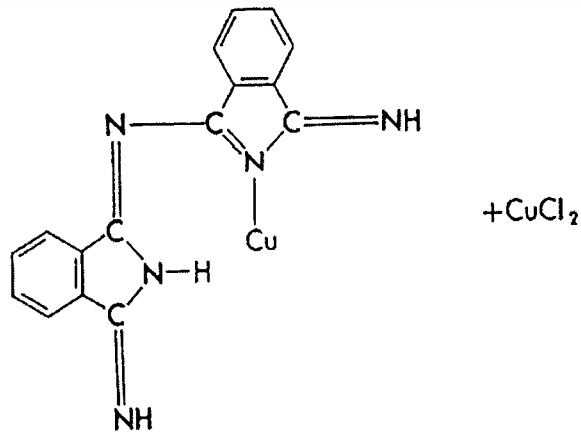

(II)

Followed by the subsequent condensation of (I) and (II) to form copper phthalocyanine and ammonia. Phthalocyanine may also be made by condensation of four molecules of phthalonitrile.

2.4 Cytochrome P-450 enzyme [35]

Cytochrome P-450 is the designation of a family of enzymes with iron porphyrin active sites that catalyze the addition of oxygen to a substrate. The most important representative of this class of reactions is the insertion reaction:

$$R\text{-}H + \tfrac{1}{2}(O2) \longrightarrow R\text{-}OH$$

The insertion of O atom into R-H bond which is just the sort of redox reaction likely to occur by an atom transfer mechanism is a part of the body's defense against hydrophobic compounds such as drugs, steroid precursors and pesticide. The hydroxylation of RH to ROH renders the target compounds more water soluble and thereby aids their elimination.

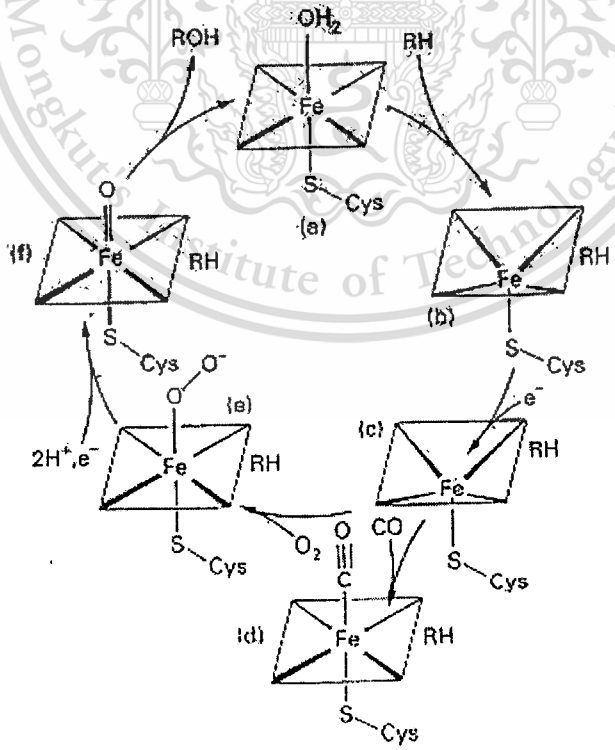

Figure 2.9 The cycle of reaction s of Cytochrome P-450

The proposed catalytic cycle for cytochrome P-450 is shown in Figure 2.9. The sequence begins at (a) in the figure with the enzyme in a resting state with iron present as Fe(III). The hydrocarbon substrate than binds (b), and one electron is transfer (c). The resulting Fe(II) complex with bound substrate proceeds to bind O_2 (e). A key reaction is the reduction of the porphyrin ring of the oxygen complex (e) by a second electron, which produces the ring radical anion. Uptake of two H^+ ions then leads to the formation of the Fe(IV) complex (f) which attacks the substrate to insert oxygen. Loss of ROH and uptake of an H_2O molecule at the vacated coordination position brings the cycle back to the resting state. The key to the cycle is the formation of the Fe(IV) oxo-complex.

2.5 Oxygen transport in the living cells

Oxygen is a recurring theme in the living organism cell because its role in respiration and its production in photosynthesis examples of a range of biologically important redox reactions, electron transfer, atom transfer and photochemical processes.

The distribution of oxygen carrier

First, we consider molecules that transport oxygen to the cell. All oxygen carriers that contain iron are found inside cells, whereas carriers that contain copper are also found in extra cellular fluids. A part of the reason for the distinction is that the cell interior is a reducing medium that can sustain iron as Fe(II). In addition, the cells supplies a porphyrin ring (shown below) as a ligand that can form a non-labile Fe(II) complex.

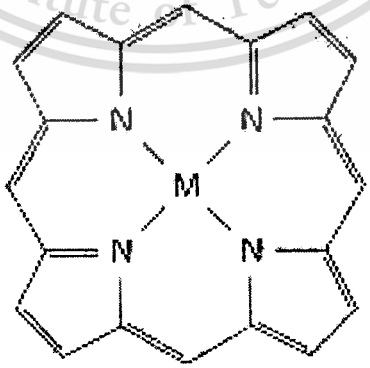

Because the porphyrin ring is susceptible to oxidative attack it also benefits from the protection of the reductases in the cell. On the other hand, both Cu(I) and Cu(II) can form strong complexes with the imidazole side chain of polypeptide residues, and the copper-based carries

may survive free in the bloodstream. The iron and copper carriers can play distinct roles in the same organism since they adopt different strategies for managing oxygen concentration gradients in the different compartments.

The most common oxygen carries are all based on helical proteins. In hemoglobin these coiled act like springs that can respond to the strain generated when oxygen binds at one site and can transmit that strain to other sites. Thus, the chemistry of O_2 complexation can be a combination of the effect complexation at the metal site and of alteration of the protein environment. The oxygen carriers are not very selective to identify of the incoming π-acceptor ligand, except in respect of its size. Thus, hemoglobin and myoglobin bind NO, CO, CN^{-1}, RNC, and SCN^{-1} as well as O_2.

2.6 Oxidation Catalyzed by Metallo Enzyme [5,36]

In recent year much attention has been devoted to the metal-catalyzed oxidation of inactivated C–H bonds in the homogeneous phase. The aim of these studies is to elucidate the molecular mechanism of enzyme-catalyzed oxygen atom transfer reactions. Additionally, such studies may eventually allow the development of simple catalytic system useful in functionalization of the organic compounds, especially in the oxidation of hydrocarbons. These methods should display high efficiency and specificity under mild conditions characteristic of enzymatic oxidation.

Many of these studies focus on modeling the oxidation by cytochrome P-450. Heme-containing mono-oxygenases known as cytochrome P-450 mediate a number of biochemical processes by incorporating one oxygen atom into the substrate. Among others they catalyze selective hydroxylation of nonactivated hydrocarbons. The oxygen atom incorporated into the substrate may derive from O_2 in the presence of a reducing agent, or may result from single oxygen atom donors.

Cytochrome P-450, however, is such a powerful oxidant that it can bring about self-degradation of its own porphyrin ligands. Because of this disadvantage metal complexes of synthetic porphyrin have been designed and used as chemical models of this enzyme. Of the different porphyrin complexes, Fe (III) and Mn (III) porphyrin exhibit the highest catalytic activity. The single oxygen atom donors most frequently used are iodosylbenzene (PhIO) and potassium hydrogen persulfate. Data for hydrogen peroxide, alkyl hydroperoxide, hypohalites, sodiumchlorate, tertiary amine *N*-oxides, and oxaziridine are also available.

The metalloporphyrin - PhIO system catalyzes the oxidation of alkane mainly to alcohols under mild conditions. High selectivity for the hydroxylation at the tertiary carbon is observed. Yields of up to 40% based on the oxidant consumed are obtained. A cyclic alkane usually exhibit very poor reactivity. A large isotope effect and retention of configuration in the oxidation of *cis*-decalin are additional important characteristics of the process.

A stepwise radical mechanism developed first for iron porphyrins and then found to be valid for manganese porphyrins as well accommodates the preceding. This mechanism is essentially the same as the one proposed for the oxidation of alkanes by cytochrome P-450. The active oxidizing species is the oxo-iron complex formed in the action of the single oxygen atom donor. The interaction0 of 8 with the alkane results in hydrogen abstraction and formation of caged radical 9. The isotope effect, the high regioselectivity, rearrangement of certain alkanes during oxidation, and the occasional decrease in stereo-selectivity testify to the radical nature of the mechanism. The reverse transfer of the OH to the carbon before diffusing out from the cage, known as the *oxygen rebound mechanism*, yields the product alcohol.

It appear that oxidation with alkyl hydroperxides has a different active species that does not include the metal. For example, in oxidation with cumyl hydroperxide the cumyloxy radical was proposed to participate in hydrogen abstraction H_2O_2, in turn, can serve as a single oxygen atom donor only oxidation with manganese porphyrins because of the activity of the manganese porphyrin- H_2O_2 system. Under these conditions, for instance, adamentane is preferentially converted to 1-adamantanol (63% selectivity at 93% conversion).

2.7 Overview of the thesis

In this thesis, the liquid phase oxidation of ethylbenzene in a stirred batch reactor under oxygen flow rate (4.2.1) and the liquid phase oxidation of cyclohexane in a pressure reactor under the pressure of oxygen (4.2.2), over zeolite BEA and zeolite EMT encapsulated cobalt phthalocyanine are studied. Cobalt phthalocyanine complexes are located in the cavities of zeolite by Ship-in-the-bottle technique [17]. Firstly, cobalt (II) ions are loaded into the cavities of zeolite using ion exchange method and impregnation method. Ligand, phthalonitrile, is then diffused into the cavities of zeolite to interact with the located cobalt (II) ion. The synthesized catalysts are characterized using conventional techniques, such as Scanning Electron Microscope (SEM), X-ray Diffraction (XRD), Fourier Transform Infrared Spectroscopy (FT-IR), Thermogravimetric Analysis (TGA), etc.

In this thesis, zeolite BEA and zeolite EMT were used as host material. Zeolite BEA is a channel structure zeolite, which is 3-dimentional system. While zeolite EMT is cage structure zeolite which is also 3-dimensional system. It is suggested that metal complex would be located in the hypercage of zeolite EMT and in the intersection of zeolite BEA. Hence, the effect of host material was studied in section 4.2.1 and 4.2.2.

It is suggested that some of the cobalt ions loaded by impregnation may not act as charge balancing cations. While all the cobalt ions loaded by ion exchange must be presented as charge balancing cations.

I. Ion exchange

All the cobalt ions loaded must be presented as charge balancing catios

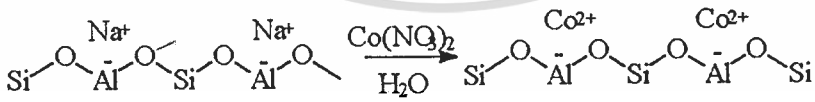

II. Impregnation

Some of cobalt ions loaded may not act as charge balancing cations

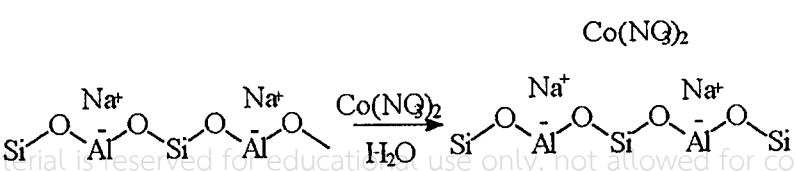

Accordingly, in this thesis, the effect of cobalt loading method was studied in the ethylbenzene oxidation section (4.2.1). According to the catalytic activity study in section 4.2.1, it was suggested that the active oxidizing species would be generated from the complexation of oxygen with cobalt phthalocyanine encapsulated in the cavities of zeolite and the free radical intermediate would play the important role in the oxidation reaction. Thus the effect of oxygen flow rate was studied in section 4.2.1. Furthermore, the purposed mechanism was clearly testified in section 4.2.2. From the purposed mechanism, it was shown that oxygen gas can serve as oxygen sources. Therefore, other oxygen source could be used as oxygen sources. Accordingly the effect of other oxygen source was studied in section 4.2.2. In this thesis the effect of solvent was also studied in section 4.2.2 using acetic acid, chloroform and dimethylformamide (DMF) as solvent.

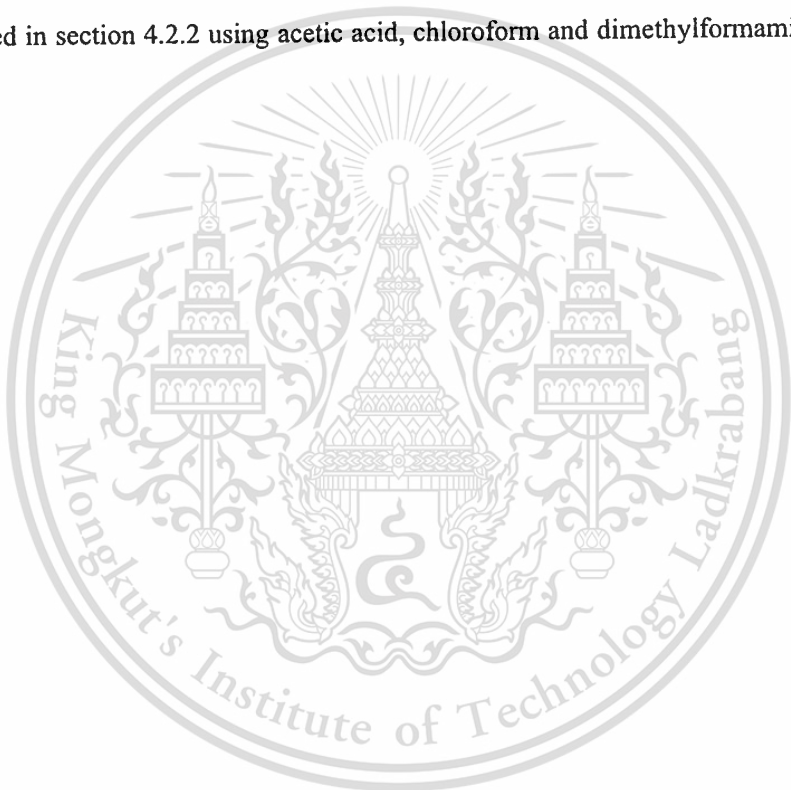

Chapter 3

Experimental

3.1 Reagents

1. Acetic acid glacial (Mallinckrodt)
2. Acetone (Fisons Analytical Reagent)
3. Air zero (TIG)
4. Aluminium ethoxide (Fluka Chemical)
5. 1-Amino-2-naphtol-4-sulphonic acid (95 %, Carlo Erba Reagenti)
6. Ammonium acetate (MERCK)
7. Ammonium molybdate ($\geq$ 99 %, Fluka Chemical)
8. Cobalt (II) nitrate (Carlo Erba Reagenti)
9. 18-Crown-6 (Fluka Chemical)
10. Cyclohexane (Carlo Erba Reagenti)
11. Deionized water
12. Dicyanobenzene (Fluka Chemical)
13. Dimethyl formamide (Carlo Erba Reagenti)
14. Ethylbenzene (Fluka Chemical)
15. Fume silica (BDH)
16. Hydrochloric acid (37 %, MERCK)
17. Hydrofluoric acid (48 %, MERCK)
18. Hydrogen peroxide (30% w/w, MERCK)
19. Hydroquinone (Carlo Erba Reagenti)
20. 8-Hydroxyquinoline (99 %, MERCK)
21. Liquid nitrogen (TIG)
22. Liquid petroleum gas (Siam Gas)
23. Ludox (colloid silica, 40% SiO_2) (Aldrich)
24. Oxygen gas (TIG)
25. Potassium bromide (BDH)
26. Pyridine (MERCK)
27. Silicic acid (Fluka Chemical)

28. Sodium aluminate (99 %, Rideal-de Haen)
29. Sodium chloride (Fisons Analytical Reagent)
30. Sodium hydrogen sulphite solution (39 %, MERCK)
31. Sodium Hydroxide (Carlo Erba Reagenti)
32. Sulfuric acid (MERCK)
33. Tartaric acid (MERCK)
34. Tetraethyl-ammonium-hydroxide (TEAOH, Fluka Chemical)

3.2 Apparatuses

1. Atomic Absorption Spectrophotometer (AA-680, Shimadzu)
2. Autoclave
3. Beaker
4. Buchner funnel
5. Burette
6. Clamp
7. Condenser
8. Dewar
9. Fourier Transformed Infrared Spectrometer (FTIR, IFS 28 Bruker)
10. Furnace (Vesstar Furnaces)
11. Gas Adsorption Analyzer (Autosorb-1, Quantachrome)
12. Gas Chromatograph (3800 Gas Chromatograph, Varian)
13. Heating mantle
14. Hot plate & stirrer
15. Magnetic stirrer
16. Nickel crucible
17. Oven
18. pH meter
19. Pipette
20. Pressure reactor (Parr autoclave)
21. Ring
22. Separation funnel (plastic)
23. Scanning Electron Microscope (SEM, Scanning Microscope 6400, Joel)

24. Suction flask
25. Thermogravimetric Analyzer (TGA-51, Dupont)
26. Thermometer (0-300 °C)
27. Universal indicator
28. UV-Vis Spectrophotometer (UV, Shimadzu)
30. Vacuum pump
31. Vial
32. Volumetric flask
33. Water circulator
34. X-ray Powder Diffractrometer (XRD, D8 Advance, Bruker)

3.3 Preparation and Characterization of catalysts

3.3.1 Synthesis of zeolites

3.3.1.1 Synthesis of zeolite EMT [37-38]

$$10SiO_2 : Al_2O_3 : 2.4Na_2O : 0.7\ 18\text{-Crown-6} : 140H_2O$$

Sodium hydroxide, 3.04 grams, was dissolved in 43.48 grams of deionized water. Sodium aluminate, 4.74 grams, was added in the mixture and the mixture was agitated until the mixture is homogeneous. Then, 5.13 grams of 18-crown-6 was added in the mixture and the mixture was agitated until the homogeneous mixture is obtained again. Afterthat, colloidal silica (Ludox®AS-40), 41.67 grams, was slowly dropped into the mixture using separating funnel, while the mixture was agitated continuously. Then, the mixture was agitated for 24 h. at 20 °C. The obtained mixture was loaded to a teflon-lined stainless-steel autoclave and crystallized at 115 °C for 168 hours. The crystalline product obtained was separated, washed with distilled water, dried at 110 °C overnight and activated by calcination in air at 550 °C (heating rate at 2 °C /min) for 3 hours in a purge of dry air. The calcination was carried out in furnace shown in Figure 3.1. Finally, the material obtained was characterized by Scanning Electron Microscope, X-ray Diffractrometer and Gas Adsorption Analyzer.

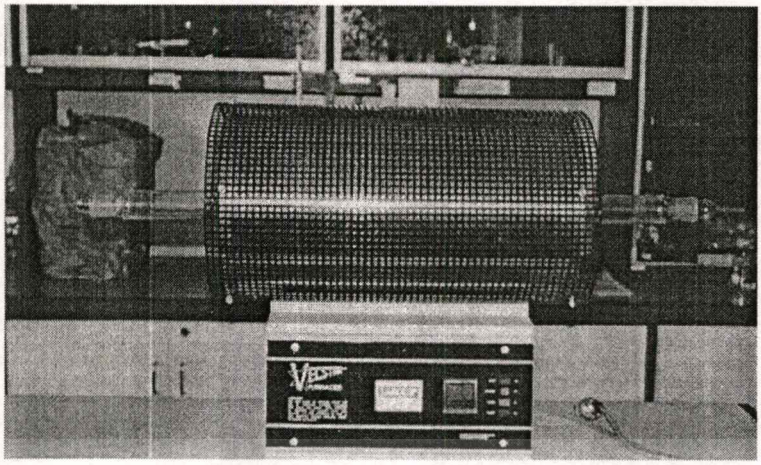

Figure 3.1 Furnace for calcination

3.3.1.2 Synthesis of zeolite BEA [39]

$$9SiO_2 : Al_2O_3 : Na_2O : 1.6TEAOH : 140H_2O$$

2.86 grams of sodium aluminate, 0.21 grams of aluminium ethoxide, 10.21 grams of tetraethylammoniumhydroxide and 12.63 grams of deionized water was mixed together. Then, the mixture obtained was agitated until it appears to be a clear solution. Afterthat, 9.54 grams of fume silica was added into the mixture and a plastic rod was used for mixing for 15 minutes. Then, the mixture was agitated by a mechanical stirrer for 2 hours. After 2 hours, solid lumps were obtained. It was transferred to a teflon-lined stainless-steel autoclave and crystallized at 170 °C for 44 hours. The crystalline product obtained was separated, washed with distilled water, dried at 110 °C overnight and activated by calcination in dry air at 550 °C (heating rate at 2 °C/min) for 3 hours. Finally, the material obtained was characterized by Scanning Electron Microscope, X-ray Diffraction and Gas Adsorption Analyzer.

3.3.2 Modification of zeolites

3.3.2.1 Ion exchange [12]

Cobalt incorporated into synthesized zeolites have been carried out by ion exchange of sodium cation by cobalt cation. First of all, 2 grams of synthesized zeolites was ion exchanged in 500 ml of 1 N aqueous solution of sodium chloride (NaCl) to result pure Na^+ form (Na-EMT and Na-BEA). A reflux at 80 °C for 20 hours was filtrated and washed 1 time using 50 ml deionized

water. Then, 2 grams of dried sodium form zeolite was ion-exchanged in 200 ml of 0.1 molar aqueous solution of cobalt (II) nitrate ($Co(NO_3)_2.6H_2O$) at 80 °C for 12 hours, this step was repeated three times. A reflux was then filtered and washed 1 time using 50 ml of distilled water at room temperature. The zeolite was dried at 100 °C for 3 hours. Finally, the solid material obtained was characterized by X-ray Diffractrometer, Gas Adsorption Analyzer and Atomic Absorption Spectrophotometer. This solid material obtained will be referred to as Ion-EMT and Ion-BEA for zeolite EMT and zeolite BEA, respectively.

3.3.2.2 Impregnation [12]

Impregnation of cobalt ions into the synthesized zeolites was done according to the following procedure: cobalt (II) nitrate hexahydrate ($Co(NO_3)_2.6H_2O$) (0.79 grams for synthesized zeolite EMT and 0.71 grams for synthesized zeolite BEA) were dissolved in a small amount of water. This solution was added to 2 grams of hot synthesized zeolites and the resulting mixture was stirred for a few minutes. Then the water was gently evaporated to dryness at room temperature. Finally, the solid material obtained was characterized by X-ray Diffraction, Gas Adsorption Analyzer and Atomic Absorption Spectrophotometer. This solid material obtained will be referred to as Imp-EMT and Imp-BEA for zeolite EMT and zeolite BEA, respectively.

3.3.2.3 Encapsulation of cobalt phthalocyanine in the cavities of zeolites [12]

2 grams of dried cobalt loaded zeolite was transferred to a glass ampoule connected with vacuum line as shown in Figure 3.2. Then, the ampoule was heated at 150 °C by heating tape for 20 hours. Afterthat, dicyanobenzene was added promptly in the ampoule, mole of dicyanobezene / mole of cobalt loaded in zeolite = 6. The ampoule connected with the vacuum line was further vacuumed for 8 hours. Then, the ampoule was sealed by free flame. The sealed ampoule was then heated in the furnace at 250 °C for 16 hours. The solid material obtained was washed directly with acetone, pyridine and acetone, respectively. After washing is completed, solid material was heated in a vacuum oven at 150 °C for 24 h. Finally, it was characterized by Scanning Electron Microscope, Fourier Transformed Infrared Spectrophotometer, Thermogravimetric Analyzer, UV/VIS spectrophotometer and Gas Adsorption Analyzer. This solid materials obtained will be referred to as Ion-EMT-encap, Ion-BEA-encap, Imp-EMT-encap and Imp-BEA-encap.

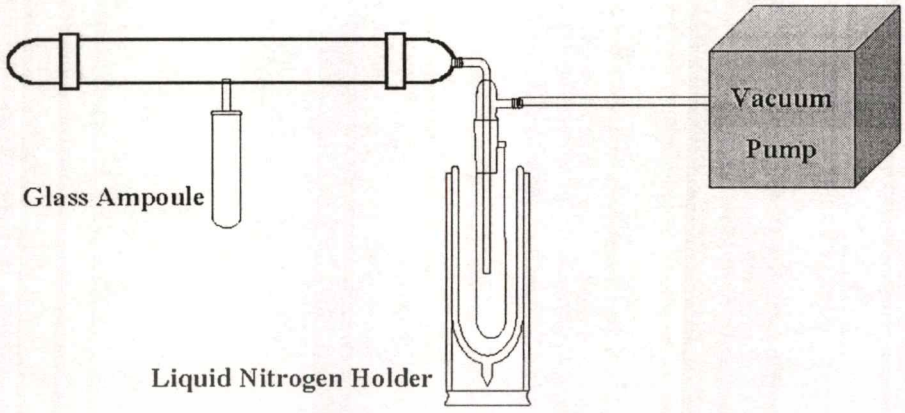

Figure 3.2 Glass ampoule contacted vacuum line

3.3.3 Catalyst characterization

3.3.3.1 Determination of crystal morphology of zeolite using Scanning Electron Microscope (SEM)

The crystal morphology and crystal size were determined by scanning electron microscope (Jeol 6400 Scanning Microscope, Chulalongkorn University Instruments Service Center). The sample was prepared by thoroughly placing zeolite onto the sample holder. It was then coated with gold thin film by ion sputtering. The sample was placed in the sample chamber of scanning electron microscope and evacuated from ambient pressure to 10^{-4} torr. The scanning electron micrographs were taken at the magnification of 1,000, 7,000, 15,000 and 20,000 times.

3.3.3.2 Determination of zeolite structure using X-ray Powder Diffractometer (XRD)

The zeolite structure was determined by X-ray diffractometer (D8 Advance, Bruker, Scientific Instruments Service Center; SISC). The sample was prepared by packing the zeolite in the sample holder. CuK$\propto$ X-ray beam was used for analysis at 40 kV, 40 mA. The sample were scanned from 2θ angle 5° to 60° with 1 second/step time and 0.04 2θ/step increment. X-ray diffraction pattern of sample was compared with the X-ray diffraction pattern of standard zeolites for structure determination.

3.3.3.3 Determination of surface area of zeolites using Gas Adsorption Analyzer (Autosorb)

Surface area of zeolite was determined by Gas Adsorption Analyzer (Autosorb-1, Quantachrome) shown in Figure 3.3. The sample was prepared by weighing 10 mg of zeolite sample into a cleaned and dried sample cell. The sample cell was attached to the out gassing station. Heating mantle was installed and the temperature was raised to 350 ^{o}C. The sample was out-gassed for 24 hours. The sample cell was then removed from the out gassing station after the nitrogen was filled and was attached to the analysis station. The equilibration time is set to 3 minutes and the adsorption was tested at the partial pressure (P/P_0) ranged from 10^{-6} to 1.0.

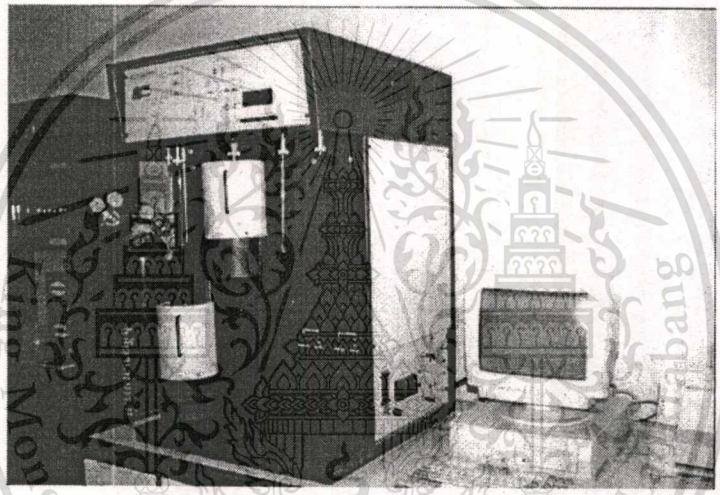

Figure 3.3 Gas Adsorption Analyzer (Autosorb-1, Quantachrome)

3.3.3.4 Determination of silicon [41]

The amount of silicon in zeolite sample was determined by UV-Vis Spectrophotometry. Zeolite was digested and the complexes of silicon with ammonim molybdate were formed and analyzed.

Preparation of reagents

- *Preparation of ammonium molybdate*

The reagent was prepared by dissolving 8.0 grams ammonium molybdate crystals in water, followed by adding of 9 ml concentrated sulfuric acid. This solution was diluted to 100 ml with distilled water.

- *Preparation of reducing agent.*

A solution (A) was prepared by dissolving 10 grams sodium hydrogensulphite in 70 ml water. Then, another solution (B) was prepared by dissolving 0.8 grams anhydrous sodium hydrogensulphite in 20 ml water, and 0.16 grams 1-amino-2-naphthol-4-sulphonic acid was added. Finally, solution A and solution B were mixed and diluted to 100 ml with distilled water. This solution must be prepared freshly in use.

Preparation of standard solution of silica and sample solution

Accurate 70.93 mg of NaZSM5 zeolite and 50 mg of standard silica (100% silicon) were weighed. Each portion was transferred to a clean nickel crucible containing 5 ml of 30% sodium hydroxide solution. The covered crucibles was heated to dull redness for about 15 minutes, the zeolite sample (or standard silica) should then have melted. The sample was carefully cooled down and the boiling water was added to dissolve the fused mass. The dissolved solution was transferred to a 1 L beaker and about 150 ml of water was added. This solution was stirred by a plastic rod and 5 ml of 1+1 hydrochloric acid was added. The sample solution was diluted to 200 times (250 ml). While, the standard solution which have been treated similarly with the sample solution, was diluted to approximately 10 ppm before further dilution. A calibration curve was constructed using 2.5, 5.0, 7.5, and 10.0 ml of the standard silica solution. After transferring of standard sample (or 5.0 ml of zeolite sample solution), pH of the solution (contained between 0.02 and 0.1 mg of silicon) was measured and adjusted to 4.5-5.0. Then, 1 ml of ammonium molybdate solution and 5 ml of 10% tartaric acid solution were added. The resulting mixed solution was further added with 1 ml of the reducing agent and diluted to 100 ml. After 20 minutes, the absorbance at 815 nm of the sample solution was measured againsted the blank. Finally, the silicon content of zeolite sample was calculated using a calibration curve.

3.3.3.5 Determination of aluminium [43]

Preparation of reagent

Reagent solution was prepared by dissolving 2 grams 8-hydroxyquinoline in chloroform to make 100 ml solution. Then, acetate buffer solution was prepared by dissolving 25 grams of ammonium acetate in 70 ml of water then 5 ml of acetic acid was added. This solution was diluted to 100 ml with water.

Preparation of standard solution of aluminium and sample solution

The accurate 44.08 mg of zeolite sample was weighed and digested with hydrofluoric acid (48 %). This solution was diluted to 100 ml in plastic volumetric flask. Then, 25 ml of the diluted sample solution and 3 ml of acetate buffer solution were mixed in a plastic beaker. The mixture should exhibit a pH 6 and it was then transferred to a separatorry funnel. After mixing, the 20 ml of 8-hydroxyquinoline solution was added and this mixture was shacked vigorously for 3 minutes. The organic phase was separated, filtered, and measured at 410 nm. against a blank. The standard aluminium solution was diluted to 50 ppm and a calibration curve was constructed by using 1, 2, 3 , and 4 ml of this standard solution. Finally, the aluminium content of zeolite sample was calculated using the calibration curve.

3.3.3.6 Determination of cobalt loaded in zeolite

Preparation of sample

50-60 mg of cobalt loaded zeolite was digested by 4-5 drops of hydrofluoric acid (48 %). This solution was neutralized by ammoniumhydroxide (NH_4OH). Then, the neutralized solution was filtered and only filtrate was transferred to 100 ml volume-metric flask. The solution was diluted to 100 ml by deionized water.

Preparation of standard solution

Standard cobalt solution 1,000 ppm was diluted in 100 ml volume metric flask by deionized water to 1, 5, 10, 20 and 30 ppm of standard cobalt solution, respectively.

3.3.3.7 Characterization by Atomic Absorption Spectrophotometer

The absorbance of standard cobalt solution prepared was measured by Atomic Absorption Spectrophotometer. After the measurement, the calibration curve could be obtained. Then, the sample solution was determined by Atomic Absorption Spectrophotometer. Finally, the cobalt-loaded content can be calculated from the calibration curves as shown in appendix F.

3.3.3.8 Characterization of catalyst by Fourier Transformed Infrared Spectrometer

The complex loaded in the cavities of zeolite can be characterized by Fourier Transformed Infrared Spectroscopy (FT-IR). The thin pallet of zeolite was prepared by compressing the mixing of, 1 microgram of dried zeolite encapsulated complex and 0.005 grams of dried potassium bromide (KBr), with 6 tons pressure loading. 16 Measurement scans was

applied in transmittance mode and the resolution was set to be 4. The sample was scanned over the frequency 4000-400cm^{-1}.

3.3.3.9 Characterization by UV-Visible spectrophotometer

After washing, 0.001 grams of the zeolite encapsulated complex was digested by 1 ml of conc. sulfuric acid. This solution was filtered by filter paper no. 40 and only filtrate was characterized by UV-Visible spectrophotometer, Shimadzu UV-Visible.

3.3.3.10 Characterization by Thermogravimetric Analyzer

After washing, 0.003-0.005 grams of the zeolite encapsulated complex was loaded in the sample holder of Thermogravimetric analyzer, TGA-51 Dupont shown in Figure 3.4. The thermogram was obtained over the range of temperature 50-800 °C with a heating rate of 10 °C/min under 50 ml/min of nitrogen gas.

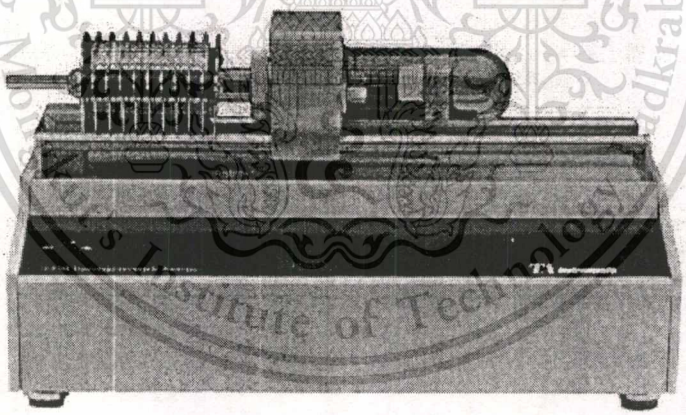

Figure 3.4 Thermogravimetric analyzer, TGA-51 Dupont

3.4 Catalytic testing

3.4.1 Oxidation of ethylbenzene

Oxidation reaction of ethylbenzene was carried out at reflux temperature (≈ 138 °C) in a 50 ml stirred reactor (shown in Figure 3.5). 0.15 grams of zeolite encapsulated complex was used

in 45 grams of ethylbenzene. Oxygen gas was subjected to flow through a glass frit to the reaction mixture. Periodically, 1 ml of reaction mixture was sampled by syringe at 2, 4, 6, 8, 10, 12, 16, 24, 50, 60, 70 and 72 hours, respectively. The solution was filtered and analyzed by gas chromatography (3800 Gas Chromatograph, Varian, as shown in Figure 3.6) with a capillary DB-FFAP column (30 m, length). 1.5 μl of liquid sample was injected to the injection port (200 °C) of gas chromatography using a split ratio of 200. The separation temperature was started at 130 °C for 5 minutes. Then, the temperature was raised to 160 °C with a heating rate of 20 °C /min and hold at that temperature for 8 minutes. Helium was used as carried gas at a flow rate of 28.1 cm/sec.

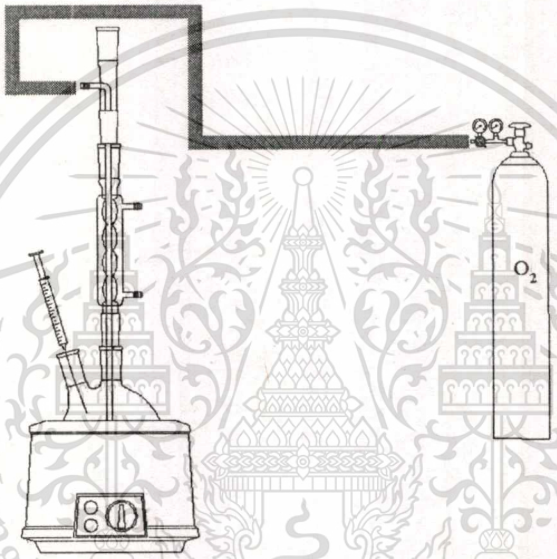

Figure 3.5 Oxidation reactor (Batch reactor)

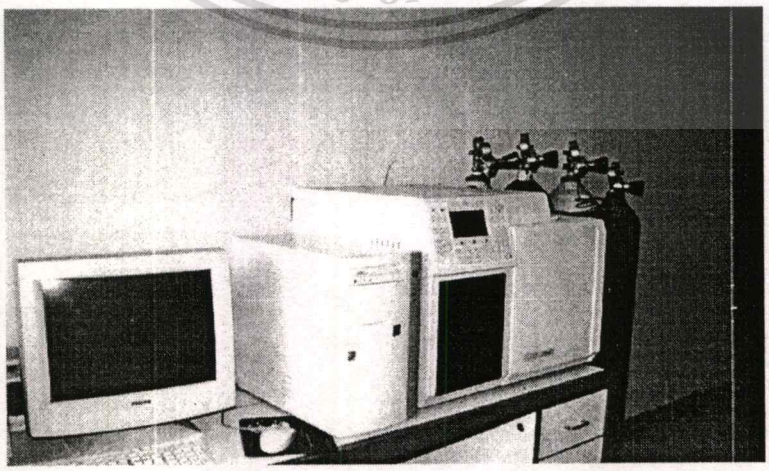

Figure 3.6 3800 Gas Chromatograph, Varian

The reaction conditions for study of oxidation of ethylbenzene were summarized in Table 3.1.

Table 3.1 The studied of oxidation reaction of ethylbenzene[a, b]

Reaction Number	Catalyst	Oxygen flow rate (ml/min)
1	None	40
2	Ion-EMT-encap	40
3	Ion-BEA-encap	40
4	Imp-EMT-encap	40
5	Imp-BEA-encap	40
6	Ion-EMT-encap	20
7	Ion-BEA-encap	20
8	Ion-EMT-encap	80
9	Ion-BEA-encap	80
10	Regen. Catalyst from reaction No. 2[c]	40
11	Regen. Catalyst from reaction No. 3[c]	40
12	Regen. Catalyst from reaction No. 8[c]	40

[a] reaction time is 72 hours

[b] the reaction mixture was sampled by syringe at 2, 4, 6, 8, 10, 12, 16, 24, 50, 60, 70 and 72 hours, respectively, for every reaction.

[c] reaction time is 24 hours

3.4.1.1 Effect of host material

The effect of host material was evaluated by the reaction using zeolite BEA and zeolite EMT as host materials. The procedures were followed by the reaction number 1-3 in Table 3.1.

3.4.1.2 Effect of reaction time

The effect of reaction time was determined by the reaction using the reaction condition followed by the reaction number 1-3 in Table 3.1.

3.4.1.3 Effect of loading cobalt method

In this research zeolite encapsulated cobalt phthalocyanine was prepared by ship-in-the-bottle strategy. Cobalt was loaded into cavities of zeolite by two methods named ion exchange and impregnation. The effect of cobalt loading method was determined by the reaction using zeolite encapsulated cobalt phthalocyanine which were prepared by ion exchange and impregnation. The procedures were followed by reaction number 2-5 in Table 3.1.

3.4.1.4 Effect of regenerated catalyst

After the reaction, the catalyst was regenerated by washing with acetone and drying at 100 °C in a vacuum oven. It was then used as a catalyst again. The effect of regeneration of catalyst was determined by the reaction using regenerated catalyst. The procedures were followed by reaction number 10-12 in Table 3.1.

3.4.1.5 Effect of oxygen gas flow rate

While the reaction was operated, the oxygen gas was introduced through a glass frit to the reaction mixture. The effect of oxygen gas flow rate was determined by the reaction using 20 ml/min, 40 ml/min and 80 ml/min of oxygen flow rate. The procedures were followed by reaction number 2, 3 and 6-9 in Table 3.1.

3.4.2 Oxidation of cyclohexane

Oxidation of cyclohexane was carried out at 70 °C in a pressure reactor (Parr autoclave, 300 ml capacity) as shown in Figure 3.4. In a typical oxidation reaction, 12.25 grams of cyclohexane, 0.375 grams of catalyst, 22.25 grams of acetic acid and 0.2 g of hygrogenperoxide were added into the reactor before a 300 psi of oxygen gas was admitted into the reactor. Afterthat, the sample was removed and the solid catalyst was filtered. Then, the sample solution was analyzed by gas chromatography, 3800 Gas Chromatograph, Varian, as shown in Figure 3.3, with a capillary DB-FFAP column (30 m). 1.5 μl of liquid sample was injected to the injection port (200 °C) of gas chromatography using a split ratio of 200. The separation temperature was started at 90 °C for 2 minutes. Then, the temperature was raised to 130 °C with a heating rate of 20 °C /min and hold at that temperature for 1 minutes. Then the temperature was raised to 140 °C with a heating rate of 20 °C /min and hold at that temperature for 7 minutes. Helium was used as carried gas at a flow rate of 28.1 cm/sec.

The reaction conditions for the study of the oxidation of cyclohexane were summarized in Table 3.2.

Table 3.2 The studied of oxidation reaction of cyclohexane at 70 °C

Reaction Number	**Catalyst**	**Time (hr.)**	**Solvent**	*Oxygen Source*	*Note*
1	None	2	Acetic acid	O_2	Without catalyst
2	None	4	Acetic acid	O_2	Without catalyst
3	None	6	Acetic acid	O_2	Without catalyst
4	None	8	Acetic acid	O_2	Without catalyst
5	None	10	Acetic acid	O_2	Without catalyst
6	None	24	Acetic acid	O_2	Without catalyst
7	Ion-BEA-encap	2	Acetic acid	O_2	-
8	Ion-BEA-encap	4	Acetic acid	O_2	-
9	Ion-BEA-encap	6	Acetic acid	O_2	-
10	Ion-BEA-encap	8	Acetic acid	O_2	-
11	Ion-BEA-encap	10	Acetic acid	O_2	-
12	Ion-BEA-encap	24	Acetic acid	O_2	-
13	Ion-EMT-encap	2	Acetic acid	O_2	-
13	Ion-EMT-encap	4	Acetic acid	O_2	-
14	Ion-EMT-encap	6	Acetic acid	O_2	-
15	Ion-EMT-encap	8	Acetic acid	O_2	-
16	Ion-EMT-encap	10	Acetic acid	O_2	-
17	Ion-EMT-encap	24	Acetic acid	O_2	-
18	Ion-BEA-encap	2	Acetic acid	O_2	0.22 g of ethylenediamine
19	Ion-BEA-encap	4	Acetic acid	O_2	0.22 g of ethylenediamine
20	Ion-BEA-encap	6	Acetic acid	O_2	0.22 g of ethylenediamine
21	Ion-BEA-encap	8	Acetic acid	O_2	0.22 g of ethylenediamine
22	Ion-BEA-encap	10	Acetic acid	O_2	0.22 g of ethylenediamine
23	Ion-BEA-encap	24	Acetic acid	O_2	0.22 g of ethylenediamine
24	Ion-BEA-encap	2	Acetic acid	O_2	0.2 g of hydroquinone
25	Ion-BEA-encap	4	Acetic acid	O_2	0.2 g of hydroquinone

Table 3.2 (continued)

Reaction Number	Catalyst	Time (hr.)	Solvent	*Oxygen Source*	*Note*
26	Ion-BEA-encap	6	Acetic acid	O_2	0.2 g of hydroquinone
27	Ion-BEA-encap	8	Acetic acid	O_2	0.2 g of hydroquinone
28	Ion-BEA-encap	10	Acetic acid	O_2	0.2 g of hydroquinone
29	Ion-BEA-encap	24	Acetic acid	O_2	0.2 g of hydroquinone
30	Ion-BEA-encap	2	Acetic acid	O_2	Without hydrogenperoxide
31	Ion-BEA-encap	4	Acetic acid	O_2	Without hydrogenperoxide
32	Ion-BEA-encap	6	Acetic acid	O_2	Without hydrogenperoxide
33	Ion-BEA-encap	8	Acetic acid	O_2	Without hydrogenperoxide
34	Ion-BEA-encap	10	Acetic acid	O_2	Without hydrogenperoxide
35	Ion-BEA-encap	24	Acetic acid	O_2	Without hydrogenperoxide
36	Ion-BEA-encap	2	Acetic acid	Air	-
37	Ion-BEA-encap	4	Acetic acid	Air	-
38	Ion-BEA-encap	6	Acetic acid	Air	-
39	Ion-BEA-encap	8	Acetic acid	Air	-
40	Ion-BEA-encap	10	Acetic acid	Air	-
41	Ion-BEA-encap	24	Acetic acid	Air	-
42	Ion-BEA-encap	2	Chloroform	O_2	-
43	Ion-BEA-encap	2	Chloroform	O_2	-
44	Ion-BEA-encap	4	Chloroform	O_2	-
45	Ion-BEA-encap	6	Chloroform	O_2	-
46	Ion-BEA-encap	8	Chloroform	O_2	-
47	Ion-BEA-encap	10	Chloroform	O_2	-
48	Ion-BEA-encap	24	Chloroform	O_2	-
49	Ion-BEA-encap	2	DMF[a]	O_2	-
50	Ion-BEA-encap	4	DMF	O_2	-
51	Ion-BEA-encap	6	DMF	O_2	-
52	Ion-BEA-encap	8	DMF	O_2	-
53	Ion-BEA-encap	10	DMF	O_2	-

Table 3.2 (continued)

Reaction Number	Catalyst	Time (hr.)	Solvent	*Oxygen Source*	*Note*
54	Ion-BEA-encap	24	DMF	O_2	-
55 [b]	Ion-BEA-encap	24	Acetic Acid	O_2	In batch reactor with O_2, 40 ml/min continuos flow

[a] DMF = Dimethylformamide

[b] the reaction mixture was sampled by syringe at 2, 4, 6, 8, 10, and 24 hour

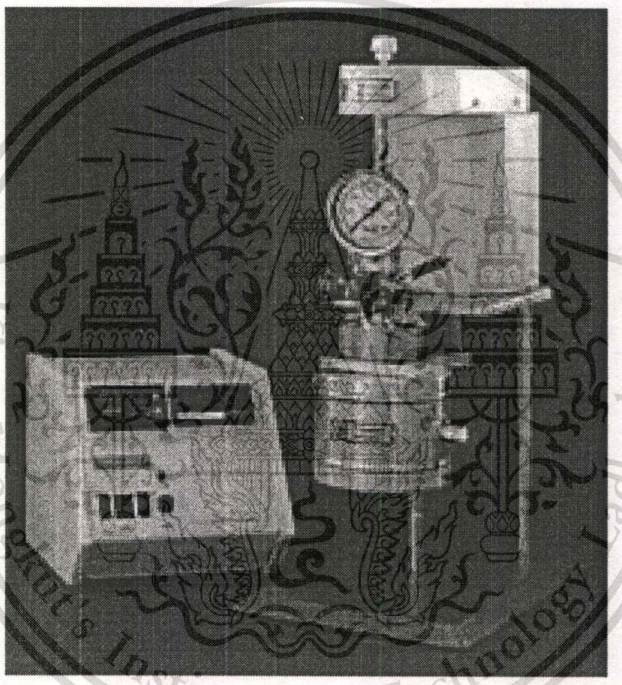

Figure 3.7 Parr reactor for cyclohexane oxidation

3.4.2.1 Effect of pressure

In the reaction at atmospheric pressure, low yields of products were obtained. Accordingly, the reaction under pressure may solve this disadvantage. The effect of pressure was determined by the reaction under pressure of oxygen and atmospheric pressure with continuous feed of oxygen gas, 40 ml/min, through a glass frit with different residential time (1-24 hours). The procedures were followed by reaction number 7-12 and 55 in Table 3.2.

3.4.2.2 Study of reaction pathway

The reaction pathway for the oxidation reaction of cyclohexane using zeolite encapsulated cobalt phthalocyanine can be tested for hypothesis that involves 3 major steps. Firstly, the active species called metal-oxo species were formed from the complexation of oxygen and the cobalt phthalocyanine encapsulated in the cavities of zeolite. Afterthat, substrate reacts with the active species. Finally, the corresponding products, ketone and alcohol are formed by the decomposition of the species obtained from the complexation of substrate and the active species. It is proposed that the free radical is the main intermediate for the decomposition step. The first step of the hypothesis was tested by adding ethylenediamine in the reaction mixture. The procedures were followed by reaction number 18-23 in Table 3.2. The decomposition step was evaluated by adding hydroquinone, a free radical inhibitor, in the reaction mixture and the procedures were followed by reaction number 24-29 in Table 3.2.

3.4.2.3 Effect of host material

The effect of host material was determined by the reaction using zeolite BEA and zeolite EMT as host materials with different residential time (1-24 hours). The procedures were followed by reaction number 7-17 in Table 3.2.

3.4.2.4 Effect of hydrogenperoxide

From the mechanistic study, it is proposed that the free radical is the main intermediate for the decomposition step. Adding hydrogenperoxide in the reaction mixture could be advantage. Hence, the effect of hydrogenperoxide was determined by the reaction with hydrogenperoxide and that without hydrogenperoxide with different residential time (1-24 hours). The procedures of study were followed by reaction number 7-12 and30-35 in Table 3.2.

3.4.2.5 Effect of oxygen partial pressure

The source of oxygen donor used in the oxidation reaction should be the major factor influencing the conversion of cyclohexane. Therefore, the effect of oxygen source was determined by the reaction using air and oxygen gas as oxygen source with different residential time (1-24 hours). The procedures were followed by reaction number 6-10 and 41-45 in Table 3.2.

3.4.2.6 Effect of solvent

It can be proposed that solvent, which mediates between reactants and active sites, is one of major factors effectively the oxidation of cyclohexane. Therefore, for comparison, three solvents including, acetic acid chloroform and di-metylformamide (DMF) are selected to use as solvent in this research. The procedures were followed by reaction number 7-12 and 42-54 in Table 3.2.

Chapter 4

Results and Discussion

4.1 Characterization of catalysts

4.1.1 X-ray Powder Diffraction, XRD

The X-ray powder diffraction pattern of synthesized sodium zeolite BEA (Na-BEA) and EMT (Na-EMT) were obtained. The X-ray powder diffraction pattern of synthesized zeolite Na-BEA coincides with a standard pattern of zeolite BEA (Appendix B). In the same way, the identical X-ray diffraction pattern of synthesized zeolite Na-EMT and standard zeolite EMT can be found (Appendix B). The X-ray diffraction pattern of synthesized zeolite Na-BEA and Na-EMT are shown in Figure 4.1.

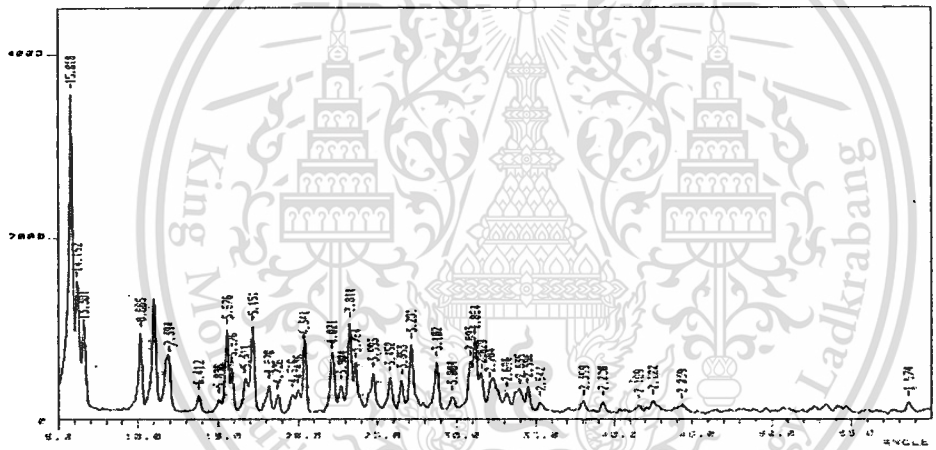

(a)

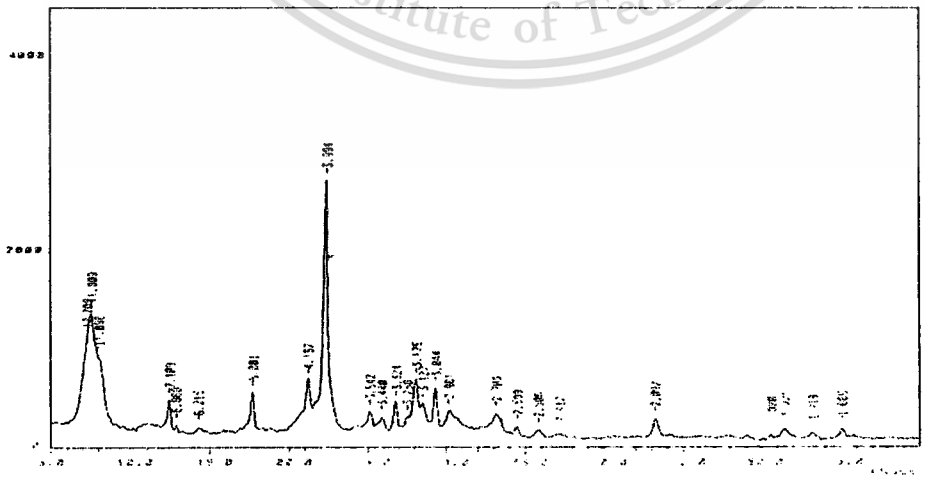

(b)

Figure 4.1 X-ray powder diffraction pattern of synthesized zeolite (a) EMT and (b) BEA

After calcination, the X-ray diffraction pattern of synthesized zeolite Na-BEA and Na-EMT remain similar to the zeolites before calcination, except that the lower intensity was found in the X-ray diffraction pattern of the zeolites after calcination. However, the synthesized zeolites are still regarded as high crystalline materials. The X-ray diffraction patterns of the calcined zeolites are shown in Figure 4.2.

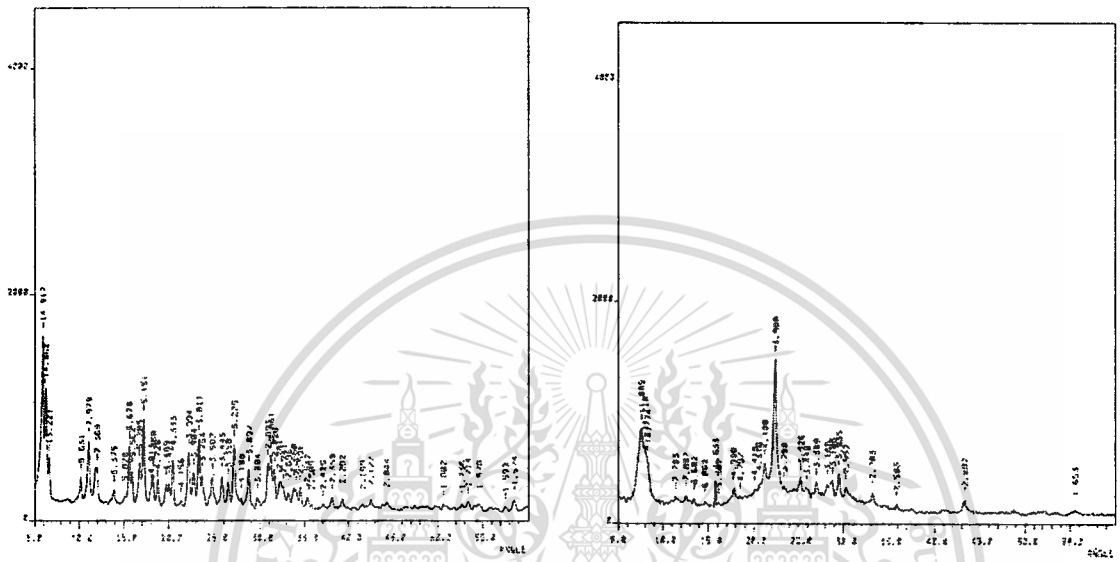

Figure 4.2 X-ray powder diffraction pattern of synthesized zeolite (a) EMT after calcination and (b) BEA after calcination

The calcined zeolites were loaded with cobalt (II) cation and the X-ray powder diffraction pattern of them were obtained. The X-ray powder diffraction patterns of modified zeolites are illustrated in Figure 4.3. The presence of cobalt (II) cation in the cavities of zeolite results in peak missing, peak splitting and intensity enhancement of some peaks. In the case of loading by ion exchange, the X-ray powder diffraction of zeolites loaded cobalt (II) cation was slightly changed, while the X-ray diffraction of zeolite loaded cobalt (II) cation was changed significantly in the case of loading by impregnation. Since cobalt cation contains a large number of electrons, the characteristics of an X-ray beam with a certain energy can be altered at a plane where a cobalt cation is located. If the altered X-ray beam is out of the condition for Bragg Law, the peak will disappear. In addition, secondary X-rays can also be generated introducing complexity to the diffraction phenomena. This results in either peak splitting or intensity

enhancement of some peaks. This makes the X-ray diffraction pattern of zeolite loaded cobalt cation become different from that of unloaded cobalt cation zeolite. Using of higher power X-ray source, i.e. tungsten (TuKα) or molybdenum (MoKα) can reduce this problem.

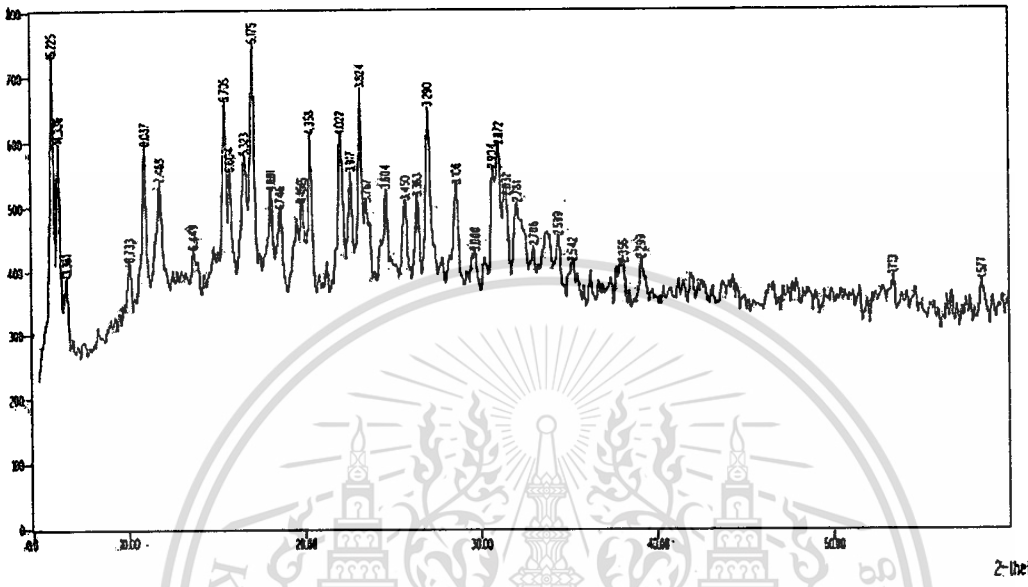

(a)

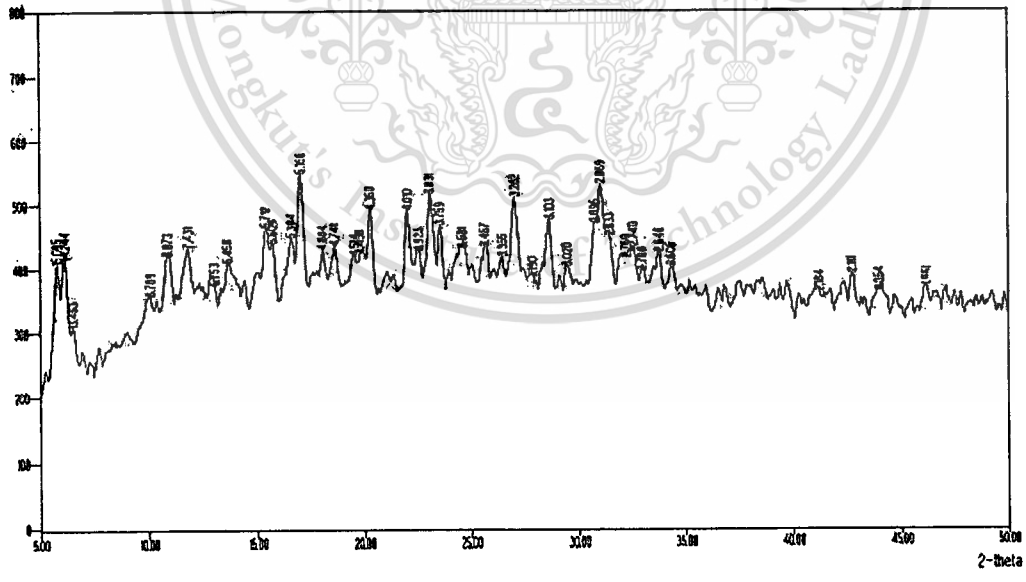

(b)

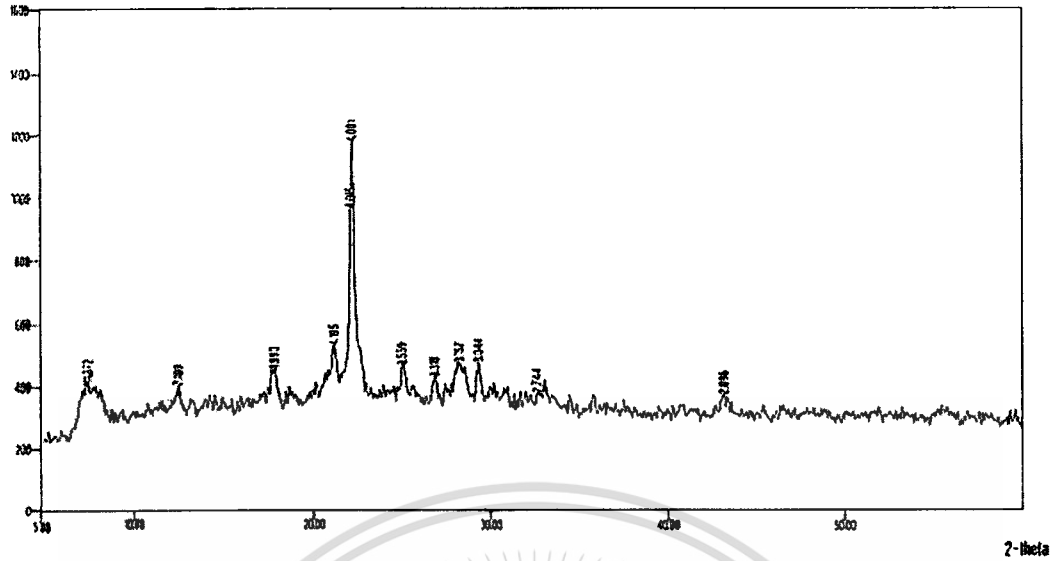

(c)

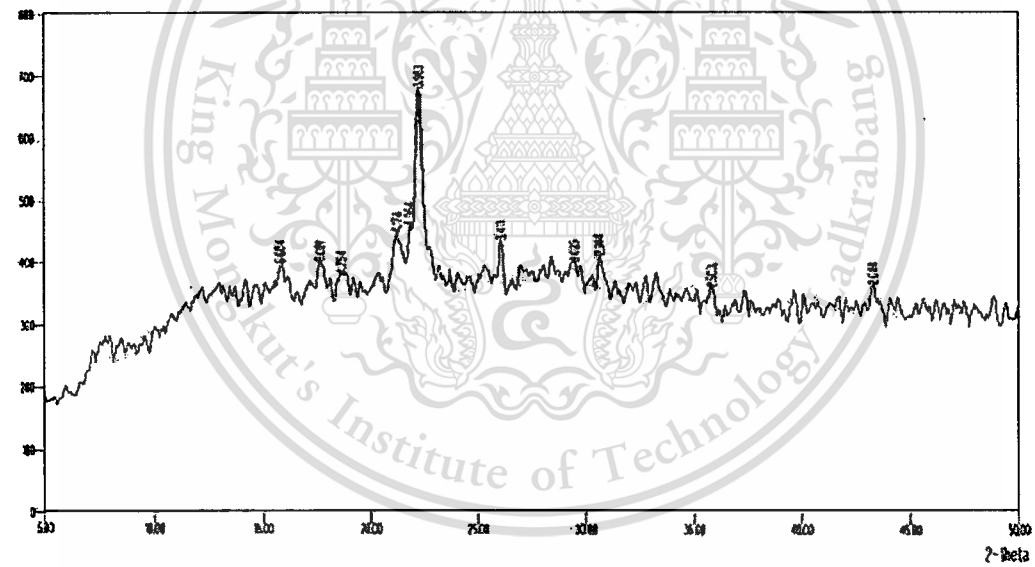

(d)

Figure 4.3 X-ray powder diffraction pattern of modified zeolites (a) Ion exchanged EMT, (b) Impregnated EMT, (c) Ion exchanged BEA and (d) Impregnated BEA

To check the crystallinity of sample, practically, the zeolite loaded cobalt cations was then re-exchanged with 1 N of sodium chloride (NaCl) solution to recover the sodium formed zeolite. Afterthat, the recovered sodium zeolite was characterized by X-ray Diffraction XRD) again and the X-ray diffraction patterns of the recovered sodium zeolites are depicted in Figure

4.4. It is found that the X-ray powder diffraction patterns of both recovered zeolite coincide with the standard patterns. Although, missing peaks, peak splitting and intensity of enhancement of some peaks was observed in the X-ray diffraction pattern of zeolite loaded cobalt cation, the zeolite loaded cobalt cations can still be regarded as a high crystallinity material. In conclusion, characterization of zeolite loaded cobalt (II) ion by X-ray powder diffraction reveals that the crystallinity of zeolite EBA and EMT after the applied modification was virtually retained.

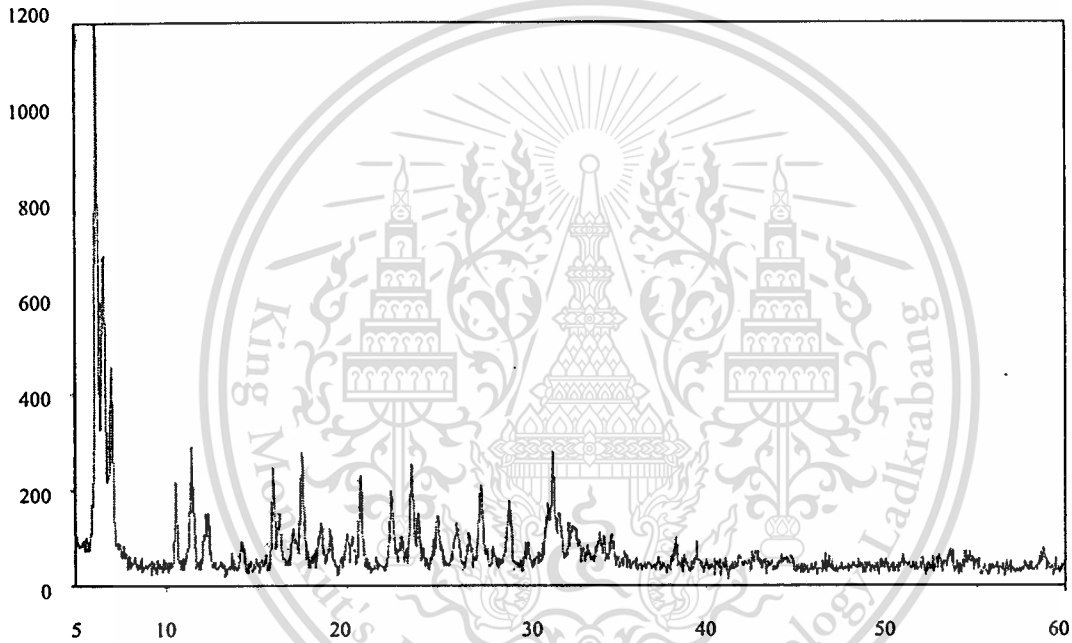

Figure 4.4 The X-ray diffraction pattern of recovery sodium zeolite

4.1.2 Scanning Electron Microscope, SEM

4.1.2.1 Characterization of parent zeolite

From the scanning electron micrograph of zeolites shown in Figure 4.5, it is found that the crystal of synthesized zeolite BEA is spherical with a crystallite size of 0.1 micron. The sample appears to be a well defines crystalline material. While the crystal of synthesized zeolite EMT is hexagonal with a crystallite size of 1 micron. Moreover, it is found that after calcination and modification by cobalt ion loading, the sample appears to be the same.

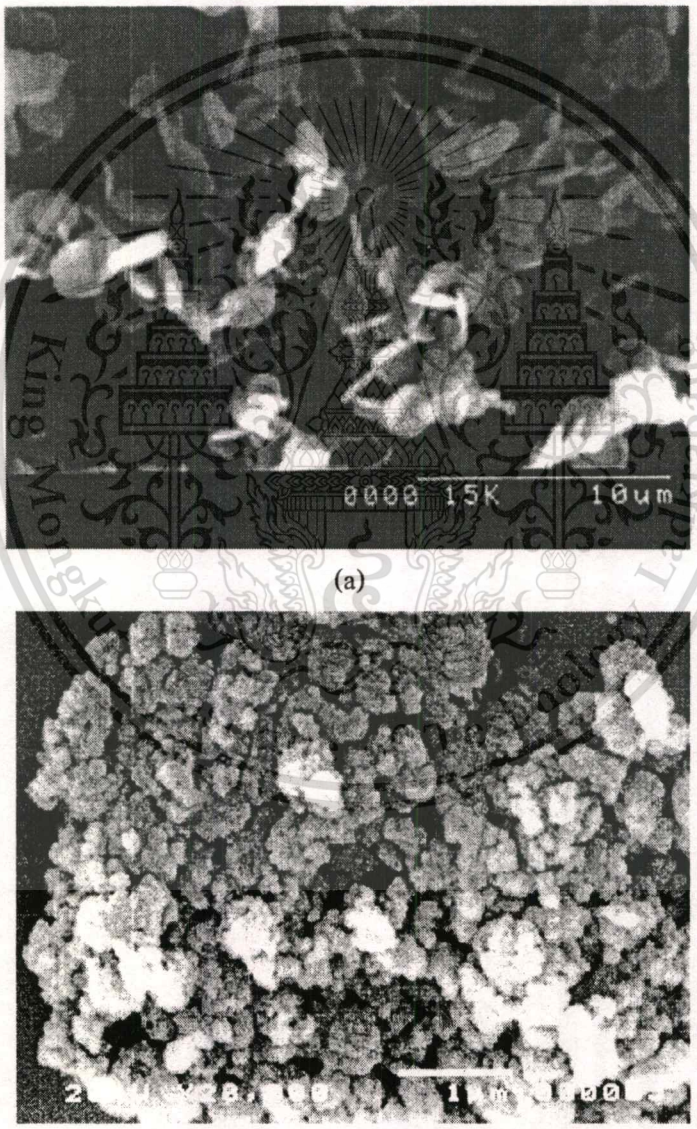

(a)

(b)

Figure 4.5 Electron micrograph of synthesized zeolites (a) EMT and (b) BEA

4.1.2.2 Characterization of encapsulated zeolites

After encapsulation of cobalt phthalocyanine, the zeolites obtained appear in dark blue. From the electron micrograph of the encapsulated zeolites presented in Figure 4.6, needle-like crystals of free cobalt phthalocyanine are also found.

(a) (b)

Figure 4.6 Electron micrographs of zeolites encapsulted cobalt phthalocyanine before solvent extraction of (a) Ion-EMT and (b) Ion-BEA

(a) (b)

Figure 4.7 Electron micrographs of zeolites encapsulted cobalt phthalocyanine after solvent extraction of (a) Ion-EMT and (b) Ion-BEA

After solvent extraction, no needle-like crystal was found with the zeolite crystals as shown in Figure 4.7. There are three steps in solvent extraction procedure. Acetone was used in first step for washing off the excess dicyanobenzene (DCB). Then, pyridine was used for washing

the complex formed at the external surface of zeolites and finally, acetone was used again for rinsing pyridine from the modified zeolite. However, the color of the modified zeolites are still dark blue. Hence, all the remaining phthalocyanine complex should be located in the intra-crystalline voids of the zeolites. Similarly, the same result could be obtained in the case of loading cobalt by impregnation.

4.1.3 Elemental analysis

The silicon and aluminium content in the zeolites were determined by the method mentioned earlier in the section 3.3.3.4 and 3.3.3.5. The silica/alumina ratio of the synthesized zeollite BEA and EMT are presented in Table 4.1. It is found that the silica/alumina ratio of both synthesized zeolite is close to the silica/alumina ratio calculated from the gel composition of zeolite BEA and zeolite EMT.

Table 4.1 Silica alumina ratio of synthesized zeolite.

Zeolite	Observed Si / Al	Si / Al calculated from gel composition
EMT	4.7	4.5
BEA	4.9	5.0

After cobalt (II) ion was loaded into zeolite BEA and EMT, the color of zeolite appear to be pink. However, in the case of loading by impregnation, the color of modified zeolite appears to be relatively darker. These indicate the presence of cobalt ion in the cavities of zeolite. The cobalt content obtained from Atomic Absorption Spectrophotometer (AA) is presented in Figure 4.8.

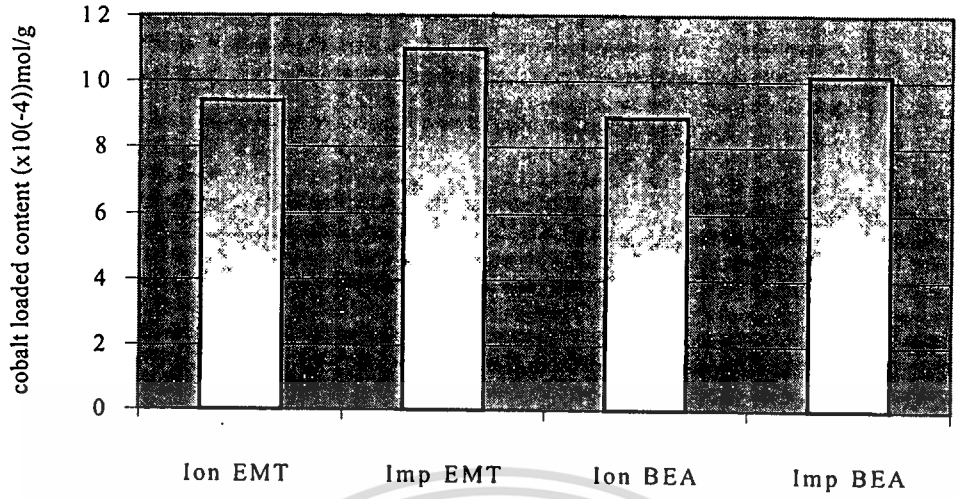

Figure 4.8 Cobalt loaded content in the cavities of catalysts (10^{-4}mol/gram of zeolite)

According to Figure 4.8, higher cobalt content is found in zeolite EMT. It is resulted from the relatively lower silica/alumina ratio of zeolite EMT. Therefore, there are a higher number of sodium ions acting as charge balancing cation, as compared to those in zeolite BEA. Accordingly, more cobalt (II) ions can replace the parent sodium ions. In addition, from Figure 4.8, it is found that loading cobalt by impregnation give more cobalt content than loading by ion exchange.

4.1.4 Fourier Transform Infrared Spectroscopy (FTIR)

After removal of phthalocyanine complexes from the external surface of the zeolite crystallites by solvent extraction, the zeolites encapsulated phthalocyanine complexes were characterized by Fourier Transformed Infrared Spectroscopy and the infrared spectra were revealed in Figure 4.9. For comparison, the spectrum of free cobalt phthalocyanine complex (CoPc) is also included. It is obvious that the major absorption bands of cobalt phthalocyanine coincide with the spectra of zeolite encapsulated phthalocyanine complex. The major absorption bands of all samples are presented in appendix C. The band at ca. 1525 cm^{-1} can be assigned to C-C stretching vibrations associated with phenyl rings and the band around 1469 cm^{-1} is attributed to C-N stretching. In the case of hydrogen phthalocyanine (H_2Pc), it is suggested that the C-C stretching of its phenyl rings and C-N stretching take place at the lower wavelength. This is resulted from the electron withdrawal of hydrogen from C-C bond which causes the shortening of

the C-C bond length. Hence the absorption band of C-C and C-N stretching of H_2Pc appear at higher frequency.

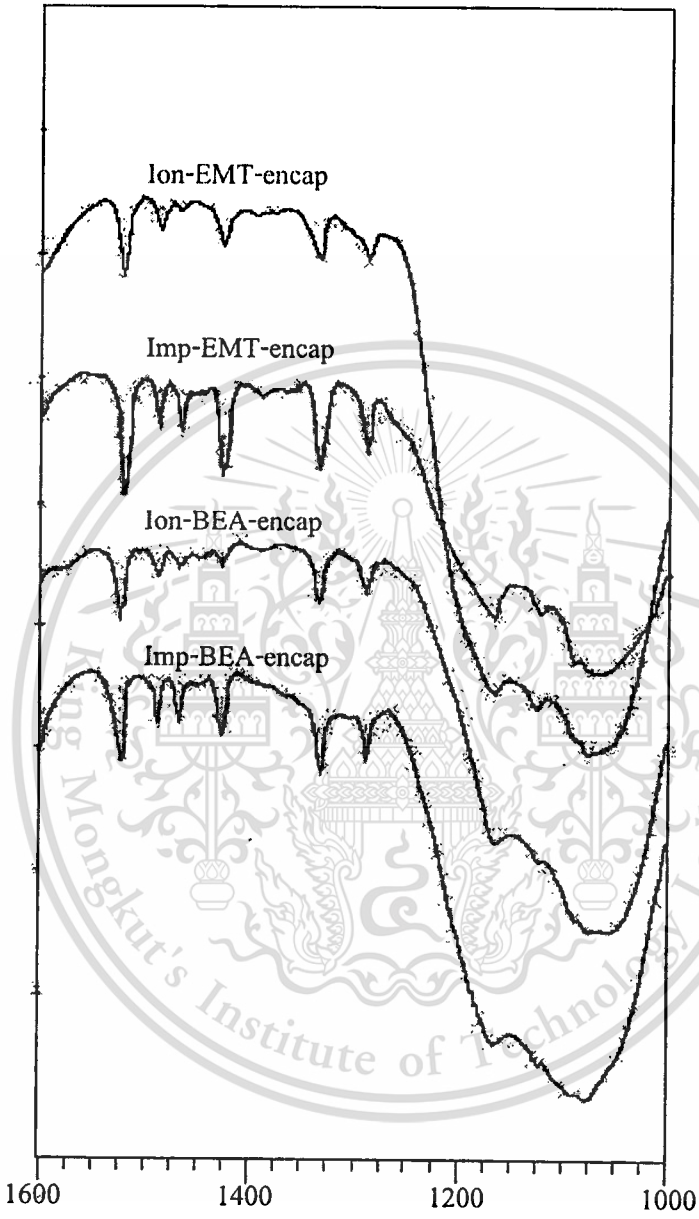

Figure 4.9 Infrared absorption band of synthesized catalyst

4.1.5 UV-Visible Spectroscopy (UV-Vis)

The zeolites without complexes on the external surface were digested by sulfuric acid and it was grinned. The greenish dark blue acid solution was characterized by UV-Visible Spectroscopy. The absorption bands of the extracted zeolites encapsulated cobalt phthalocyanine complex are shown in Figure 4.10 and appendix D. It is found that the encapsulated cobalt phthalocyanine complexes absorb at the wavelength of 690 and 780 and it is obvious that the major absorption bands of free cobalt phthalocyanine coincide with that of the encapsulated metal phthalocyanine complex [13]. From this result, it is again confirmed that there are cobalt phthalocyanine complexes in the cavities of zeolite.

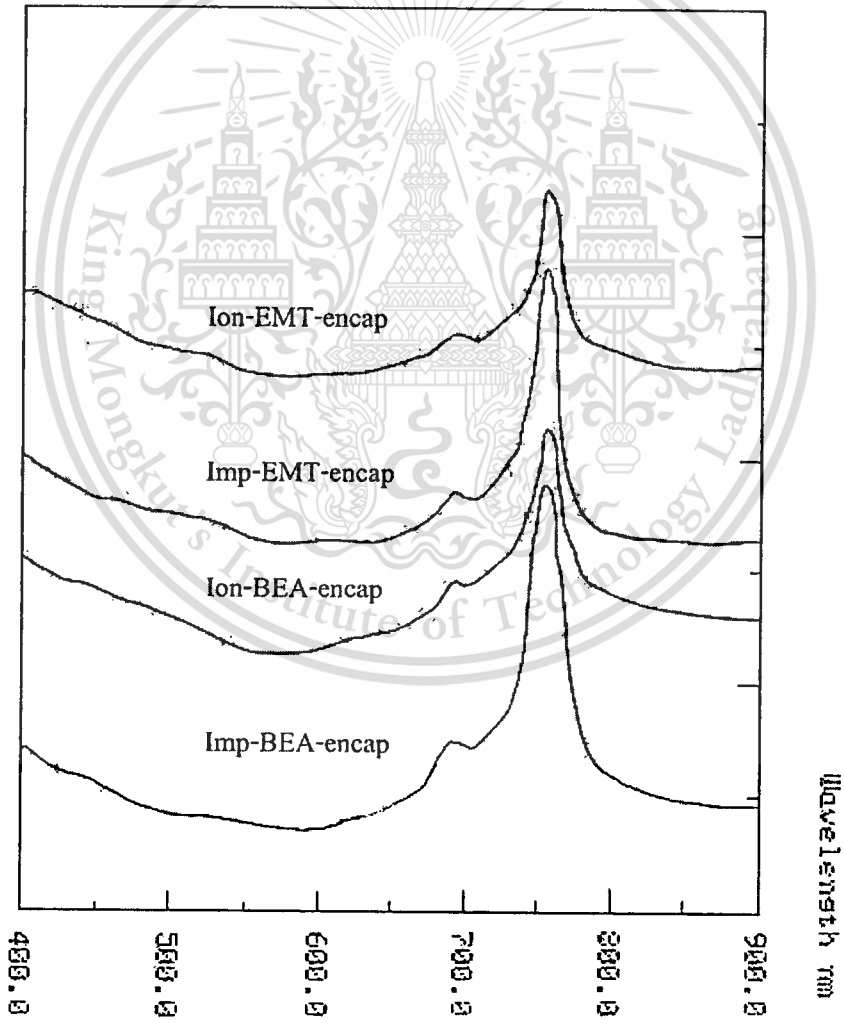

Figure 4.10 UV-Visible absorption band of encapsulated cobalt phthalocyanine

4.1.6 Thermogravimetric Analyzer, (TGA)

The zeolites encapsulated phthalocyanine complex after washing off the external on the surface were analyzed by Thermogravimetric Analyzer. The temperature range of 50–800 °C and heating rate of 10 °C/min were used for the measurement. Thermal decomposition pattern and decomposition temperature of cobalt phthalocyanine encapsulated in the cavities of zeolites are presented in Figure 4.11 and 4.12, respectively. It is found that there is one step for the decomposition of encapsulated cobalt phthalocyanine in zeolite EMT at 500-510 °C, which is similar to the decomposition temperature of free cobalt phthalocyanine [13]. In the case of zeolite BEA, there is also one step of the decomposition at ca. 450-460 °C, which is lower than that of free cobalt phthalocyanine. The decomposition of H_2Pc taking place at temperature over 600 °C, was not detected in all of the synthesized catalyst [12].

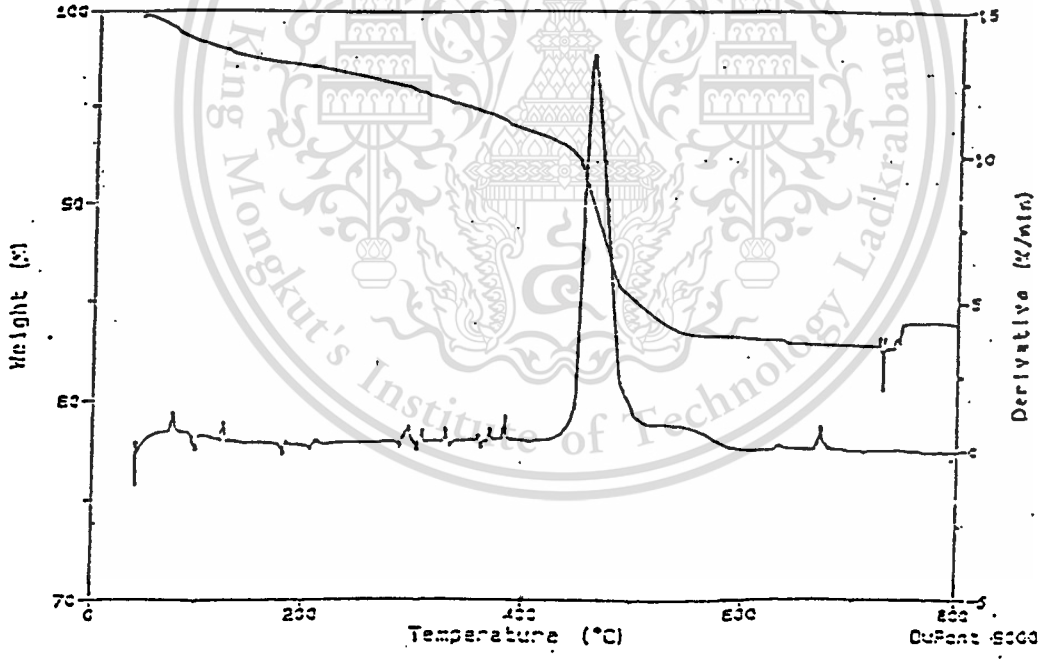

Figure 4.11 Thermal decomposition pattern of the encapsulated cobalt phthalocyanine

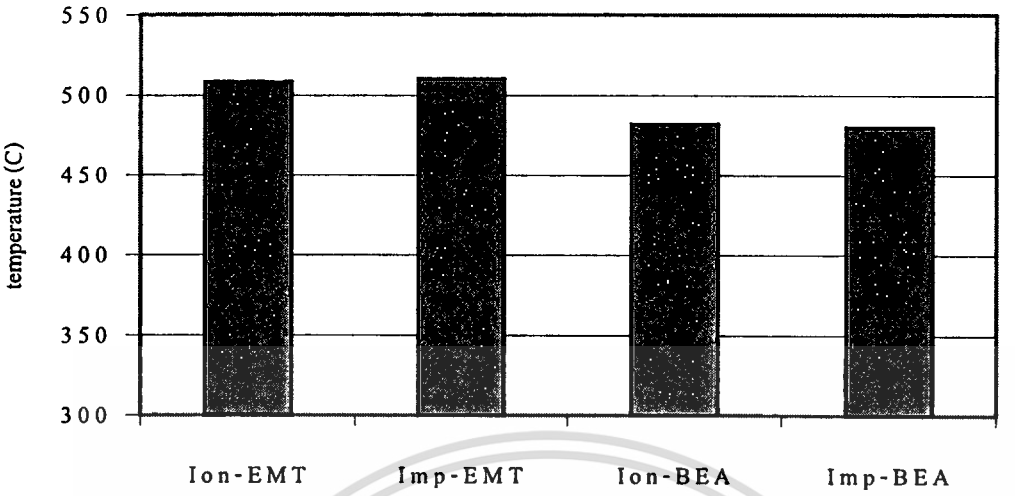

Figure 4.12 Decomposition temperature of the synthesized catalysts

It is suggested that there are cobalt phthalocyanine complexes encapsulated presumably in the hypercage, the 12 angstrom cage, of zeolite EMT. This allows cobalt phthalocyanine, 13 angstrom diameter, to be located with very little strain. Accordingly, this complex is thermally stable in a manner similar to the free cobalt phthalocyanine crystalline. In the case of zeolite BEA, it can be explained that the channel structure of zeolite BEA is about 7 angstrom. Therefore, no complexes with a diameter of 13 angstrom can be formed around here. Accordingly, it is suggested that the cobalt phthalocyanine is likely to be formed in the intersection of the channel, where larger space is available for the complex formation as illustrated below.

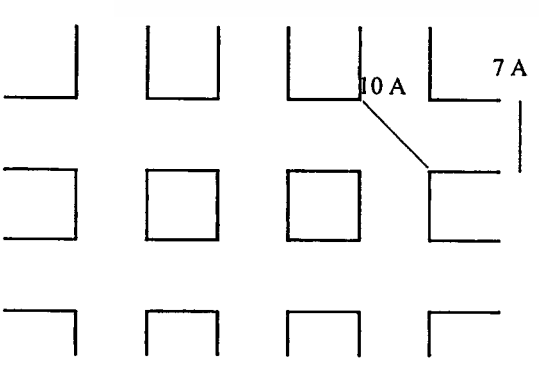

Channel structure of zeolite BEA

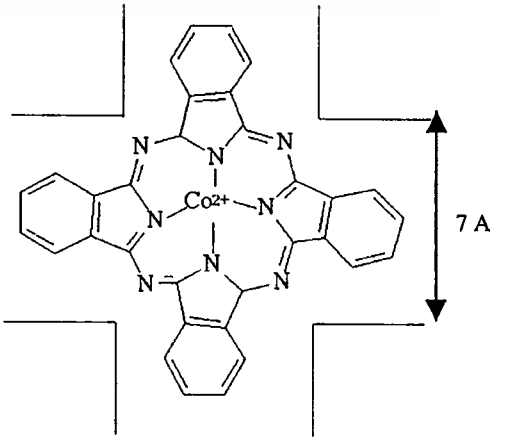

The restricted intersection could make the complex appear to be distorted. If this is the case, the complexes encapsulated in zeolite BEA would be relatively unstable, as compared to that in zeolite EMT. This can result in a lower decomposition temperature of cobalt phthalocyanine encapsulated in zeolite BEA, as compared to that in zeolite EMT and the free cobalt phthalocyanine.

The amount of cobalt phthalocyanine encapsulated in the zeolites can be calculated from the Thermogravimetric Analysis, as shown in Figure 4.13.

Figure 4.13 Amount of cobalt phthalocyanine complex formed in catalysts

It is found that loading of the cobalt ion by impregnation provide higher yields of cobalt phthalocyanine complex encapsulated in the zeolite, as compared to that by ion exchange. This is because relatively more cobalt ions can be obtained from loading by impregnation which is confirmed by Atomic Absorption Spectrophotometry in section 4.1.3. Hence, there is more cobalt phthalocyanine complexes formed in the cavities of zeolite when impregnation is used for cobalt loading. In addition, it is suggested that some of the cobalt ions loaded by impregnation may not act as charge balancing cations. While all the cobalt ions loaded by ion exchange must be presented as charge balancing cation.

Ion exchange

All the cobalt ions loaded must be presented as charge balancing catios

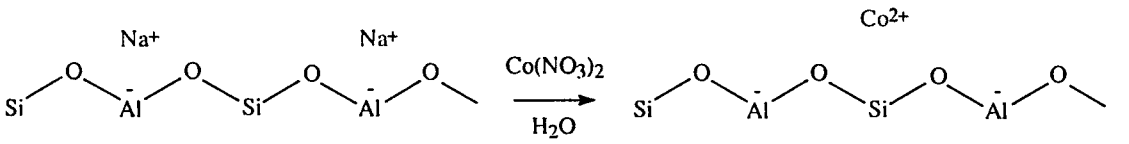

Impregnation

Some of cobalt ions loaded may not act as charge balancing cations

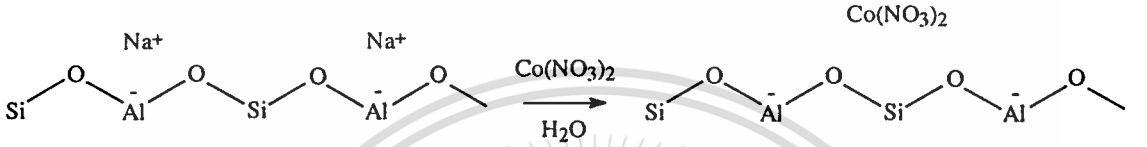

According to this propose, it can be suggested that two forms of the complex should be presence for cobalt loading by impregnation. From the reaction pathway for the formation of phthalocyanine by *Heinrich Zollinger* [33] shown in Figure 4.14, it can be proposed that there are two forms of the cobalt phthalocyanine immobilized in the cavities of zeolite as depicted in Figure 4.15.

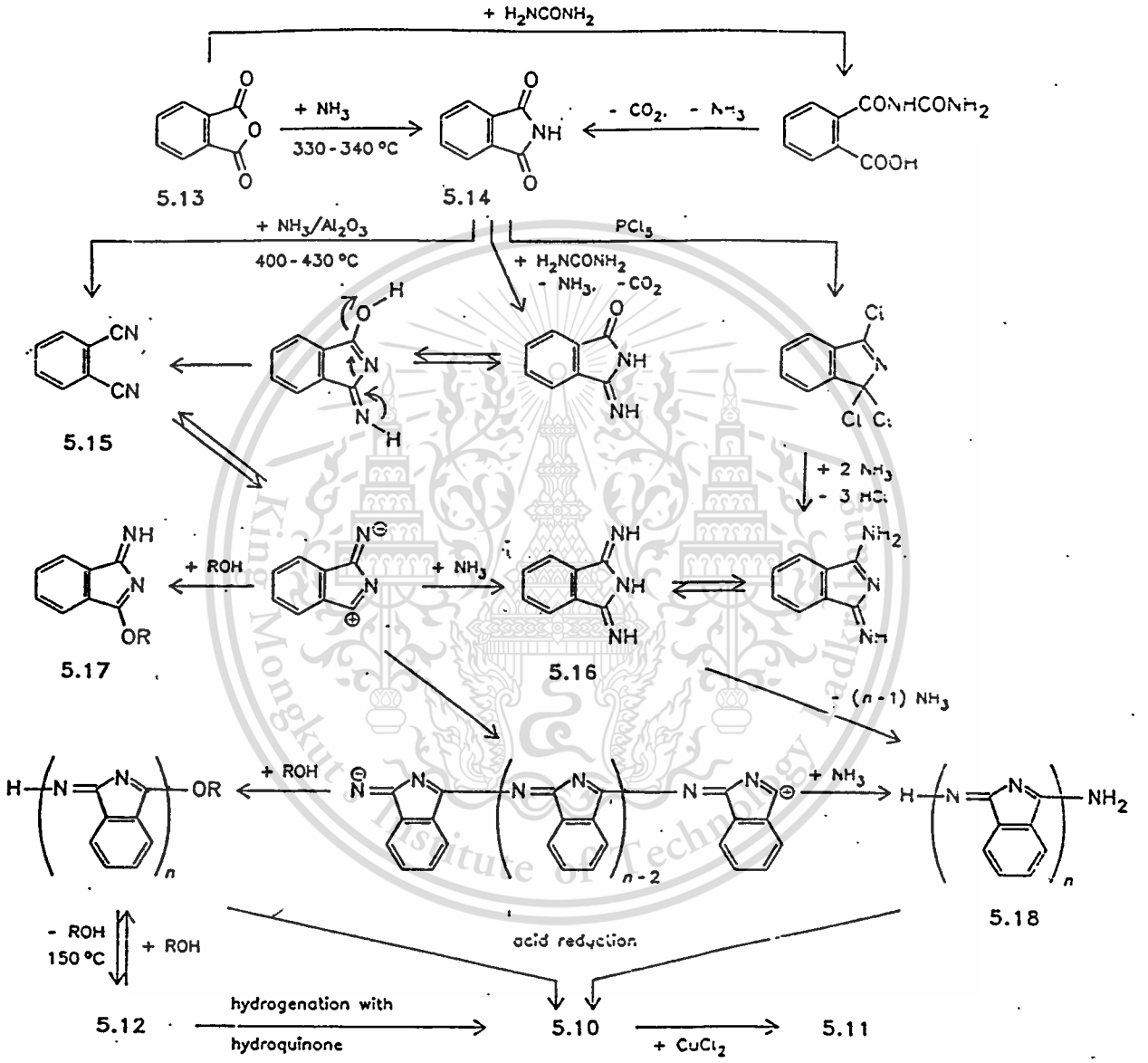

Figure 4.14 Reaction pathway for the formation of phthalocyanine

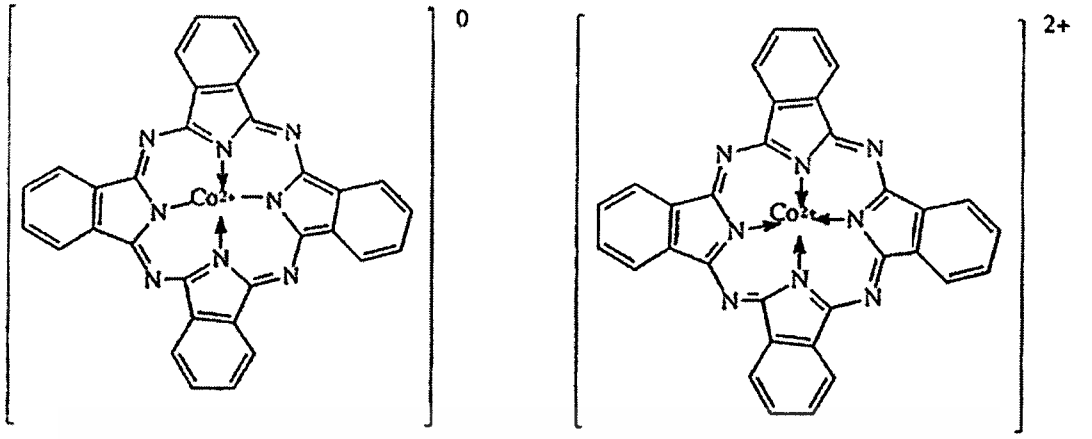

(a) (b)

Figure 4.15 Complex formed in the cavities of zelite; (a) cobalt-hydro-phthalocyanine and (b) cobalt- dehydro-phthalocyanine cation

The complex shown in Figure 4.15 (a) is reacted and can be formed in the presence of a reducing agent. In the case of loading by impregnation, some of cobalt (II) ions can be oxidized to facilitate the formation of cobalt phthalocyanine complex from cobalt nitrate ($Co(NO_3)_2$).

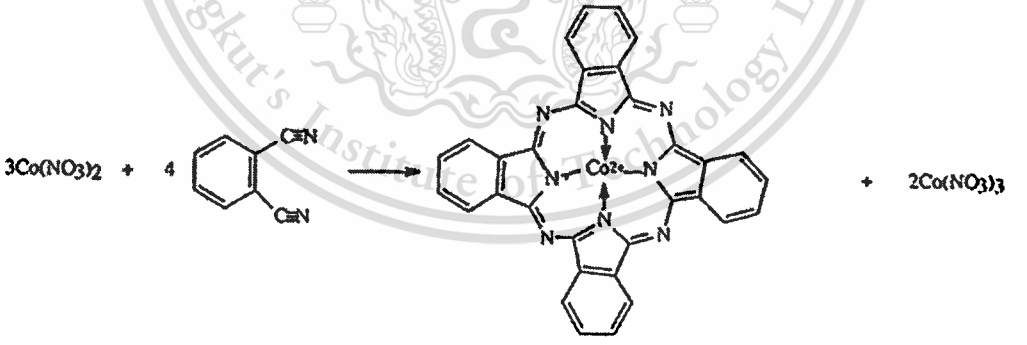

$$Co^{2+} \longrightarrow Co^{3+} + e^-$$

In contrast, the complex shown Figure 4.15 (b) possess a positive charge and can be formed without reducing agent. This is likely to be the case for the complex formation in the cobalt zeolite loading by ion exchange because the cobalt (II) ion would act as charge balancing cations and cannot readily be oxidized. In addition, it is unlikely that cobalt (III) ion can be

presented as a charge balancing cation due to an improper site proximity. Accordingly, cobalt phthalocyanine cation complex (Figure 4.15 (b)) formed in the case of ion exchange would also act as a charge balancing cation as shown below;

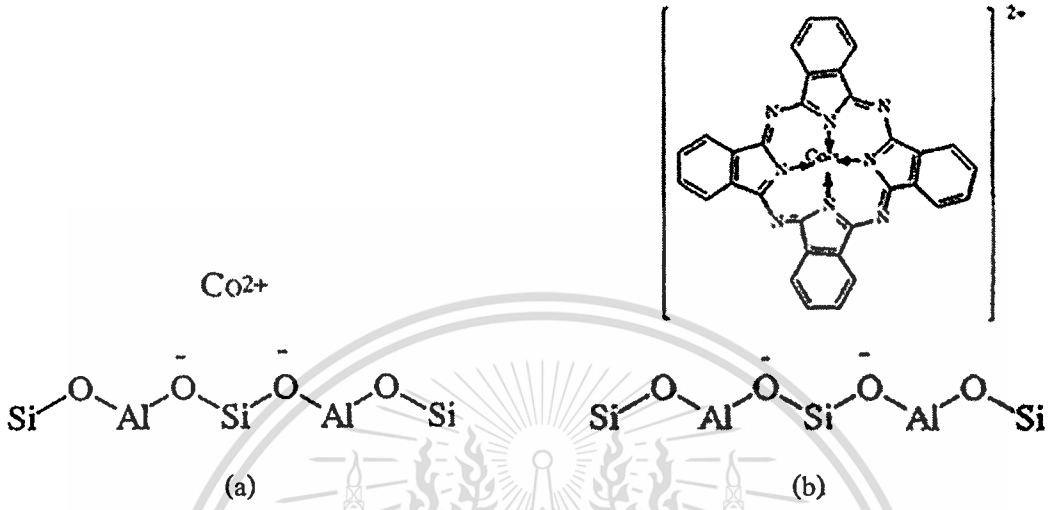

Figure 4.16 Charge balancing cation (a) before complex formation and (b) after complex formation

Furthermore, it is found that there is more cobalt phthalocyanine complexes formed in the cavities of zeolite EMT, as compared to that formed in the cavities of zeolite BEA. This can be explained by the elemental analysis (section 4.1.3), which shows that the silica/alumina ratio of zeolite EMT is 4.7, while that of zeolite BEA is 4.9. The lower silica/alumina ratio provides higher number of sodium ions acting as charge balancing cations in the cavities of zeolite. As a result, more cobalt ion can be exchanged with the parent sodium ion. In addition, more sodium ion in zeolite EMT also provide higher electrostatic field that can induce more cobalt ion to be in the cavities of zeolite EMT when impregnation is used for cobalt loading. Accordingly, it can be explained that since there are more cobalt ion loaded in the cavities of zeolite EMT, more cobalt phthalocyanine complex can be formed in zeolite EMT. This explanation could be confirmed by the result from the characterization of cobalt loaded in zeolite by Atomic Absorption Spectrophotometer in the elemental analysis (Figure 4.8).

4.1.7 Surface Analysis

Parent zeolites, zeolite loaded cobalt (II) ion and zeolites encapsulated cobalt phthalocyanine complex were analyzed by Gas Absorption (Autosorb). The BET specific surface area of the synthesized zeolites are presented in Table. 4.2, and the BET specific surface area of the zeolite loaded cobalt (II) ion and the zeolite encapsulated cobalt phthalocyanine complex are shown in Figure 4.17

Table 4.2 BET surface area of synthesized zeolite

Zeolite	BET surface area (m^2/g)
Synthesized EMT	821.6
Synthesized BEA	782.5

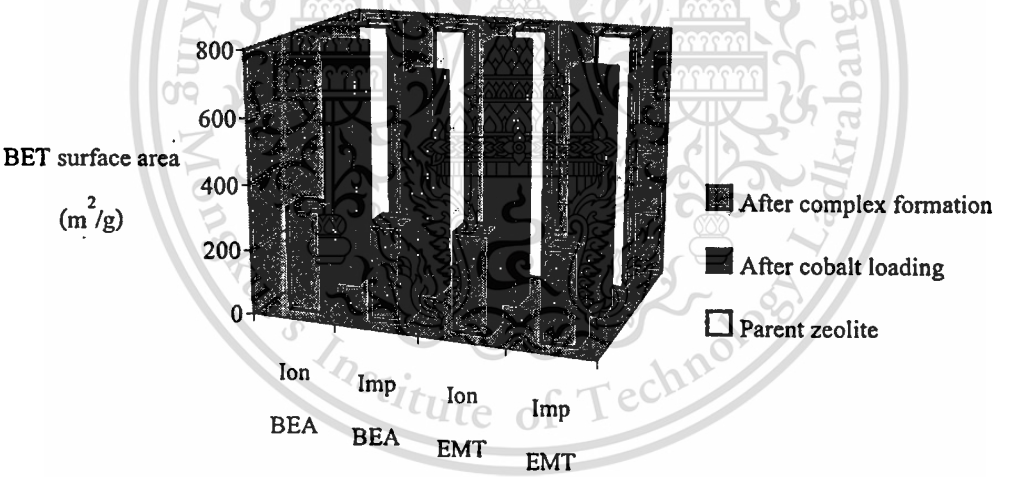

Figure 4.17 BET surface of zeolites in each step of catalyst preparation

There appears to be no difference in the specific surface area of the parent zeolite (Na-EMT and Na-BEA) and zeolite loaded cobalt (II) ion by ion exchange (Ion-EMT and Ion-BEA). As no significant reduction in the volume of nitrogen (N_2) adsorbed, the large internal pore volume is still accessible to nitrogen. While, the specific surface area of the zeolite loaded cobalt ion by impregnation (Imp-EMT and Imp-BEA) is decreased, as compared to the parent zeolite

(Na-EMT and Na-BEA). These support the result from the determination of the cobalt (II) ion loading in the zeolite, that there is addition cobalt (II) species formed by loading cobalt (II) ion by impregnation. These species may well encage in the pore of the zeolites. Hence, lesser surface area is obtained when impregnation is used for incorporating cobalt ions into the zeolite cavities. In the same manner, the surface area of zeolite encapsulated cobalt phthalocyanine complex (Ion-EMT-encap, Imp-EMT-encap, Ion-BEA-encap and Imp-BEA-encap) decrease obviously. These results provide direct evidences for the presence of cobalt phthalocyanine inside the zeolite cavities.

From all the result in this characterization section, it can be concluded that cobalt phthalocyanine is indeed immobilized in the cavities of zeolite BEA and zeolite EMT. It was found that relatively more complexes were formed in the cavities of zeolite EMT. Although, there is no solid evidence for the exact location of cobalt phthalocyanine in the zeolite cavities, it is suggested that in this study, that in the case of zeolite EMT, the complexes is likely to immobilize in the hypercage, while the complexes seem to be encapsulated in the intersection void in the case of zeolite BEA. As a result, the complexes formed may well be distorted. This leads to the difference in their stability and possibly to the catalytic activity, which will be intensively discussed in the next section.

4.2 Catalytic testing

4.2.1 Oxidation of ethylbenzene

4.2.1.1 Effect of host material

Catalytic activity

In this research, cobalt phthalocyanine was encapsulated in two types of host material such as zeolite BEA and zeolite EMT. To study the effect of the host material, the synthesized catalyst, Ion-BEA-encap and Ion-EMT-encap, are used as catalysts in the liquid phase oxidation of ethylbenzene in the batch reactor under the continuous flow of oxygen, 40 ml/min, at the reflux temperature (around 138 °C) with a continuous stirring. The conversion of ethylbenzene is depicted in Figure 4.18.

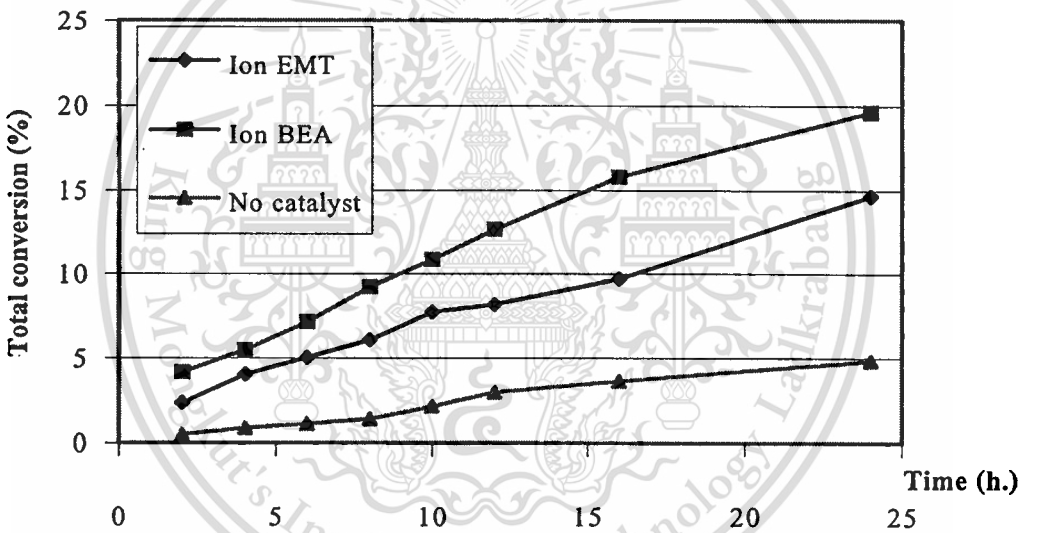

Figure 4.18 Result of oxidation of ethylbenzene using Ion-EMT-CoPc and Ion-BEA-encap as catalyst; *ethylbenzene 45 g, catalyst weight = 0.15 g, reaction time = 24 hr. temperature = 138 °C, oxygen flow rate 40 ml/min*

It is found that cobalt phthalocyanine complex encapsulated in zeolite EMT and BEA are able to catalyze ethylbenzene oxidation under the experimental conditions. It appears that low conversion of ethylbenzene was observed in the reaction without catalyst. It is suggested that this is the result of cobalt phthalocyanine encapsulated in the cavities of zeolite. Generally, it has been known that metal-phthalocyanine behaves mechanically like cytochrome P-450 [6] which is a well-known oxygenation enzyme in many kinds of living organisms. In addition, it can promote

the oxidation of alkane. The oxidation by cytochrome P-450 was suggested to proceed via two steps. The first is activating the molecular oxygen by iron porphyrin to generate the oxo-iron porphyrin. The latter is the oxygen transfer to the substrate as shown below.

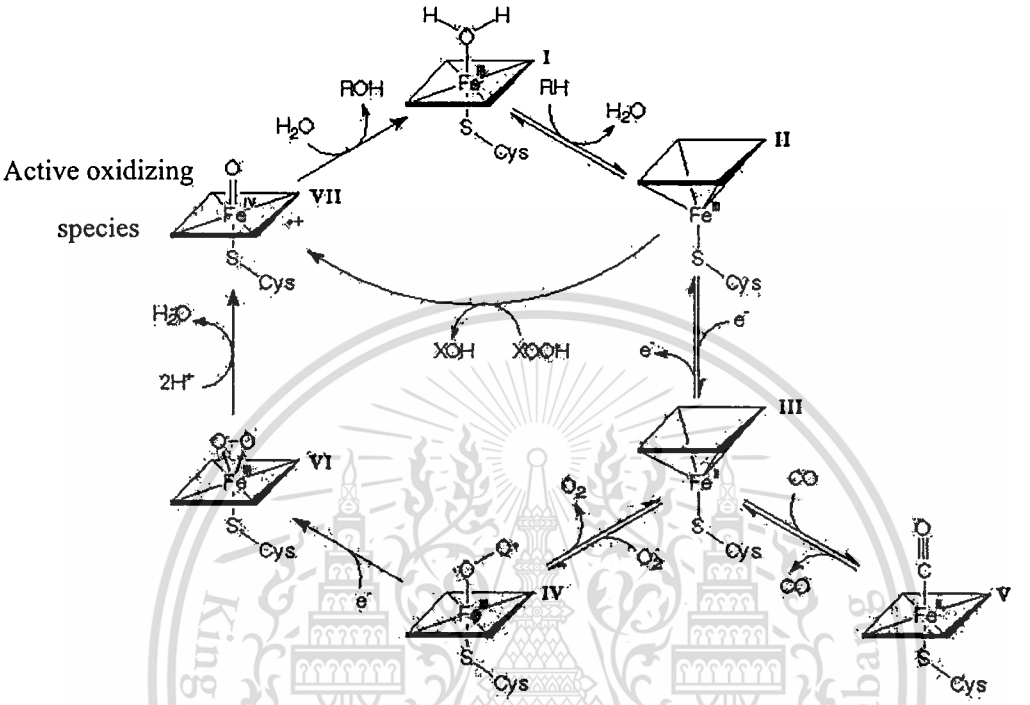

From the mechanism illustrated above, it is also shown that the active oxidizing species of cytochrome P-450 can be generated directly from other oxygen atom donor, peroxide compound [6]. In the same way, it can be proposed that metal phthalocyanine immobilized in the cavities of zeolite would dissociate the molecular oxygen and acts as an oxygen atom carrier. This then transfers the oxygen atom to the hydrocarbon substrate. The model of proposed mechanism is shown below.

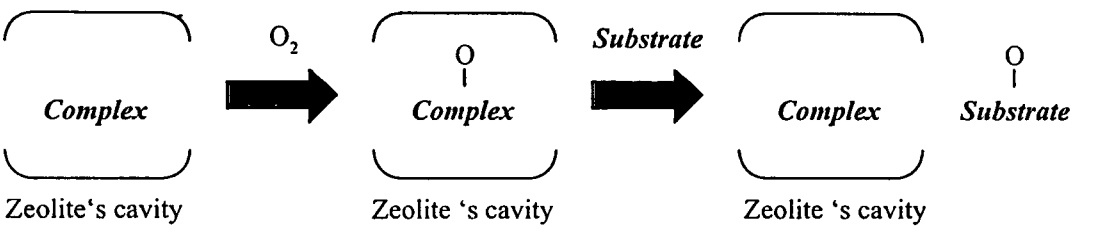

From the above model, the proposed mechanism could be explained clearly that the reaction pathway for the oxidation of ethylbenzene using zeolite encapsulated cobalt phthalocyanine involves 3 major steps [38]. Firstly, the active species called metal-oxo species [38] were formed from the complexation of oxygen with the cobalt phthalocyanine encapsulated in the cavities of zeolite. This leads to the formation of a high-valent metal-oxo species (1) located in the cavities of zeolite as shown below. This species is highly reactive and is responsible for the oxidation of hydrocarbons to alcohols and ketones.

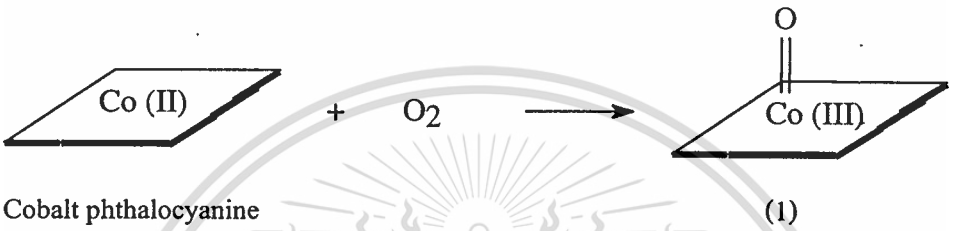

Cobalt phthalocyanine (1)

In the second step, substrate would react with the active species (1) forming an intermediate complex (2). Finally, the corresponding products, ketone and alcohol are formed by the decomposition of the intermediate species (2). It is proposed that the decomposition step of the intermediate species proceed via free radical mechanism [38].

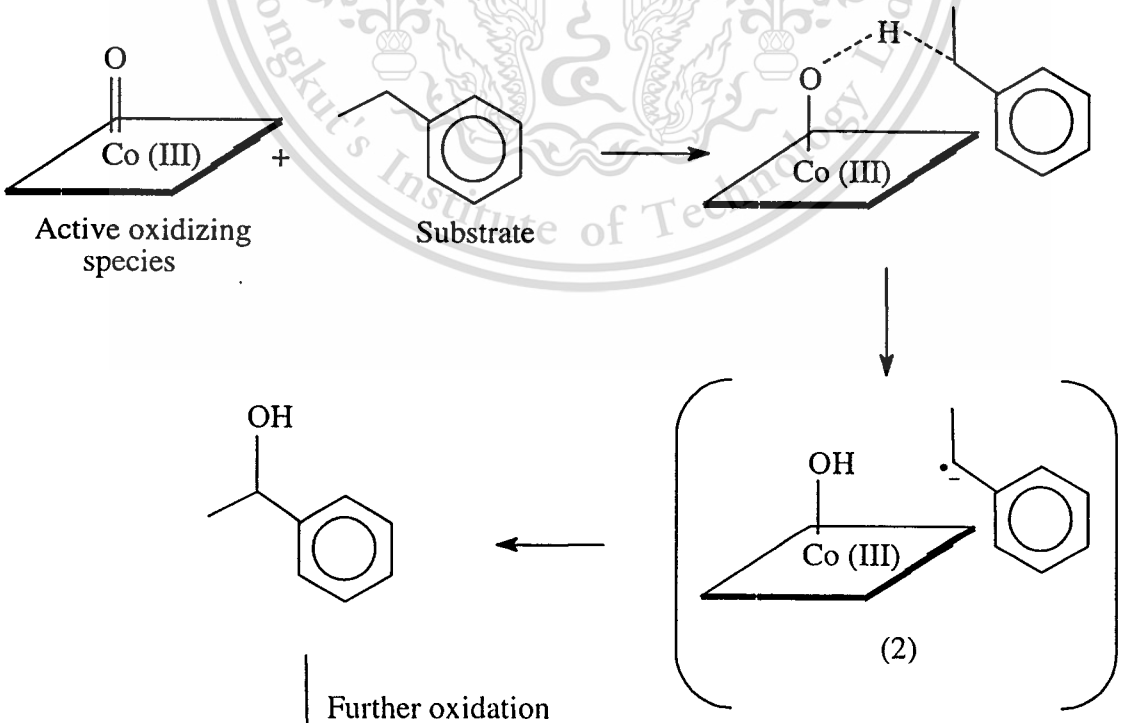

Since the mechanism for catalytic oxidation by cobalt phthalocyanine proceed via the oxidative addition of oxygen onto cobalt phthalocyanine complex, it seems that the complexation of oxygen with the metal phthalocyanine is essential for the generation of active oxidizing species. Consequently, in the reaction without catalyst, the dissociation of molecular oxygen cannot be facilitated. Only the homogeneous oxidation can take place. Therefore, small amounts of product can be observed in the reaction without catalyst.

As seen from Figure 4.18, it is also found that a higher conversion could be observed when Ion-BEA-encap was used as a catalyst. This indicates that Ion-BEA-encap is more active than Ion-EMT-encap. This is because cobalt phthalocyanine complexes encapsulated in zeolite BEA is likely to be formed in the more restricted intersection of the channel (shown below), as suggested earlier in section 4.1.6.

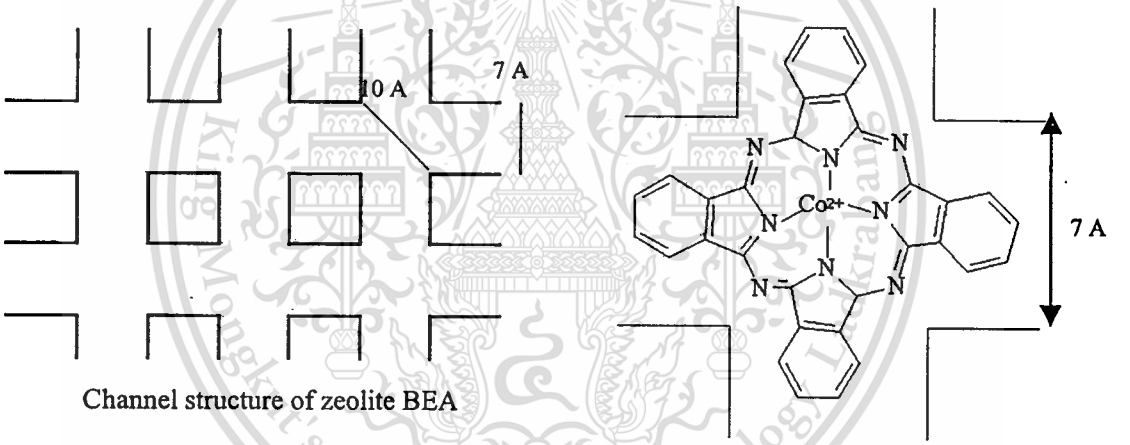

Channel structure of zeolite BEA

This result in higher strain configuration of cobalt phthalocyanine complex encapsulated in zeolite BEA. Under such strain configuration, delocalization of π-electron in the kelated ligand would be perturbed leading a higher degree of coordinative unsaturation of cobalt active site. This would enhance an addition complexation with other ligand. In the other words, the complex would be more active for lewis base ligand association and, even oxidative addition. Therefore, cobalt phthalocyanine complex encapsulated in the intersection of zeolite BEA with high degree of coordination unsaturation would possess relatively oxygen affinity than that in zeolite EMT. Hence, the active oxidizing species would be readily formed in the case of cobalt phthalocyanine complex encapsulated in zeolite BEA causing higher catalytic activity, as obtained in Figure 4.18.

Selectivity

It was found that the oxidation of ethylbenzene give only 1-phenylethanol and acetophenone as products. No CO, CO_2 and the other high molecular weight products could be detected. The selectivity of acetophenone in the oxidation of ethylbenxene over Ion-BEA-encap and Ion-EMT-encap is shown in Figure 4.19.

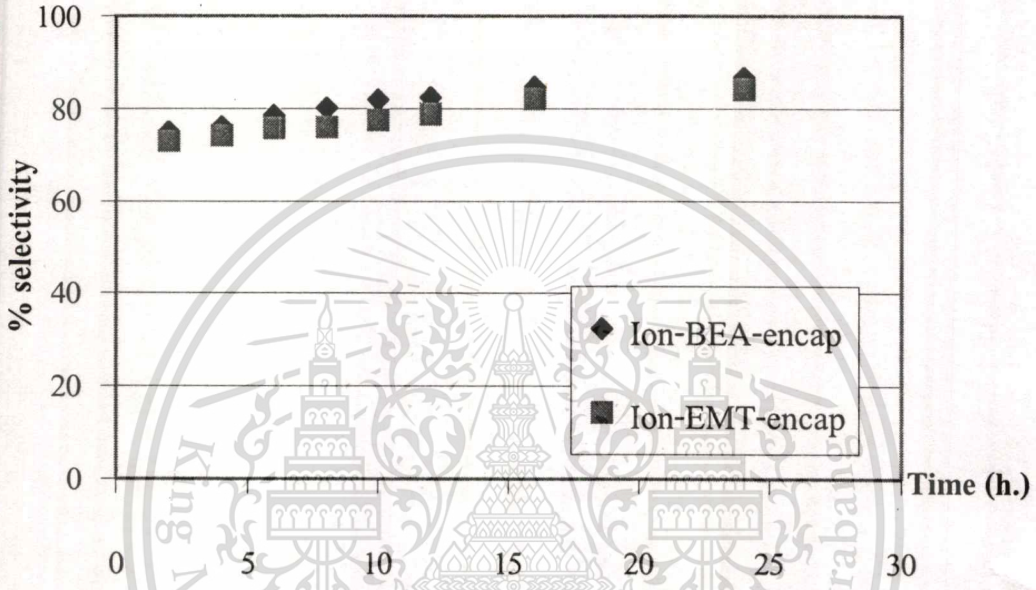

Figure 4.19 Percent selectivity of acetophenone from the oxidation of ethylbenzene using Ion-BEA-encap and Ion-EMT-encap as a catalyst; *ethylbenzene 45 g, catalyst weight = 0.15 g, reaction time = 24 hr. temperature = 138 °C, oxygen flow rate 40 ml/min*

It can be seen from Figure 4.19 that slightly higher selectivity of acetophenone was observed when the reaction time was increased for both reactions. This is because acetophenone are produced as a secondary product in a series reaction. It is suggested that ethylbenzene was primary oxidized over metal complexes to 1-phenylethanol, which is then further oxidized to acetophenone. As increasing the reaction time, a large amount of acetophenone is subsequently produced. The pathway for this series reaction is illustrated below.

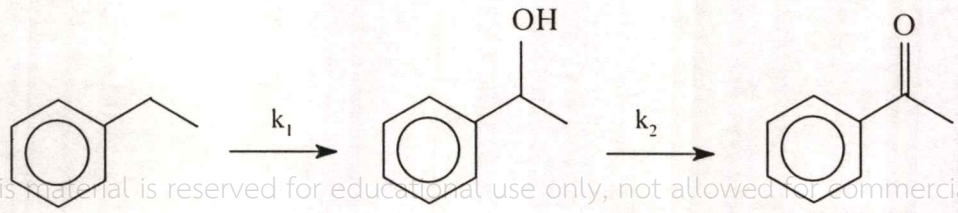

It was also found that a higher selectivity of acetophenone was observed when Ion-BEA-encap was used as a catalyst. This is because of the advantage in structure of zeolite BEA, as compared to that of zeolite EMT. Since, zeolite BEA is a channel structure zeolite, while zeolite EMT possess a cage structure. A relatively more open framework structure can be seen in zeolite BEA, as shown in Figure 4.20.

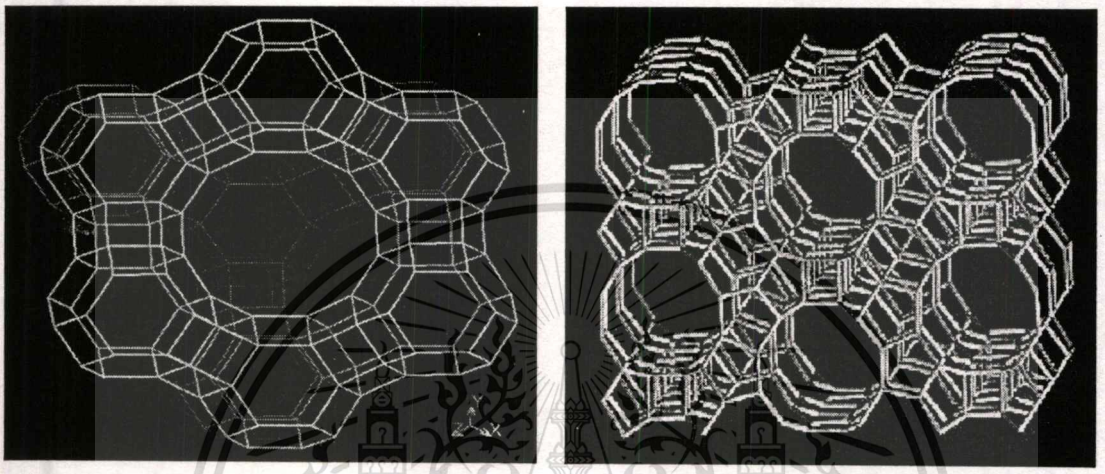

(a) (b)

Figure 4.20 Structure of zeolite (a) EMT and (B) BEA

This feature could result in a better accessibility of encapsulated complexes for reactant molecule. Hence, at a certain period time, more reactant molecules can reach to the active site in the cavities of zeolite BEA. Moreover, according to the better accessibility of zeolite BEA, the product form the oxidation of ethylbenzene can diffuse out of the cavities zeolite easily. These result in higher selectivity of acetophenone can be observed when the used catalyst is Ion-BEA-encap. The higher selectivity of acetophenone observed when Ion-BEA-encap was used as a catalyst also indicates that the rate of oxidation of 1-phenylethanol (k_2) over Ion-BEA-encap is relatively faster than that over Ion-EMT-encap.

4.2.1.2 Effect of reaction time

The effect of reaction time was further investigated at a resident time higher than 24 hours, as depicted in Figure 4.21.

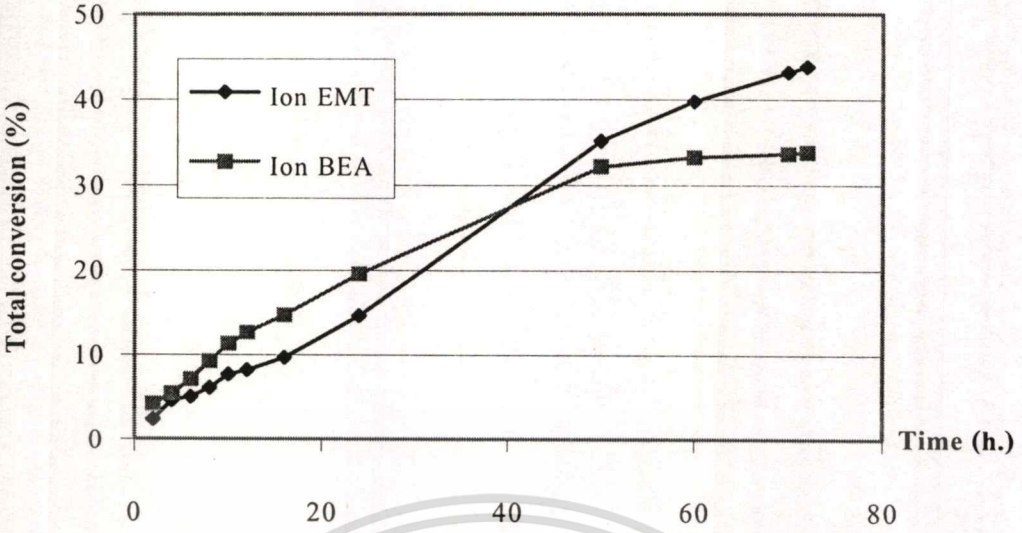

Figure 4.21 Result of oxidation of ethylbenzene using Ion-EMT-encap and Ion-BEA-encap as catalyst; *ethylbenzene 45 g, catalyst weight = 0.15 g, reaction time = 72 hr. temperature = 138 °C, oxygen flow rate 40 ml/min*

It can be seen that although, the conversion of ethylbenzene increase with time for both reaction, lower extent conversion of ethylbenzene increased was observed in the case of using Ion-BEA-encap as a catalyst when the reaction time is higher than 50 hours. Moreover, the reaction using Ion-BEA-encap give a lower conversion of ethylbenzene than that using Ion-EMT-encap at high resident time. It can be described that the deactivation of catalyst may well occur due to partial oxidative destruction of cobalt phthalocyanine encapsulated particular in zeolite BEA. Since it was found that cobalt phthalocyanine encapsulated in the cavities of zeolite BEA appeared to be relatively unstable due to the distort conformation. The oxidation of cobalt phthalocyanine may well take place on long exposures of oxygen stream at high temperature. However, this appears not to be the case of Ion-EMT-encap. As described in section 4.1.6, in zeolite EMT, the cobalt phthalocyanine is loaded in the non-restrict environment. Consequently, the cobalt phthalocyanine encapsulated in zeolite EMT is relatively more stable, as compared to that in zeolite BEA. To prove this suggestion, both of synthesized catalyst, Ion-EMT-encap and Ion-BEA-encap, was regenerated by washing with acetone and drying at 100 °C in a vacuum oven. It was then reused as a catalyst in the ethylbenzene oxidation under the same experimental conditions. The ethylbenzene conversion obtained from regenerated catalysts is shown in Figure. 4.22.

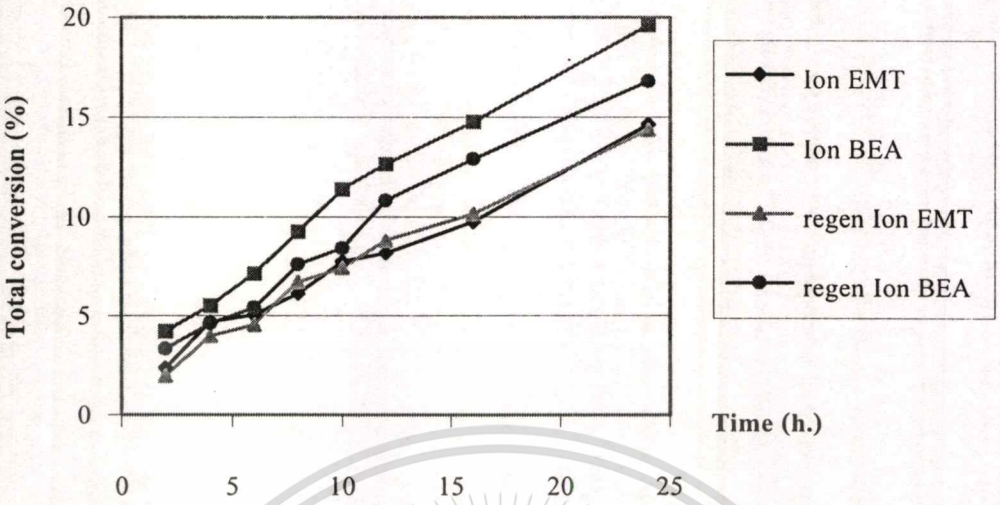

Figure 4.22 Result of oxidation of ethylbenzene using Ion-EMT-CoPc, Ion-BEA-encap, regenerated Ion-EMT-CoPc and regenerated Ion-BEA-encap as catalyst; *ethylbenzene 45 g, catalyst weight = 0.15 g, reaction time = 24 hr. temperature = 138 °C, oxygen flow rate 40 ml/min*

It can be clearly seen that a similar activity of the fresh counterpart is observed for the regenerated Ion-EMT-encap. While a lower activity was obtained when the Ion-BEA-encap was reused. This supports the suggestion that the deactivation of the Ion-BEA-encap occur at higher reaction time while this was not to be in the case for Ion-EMT-encap.

4.2.1.3 Effect of cobalt loading method

In this research, cobalt ion was loaded into the cavities of zeolite by ion exchange and impregnation. To study the effect of cobalt loading method, Ion-EMT-encap, Imp-EMT-encap, Ion-BEA-encap and Imp-BEA-encap are used as catalysts in the liquid phase oxidation of ethylbenzene in the batch reactor under the continuous flow of oxygen, 40 ml/min, at the reflux temperature (around 138 °C) with a continuous stirring. The results of the oxidation over both of host material are shown in Figure 4.23 and 4.24.

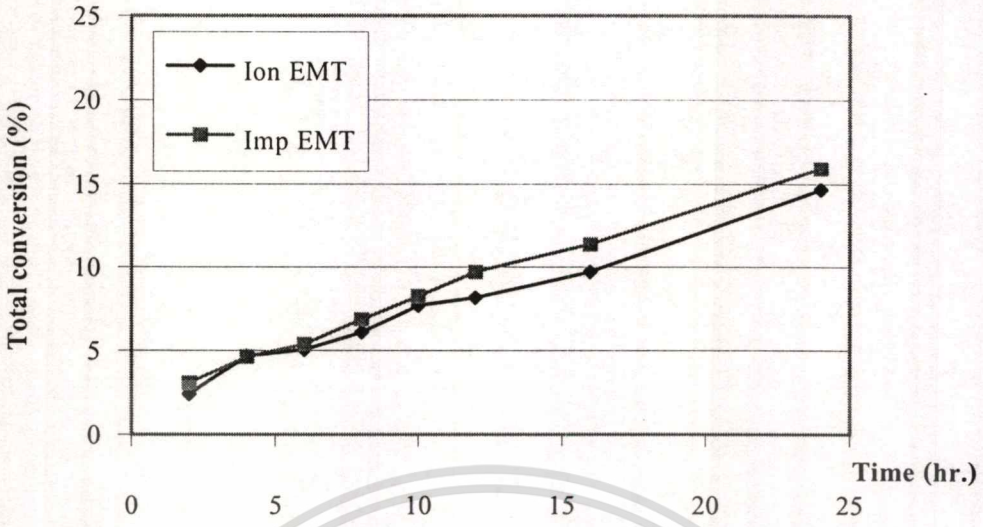

Figure 4.23 Result of oxidation of ethylbenzene using Ion-EMT-CoPc and Imp-EMT-encap as a catalyst; *ethylbenzene 45 g, catalyst weight = 0.15 g, reaction time = 24 hr. temperature = 138 °C, oxygen flow rate 40 ml/min*

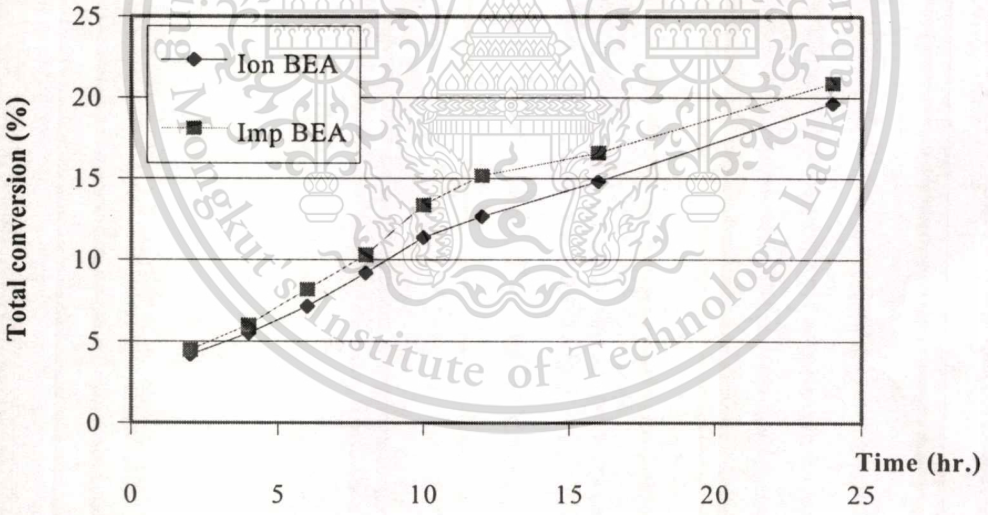

Figure 4.24 Result of oxidation of ethylbenzene using Ion-BEA-CoPc and Imp-BEA-encap as a catalyst; *ethylbenzene 45 g, catalyst weight = 0.15 g, reaction time = 24 hr. temperature = 138 °C, oxygen flow rate 40 ml/min*

A higher conversion of ethylbenzene can be observed when the catalyst is prepared by impregnation. This is because more complexes were formed in the catalyst prepared by impregnation which is evident by Thermogravimetric Analysis (Figure 4.13) that the cobalt

loading by impregnation gives a relatively higher amount of cobalt phthalocyanine in the cavities of zeolite. According to the proposed mechanism, the higher yield of cobalt phthalocyanine encapsulated in the cavities of zeolite would provide a higher number of active species. Consequently, more activity could be obtained when more complexes are formed in the cavities of zeolite. This results in a relatively higher yield of products. However, the reduced activity of Imp-EMT-encap as compared to Ion-EMT-encap was observed when the reaction time exceeds 50 hours. The result of the oxidation of ethylbenzene at the reaction time of 72 hours is shown in Figure 4.25.

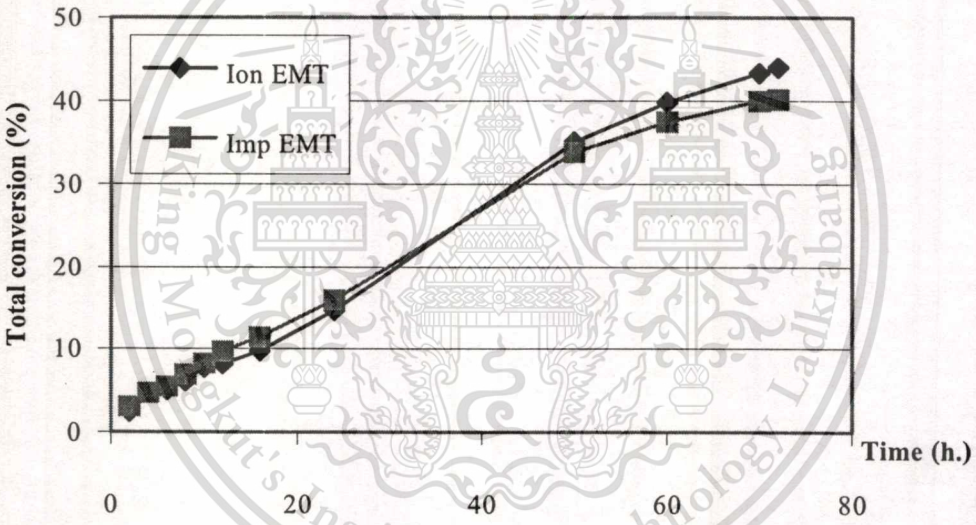

Figure 4.25 Result of oxidation of ethylbenzene using Ion-EMT-CoPc and Imp-EMT-encap as a catalyst; *ethylbenzene 45 g, catalyst weight = 0.15 g, reaction time = 72 hr. temperature = 138 °C, oxygen flow rate 40 ml/min*

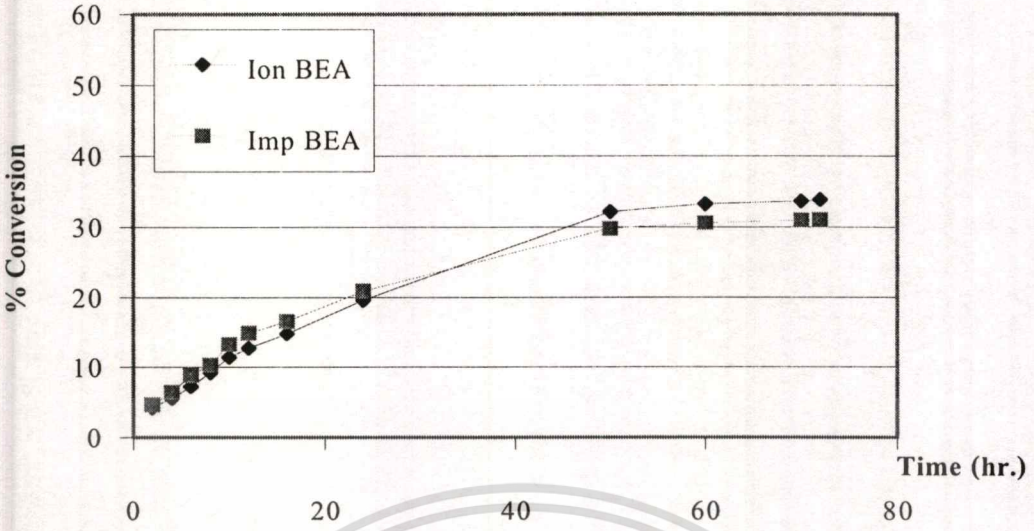

Figure 4.26 Result of oxidation of ethylbenzene using Ion-BEA-CoPc and Imp-BEA-encap as a catalyst; *ethylbenzene 45 g, catalyst weight = 0.15 g, reaction time = 72 hr. temperature = 138 °C, oxygen flow rate 40 ml/min*

This can be tentatively interpreted as a result of the high loading of metal complex in the cavities of zeolite by impregnation. This not only give a high reaction rate but also reduces the internal pore volume as indicated by a diagram in the surface area when the catalyst were prepared by impregnation (Table 4.3)

Table 4.3 The specific area of zeolite encapsulated metal complex prepared by ion exchange and impregnation (m^2/g).

	Zeolite BEA	**Zeolite EMT**
Ion exchange	318.2	302.3
Impregnation	297.9	284.6

As a large amount of products are formed increasingly and accumulated in the cavities of zeolite, the reactants would be gradually restricted in access into the active sites. Consequently, a lower rate of the reaction is observed at long residential time (around 50 hours). While, this is not in the case for catalyst with the lower metal complex loading by ion exchange.

4.2.1.4 Effect of Regenerated Catalyst

The Ion-EMT-encap and Ion-BEA-encap were regenerated by washing with acetone and drying at 100 °C in a vacuum oven. It was then reused as catalyst in ethylbenzene oxidation under the same experimental conditions. The ethylbenzene conversion obtained from regenerated Imp-EMT-encap and Ion-BEA-encap are shown in Figure 4.27 and 4.28, respectively.

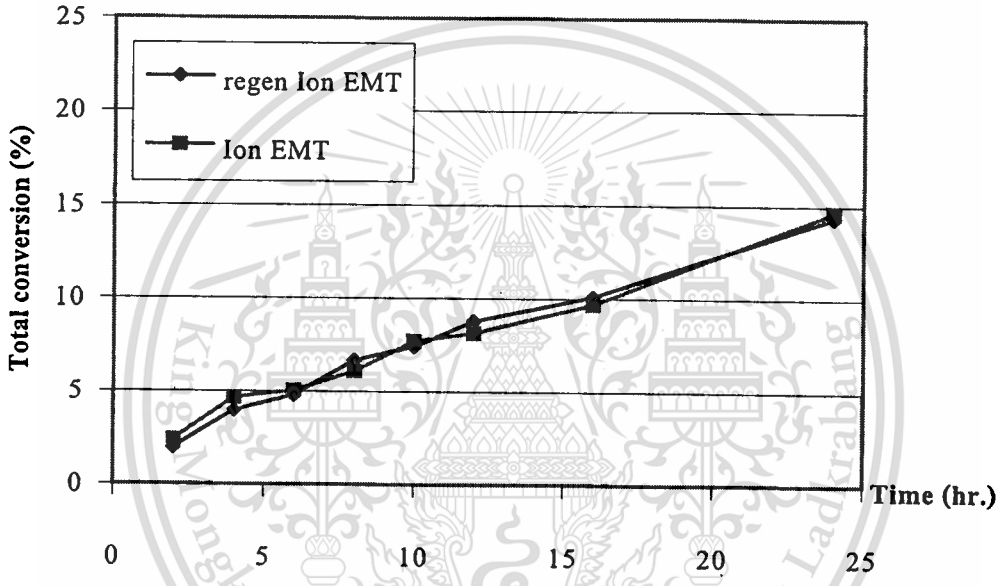

Figure 4.27 Result of oxidation of ethylbenzene using Ion-EMT-encap and regenerated Ion-EMT-encap as a catalyst; *ethylbenzene 45 g, catalyst weight = 0.15 g, reaction time = 24 hr. temperature = 138 °C, oxygen flow rate 40 ml/min*

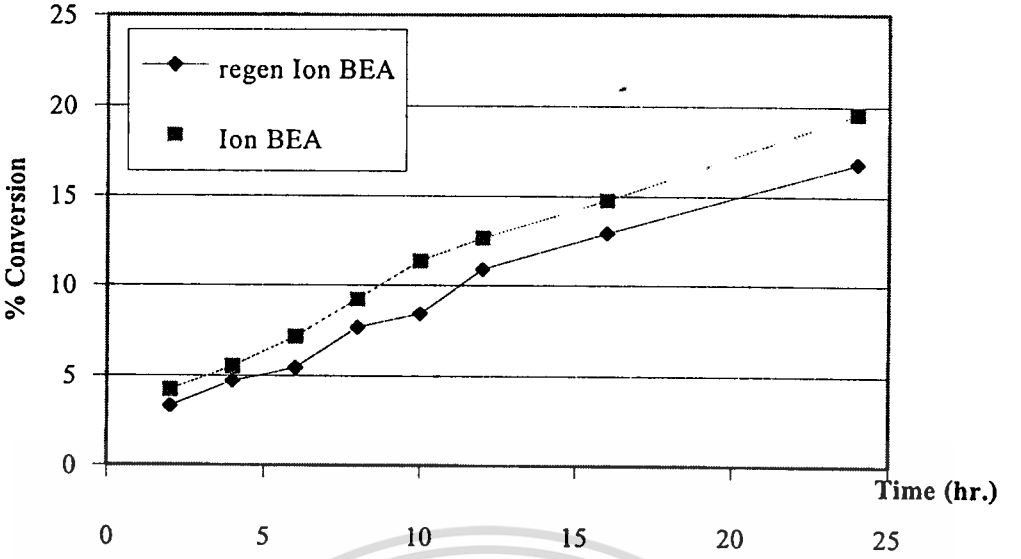

Figure 4.28 Result of oxidation of ethylbenzene using Ion-BEA-encap and regenerated Ion-BEA-encap as a catalyst; *ethylbenzene 45 g, catalyst weight = 0.15 g, reaction time = 24 hr. temperature = 138 °C, oxygen flow rate 40 ml/min*

In the case of using zeolite EMT as host material, the decrease in the activity at long reaction time is not due to the destruction of the complex loaded into the cavities of zeolite EMT because no decrease in activity of the regenerated Ion-EMT-encap can be observed. It is found that the activity is retained. This is also confirmed that the cobalt phthalocyanine encapsulated in the cavities of zeolite was not deactivated and leached out during the reaction. However, deactivation seems to be the case for zeolite BEA. According to the study of host material, it is know that when the zeolite BEA was used as host material, the deactivation of catalyst occurs at higher reaction time (Figure 4.22). Hence, the reduced activity was observed when the regenerated Ion-BEA-encap was reused in the reaction (Figure 4.28). From this result, it can be concluded that the reduced activity of the use of Ion-BEA-encap and Ion-EMT-encap was caused from the reducing in the internal pore volume. However, in the case of Ion-BEA-encap, the reduced activity of catalyst also cause from the deactivation of catalyst occur at higher reaction.

4.2.1.5 Effect of oxygen gas flow rate

The conversion of the reaction using Ion-EMT-encap and oxygen gas flow rate of 20, 40 and 80 ml/min is shown in Figure 4.29.

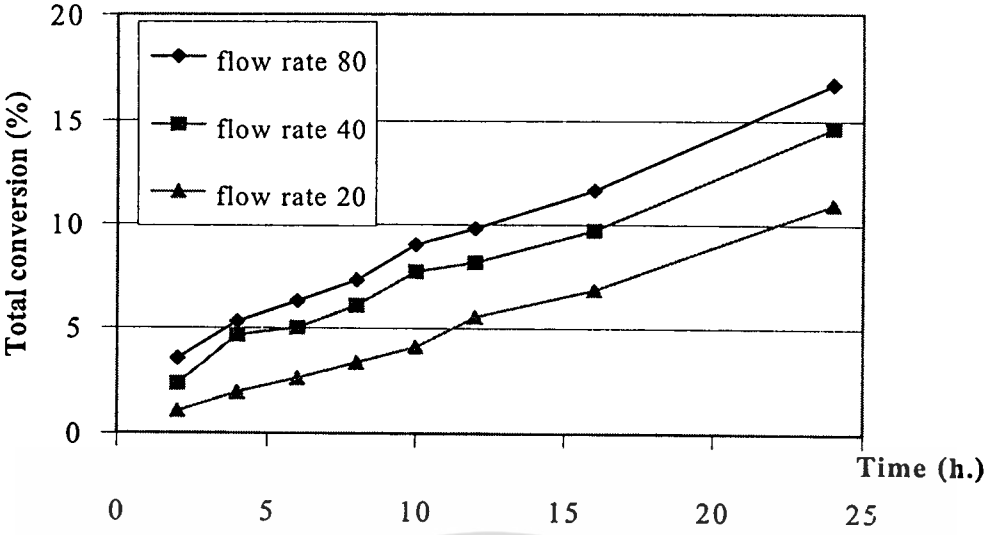

Figure 4.29 Result of oxidation of ethylbenzene using Ion-EMT-CoPc as a catalyst; *ethylbenzene 45 g, catalyst weight = 0.15 g, reaction time = 24 hr. temperature = 138 °C, oxygen flow rate 20, 40 and 80 ml/min*

It is found that the higher conversion of ethylbenzene is observed when a higher flow rate of oxygen is used in the reaction. According to the catalytic study above, it is described that ethylbenzene is oxidized by the interaction of ethylbenzene and the active species, which are formed by the complexation of molecular oxygen with cobalt phthalocyanine, encapsulated in the cavities of zeolite. Hence, the more the oxygen presents in the reaction, the more the active species. Accordingly, higher yield of the products could be obtained when the higher numbers of active species were generated in the reaction.

However, at the resident time higher than 50 hours, the lower activity could be observed when the oxygen flow rate of 80 ml/min was used. The conversion of ethylbenzene using Ion-EMT-encap with 72 hours reaction time was shown in Figure 4.30.

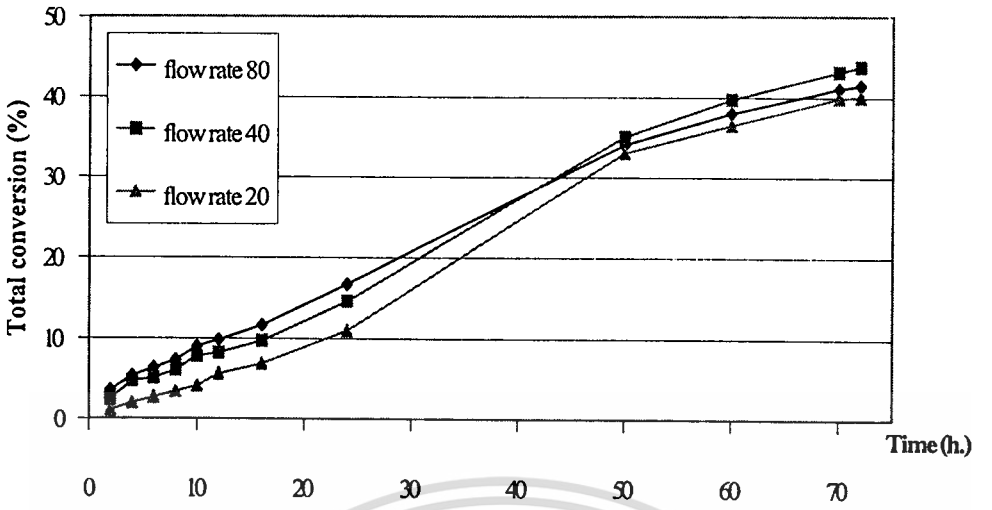

Figure 4.30 Result of oxidation of ethylbenzene using Ion-EMT-CoPc as a catalyst; *ethylbenzene 45 g, catalyst weight = 0.15 g, reaction time = 72 hr. temperature = 138 °C, oxygen flow rate 20, 40 and 80 ml/min*

The reduced activity at high reaction time appears not to be the case for the reaction with milder condition (oxygen flow rate of 20 and 40 ml/min). It can be suggested that the deactivation of catalyst occur due to a partial oxidative destruction of cobalt phthalocyanine encapsulated in zeolite. Since the molecular oxygen has to form complex with cobalt phthalocyanine, the oxidation of cobalt phthalocyanine may well take place when at long exposures of high flow rate of oxygen stream at high temperature. To prove this suggestion, the Ion-EMT-encap which are used in the reaction with oxygen flow rate of 80 ml/min was regenerated by washing with acetone and drying at 100 °C in a vacuum oven. It was then reused as catalyst in the ethylbenzene oxidation under the same experimental conditions. The ethylbenzene conversion obtained from the regenerated catalysts is shown in Figure 4.31. It is found that lower conversion was observed when the regenerated catalyst was used in the oxidation reaction. This result show that the deactivation of catalyst occurred due to partial oxidatively destruction of the metal complex encapsulated in the cavities of zeolite when the oxygen flow rate of 80 ml/min was used. This leads the formation of the lower amount of active oxidizing species, as compared to that generated form the fresh catalyst. From this result, it can be concluded that activity would be increase when the increase of oxygen flow rate was applied in the reaction. However, when too much of oxygen flow rate was used in the reaction, it can result in the reduction in activity due to

the partial oxidation of cobalt phthalocyanine encapsulated in both of zeolite EMT and BEA. This can be concluded that excess of oxygen flow rate cause low stability of the catalyst as well.

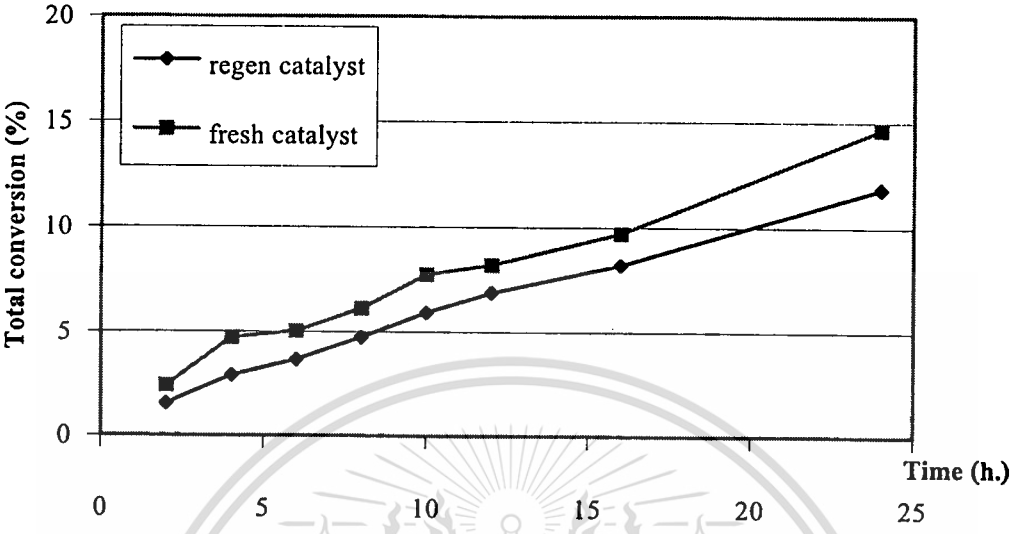

Figure 4.31 Result of oxidation of ethylbenzene using regenerated Ion-EMT-CoPc obtained from the reaction using 80 ml/in oxygen flow rate as a catalyst; *ethylbenzene 45 g, catalyst weight = 0.15 g, reaction time = 72 hr. temperature = 138 °C, oxygen flow rate 40 ml/min*

According to the results obtained from the catalytic testing in the oxidation of ethylbenzene, it is found that a relatively more active catalyst can be obtained from the use of zeolite BEA as a host material for the cobalt phthalocyanine encapsulation. However, the lower activity was observed at the long reaction time. This is suggested that cobalt phthalocyanine is relatively unstable, as compared to that encapsulated in zeolite EMT which can be confirmed by the lower decomposition temperature obtained by Thermogravimetric Analysis (section 4.1.6). In addition, the higher conversion was observed when impregnation was used for cobalt loading method in both zeolite EMT and zeolite BEA. This method provides the higher amount of metal complexes in the cavities of zeolite, which can be confirmed by Thermogravimetric Analysis and Surface Area Analysis. However, a reduced activity was observed at the long reaction time over the catalyst with high loading of metal complex in the cavities of zeolite. This is not due to the decomposition of cobalt phthalocyanine but suggested to be a result of a reduced internal pore volume which inhibit the diffusion of reactants into the active site. While, there are lower metal

complex loaded into the cavities of zeolite by ion exchange. Hence, substrate and products can access into the cavities of zeolite somewhat more easily even at a long reaction time. Moreover, it is found that conversion of ethylbenzene also depends on the oxygen flow rate. Higher conversion can be obtained when the oxygen flow rate is increased. However, at high oxygen flow rate (i.e. 80 ml/min) the reduced activity can be obtained at the long reaction time. This is suggested to be resulted from the reduced stability of cobalt phthalocyanine encapsulated in zeolite BEA under strong oxidation conditions. It is likely that some of the cobalt phthalocyanine encapsulated in the cavities of zeolite can be oxidized at high oxygen flow rate. The choice of oxygen flow rate is determined by a satisfied catalytic activity and stability of catalyst. It is found in this experiment that the oxygen flow rate of 40 ml/min gives an optimum result. From this study, it seems that cobalt phthalocyanines encapsulated in zeolite BEA and zeolite EMT are effective catalysts for the oxidation of hydrocarbon. These catalysts will be used for the study of the oxidation of cyclohexane in the next section. Only, the catalysts prepared by ion exchange will be used since a long catalyst lifetime can be obtained.

4.2.2 Oxidation of cyclohexane

4.2.2.1 Effect of pressure

According to the results from the oxidation of ethylbenzene, Ion-BEA-CoPc and Ion-EMT-CoPc were selected to use as catalysts in the liquid phase oxidation of cyclohexane in the stirred batch reactor under oxygen flow rate of 40 ml/min. The reaction was carried out at 70 °C for 24 hours. It was found that a low conversion was observed. This can be suggested that cyclohexane is a saturated hydrocarbon which is relatively more resistant to the heterogeneous oxidation process, as compared to ethylbenzene. Therefore, the oxidation of cyclohexane could not readily take place under atmospheric pressure. Hence, a pressure reactor was applied to overcome this problem. The oxidation of cyclohexane was then carried out at 70 °C under pressure of oxygen (300 psi). The result of oxidation reaction of cyclohexane is shown in Figure 4.32.

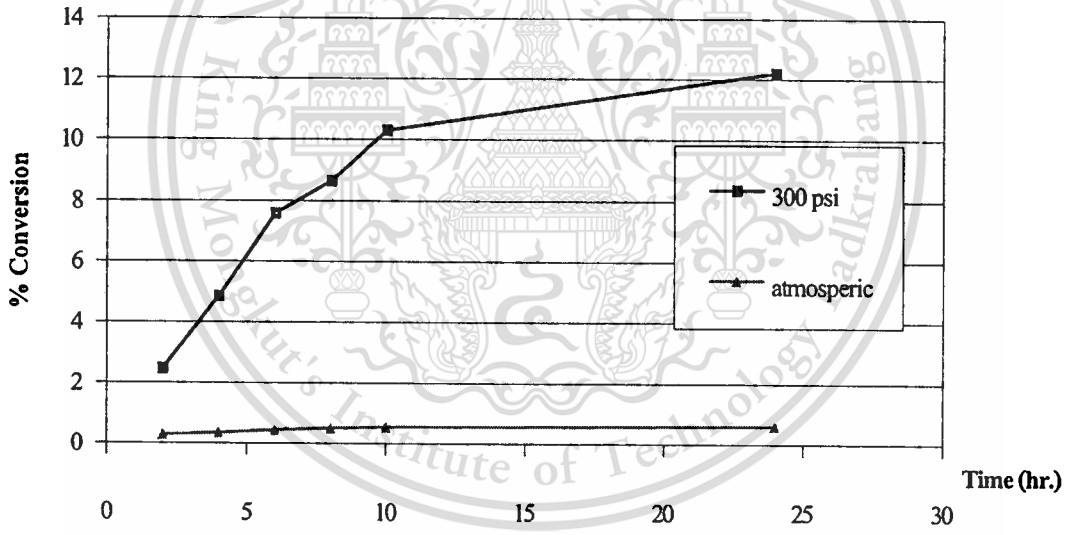

Figure 4.32 The conversion of the reaction under pressure; *cyclohexane = 12.25 g, catalyst (Ion-BEA-CoPc) weight = 0.375 g, reaction time = 24 hr. temperature = 343 K, solvent (acetic acid) = 22.25 g, oxygen 300 psi,* H_2O_2 *= 0.2 g.* and atmospheric pressure; *cyclohexane = 45 g, catalyst (Ion-BEA-CoPc) weight = 0.375 g, reaction time = 24 hr. temperature = 343 K, oxygen = 40 ml/min*

It can be clearly seen that the conversion of cyclohexane in the reaction under high pressure is higher than that at atmospheric pressure. From this result, it can be explained that under high pressure the oxygen molecules were compressed. As a result, more oxygen in gaseous

phase can distribute into the liquid phase of the reaction mixture. In other words, more oxygen can be readily dissolved. This facilitates the interaction of the oxygen with the encapsulated cobalt phthalocyanine, forming the active species. Moreover, the reaction under pressure could provide a high concentration of the reactants around the active sites. As a result, higher conversion could be obtained in the reaction under pressure.

4.2.2.2 Study of Reaction Pathway

Thermodynamically, the oxidation of cyclohexane can homogeneously take place under high pressure. However, The reaction is typically carried out at high temperature, generally in a gas phase. At the condition used in this study, it is shown in Figure 4.33 that, without aid of the catalyst, the reaction gives much lower conversion at 70 °C. On the other hand, the higher conversion of cyclohexane was obtained when catalyst was used. Thus, it can be concluded that the oxidation of cyclohexane, reported in the present study, is indeed catalyzed by the cobalt phthalocyanine complex encapsulated in the zeolite matrix.

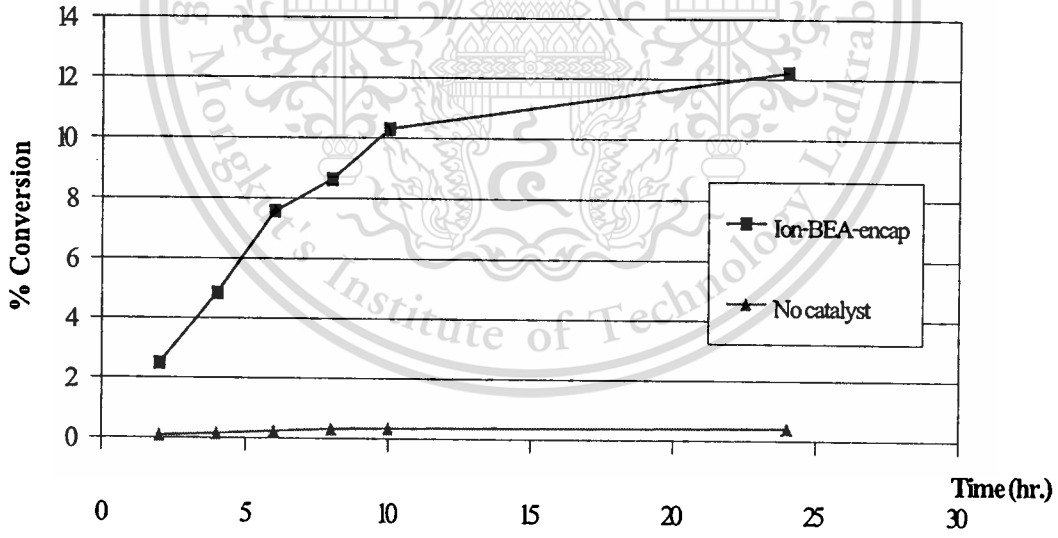

Figure 4.33 The conversion of cyclohexane; *cyclohexane 12.25 g, catalyst weight = 0.375 g, reaction time = 24 hr. temperature = 343 K, solvent (acetic acid) = 22.25 g, oxygen 300 psi,* H_2O_2 *= 0.2 g.*

The mechanism for the catalytic oxidation by cobalt phthalocyanine encapsulated in the cavities of zeolite was suggested to proceed via oxidative addition of oxygen onto the cobalt phthalocyanine encapsulated in the cavities of zeolite. This species became the active sites for

further oxidation of alkane substrate, in the similar manner as described in the oxidation of ethylbenzene (section 4.2.1). It seems that complexation of oxygen with the cobalt phthalocyanine is essential for the generation of the active oxidizing species. To testify the complexation of oxygen with metal complex, ethylenediamine was added into the reaction mixture. According to the spectrochemical series, it is expected that cobalt prefer complexation with ethylenediamine to that with oxygen. The result of the effect of ethylenediamine is revealed in Figure 4.34.

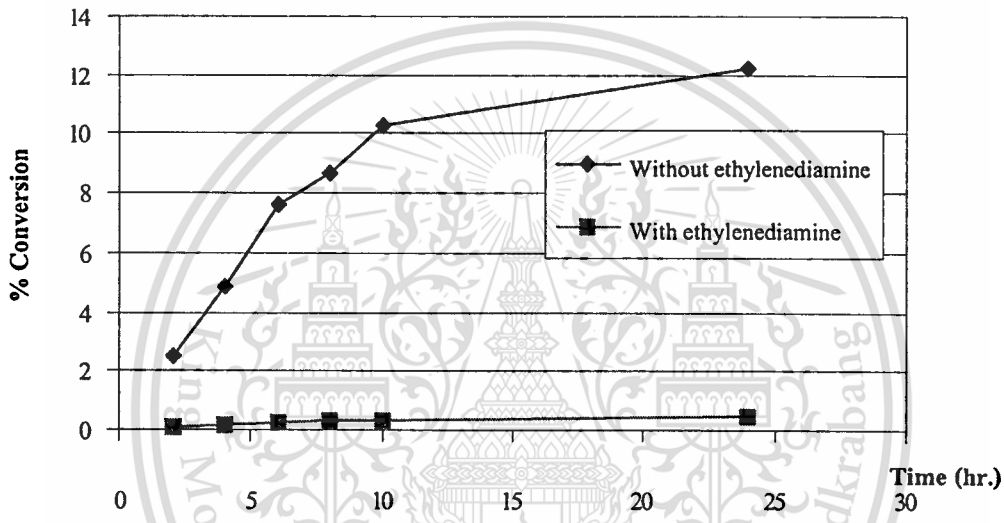

Figure 4.34 Influence of ethylenediamine on cyclohexane conversion; *cyclohexane = 12.25 g, acetic acid = 22.25 g, hydrogenperoxide = 0.2 g, catalyst (Ion-BEA-CoPc) weight = 0.375, O_2 300 psi, reaction time = 8 hr (with 0.23 g of* ethylenediamine*)*

As expected, it is found that a negligible activity was obtained when etylenediamine was added into the reaction mixture. Ethylenediamine can readily form a complex with cobalt as illustrated below:

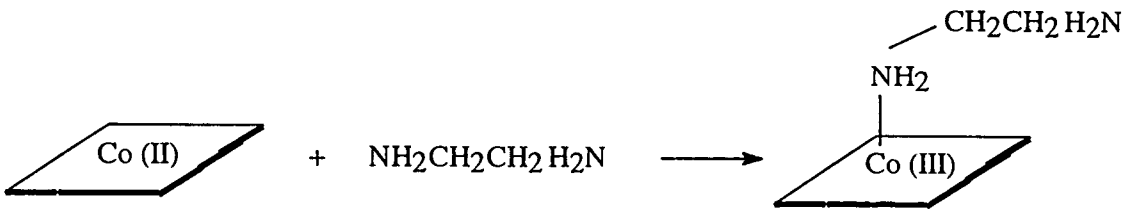

As a result, the active oxidizing species, called metal-oxo complex, could not be generated in the presence of ethylenediamine. Consequently, a low conversion was observed.

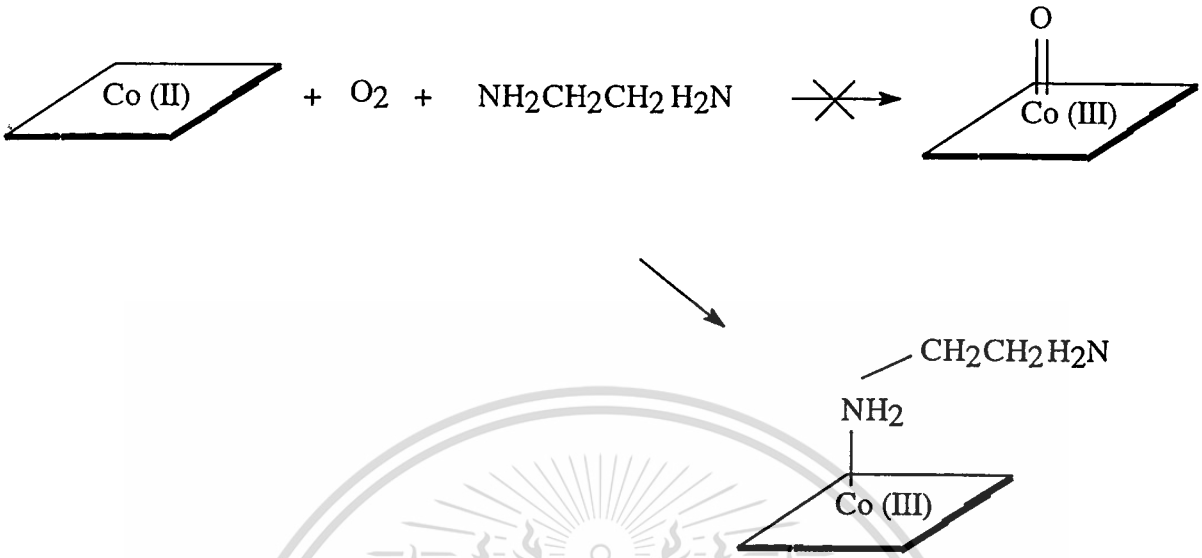

Accordingly, it can be concluded that the active oxidizing species must be initially formed by the complexation of oxygen with the cobalt phthalocyanine and this step is significant for the oxidation reaction using cobalt phthalocyanine encapsulated in the cavities of zeolite. The active oxidizing species generated by the complexation with oxygen is suggested to interact with substrate (cyclohexane) forming a radical by hydrogen abstraction (I). The decomposition of such complex involves the reverse transfer of the hydroxyl group (OH) to the carbon radical, as shown below. This reverse transfer step, known as the oxygen rebound mechanism [38], yields the alcohol product.

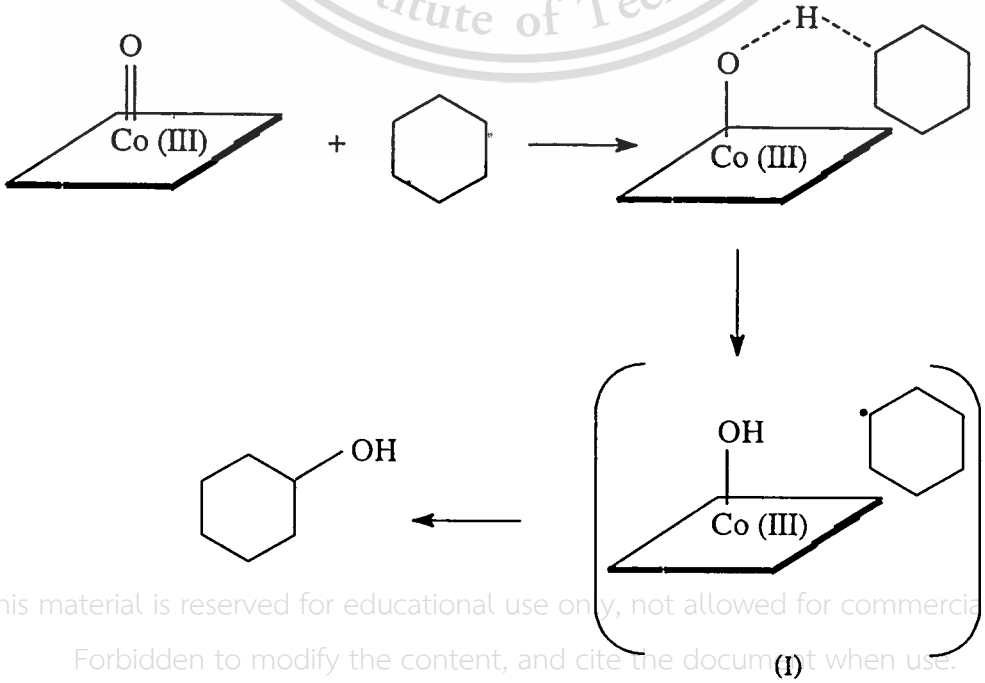

(I)

It can be seen that there are free radical species (I) involved in the proposed mechanism. The yield of products is suggested to be directly influenced by the formation of such intermediate. The significant of radical formation were tested by adding hydroquinone, a free radical inhibitor, in the reaction mixture. The result of the effect of free radical inhibitor is illustrated in Figure 4.35.

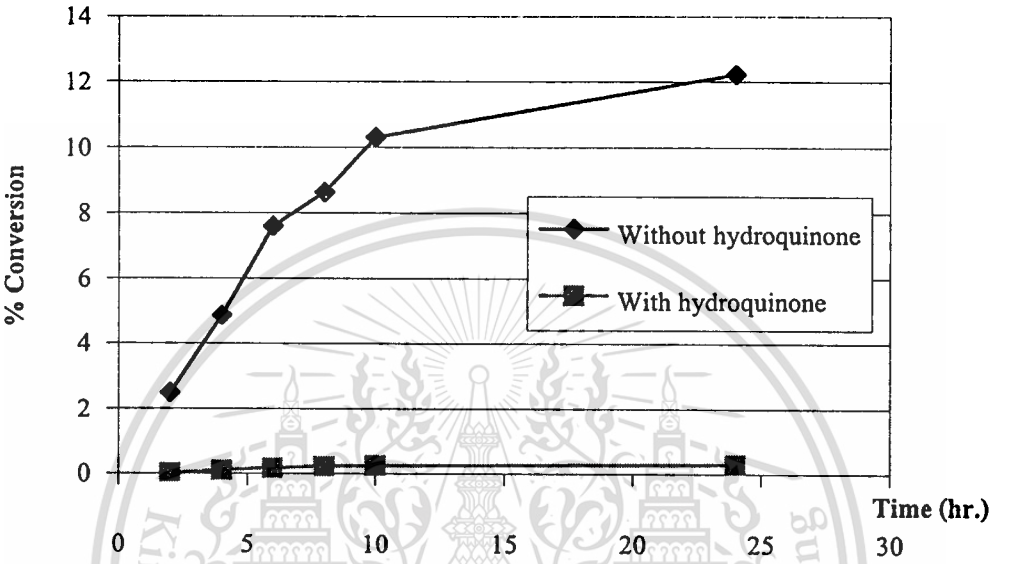

Figure 4.35 Influence of hydroquinone on cyclohexane conversion; *cyclohexane = 12.25 g, acetic acid = 22.25 g, hydrogenperoxide = 0.2 g, catalyst (Ion-BEA-CoPc) weight = 0.375, O_2 300 psi, reaction time = 8 hr (with 0.23 g of hydroquinone)*

It can be seen that a much lower conversion is obtained when hydroquinone is added. This is the result of the formation of stable hydroquinone radical as shown below, instead of free radical species proposed in the mechanism suggested earlier.

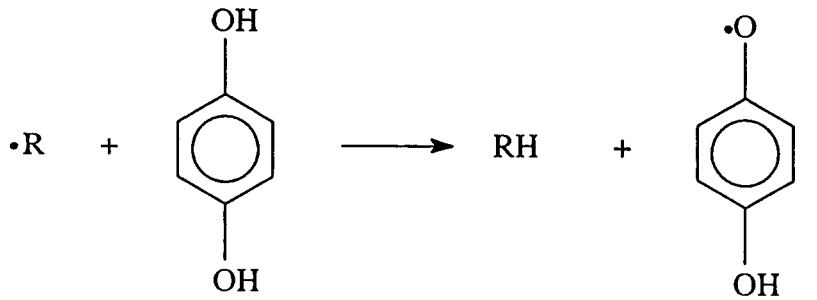

Generally, alkyl radical is not stable, as compared to the phenolic radical due to the lack of resonance stabilized structure [43-44], as observed in the radical inhibitor.

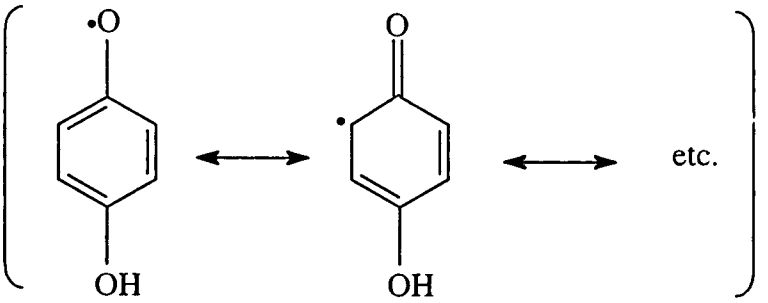

When cyclohexyl radical species are generated, this induces the homolytic cleavage of O-H bond of hydroquinone forming a stable hydroquinone radical in the reaction mixture. No further formation of the alkyl radical species can be found. The free radical generated from hydroquinone is so stable that no reaction with any species in the reaction mixture can be observed. In other words, the stable hydroquinone radical cannot induce further radical disproportionation. As a result, a lower conversion could be observed when the hydroquinone is added in the reaction mixture.

To evaluate the significant of the effect of ethylenediamine and hydroquinone on the conversion of cyclohexane, the conversions obtained from the both approaches are plotted simultaneously in Figure 4.36.

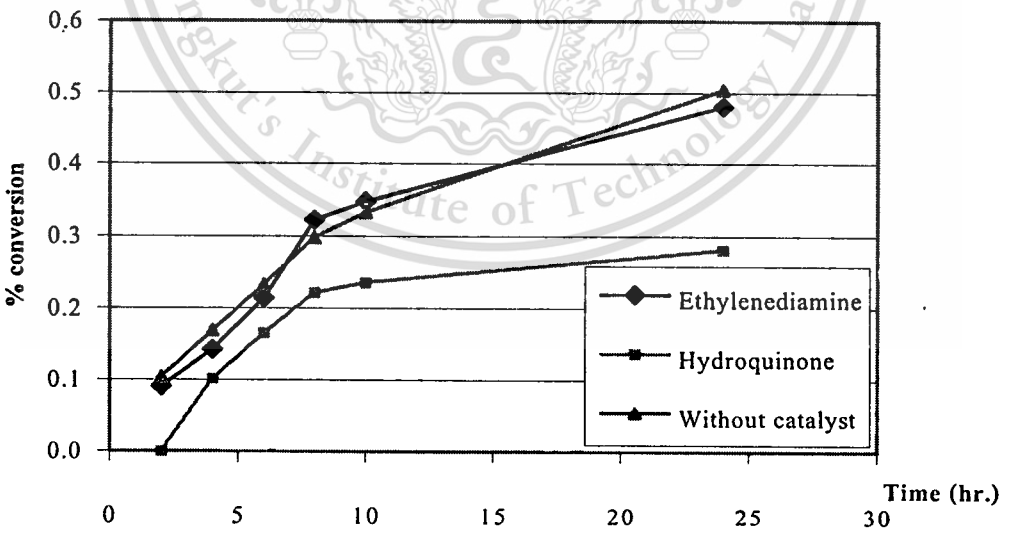

Figure 4.36 Comparison between the effect of ethylenediamine and the effect of hydroquinone: *cyclohexane = 12.25 g, acetic acid = 22.25 g, hydrogenperoxide = 0.2 g, catalyst (Ion-BEA-CoPc) weight = 0.375, O_2 300 psi, reaction time = 8 hr (with 0.23 g of ethylenediamine or with of hydroquinone)*

It can be seen that in the reaction with ethylenediamine and the reaction without catalyst, the similar manner in activity was obtained. When ethylenediamine was added in the reaction mixture, active oxidizing species cannot be generated because the complexation with oxygen is inhibited by the competitive complexation of added ethylenediamine as discussed earlier. It is suggested that in the presence of ethylenediamine the products were obtained by only the homogeneous oxidation, which is supposed to proceed via the free radical pathway as shown below.

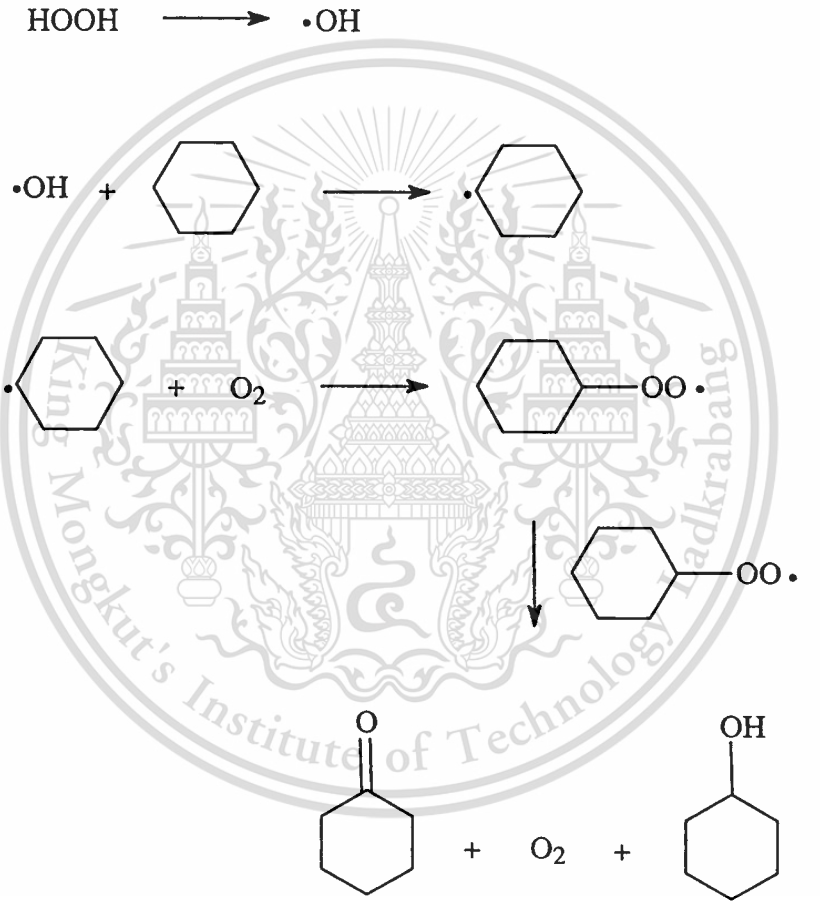

In the same way, as the reaction with catalyst, the formation of active oxidizing species cannot be possibly promoted. Therefore only the homogeneous oxidation may well take place in the reaction. Accordingly, the similar activity can be observed in the reaction added ethylenediamine and the reaction without catalyst.

It is also found that the relatively lower conversion of cyclohexane was observed in the reaction added hydroquinone, as compared to that obtained from the reaction without catalyst. This is suggested that although the active species could be generated in the reaction mixture of the reaction with hydroquinone, the active intermediate species (I) discussed earlier cannot be formed. This leads to no further formation of any products. At the same time, the homogeneous oxidation like the case of the reaction without catalyst is unlikely to occur because the inhibition of hydroquinone, the free radical inhibitor. This is the cause of the relatively lower conversion when hydroquinone was added into the reaction mixture. Accordingly, it can be concluded that the effect of hydroquinone on the conversion of cyclohexane is relatively stronger than that by ethylenediamine. This result shows that the decomposition step (species (I) described earlier) is more important than the formation of active oxidizing species. From the result mentioned earlier, the overall proposed mechanism could be illustrated below;

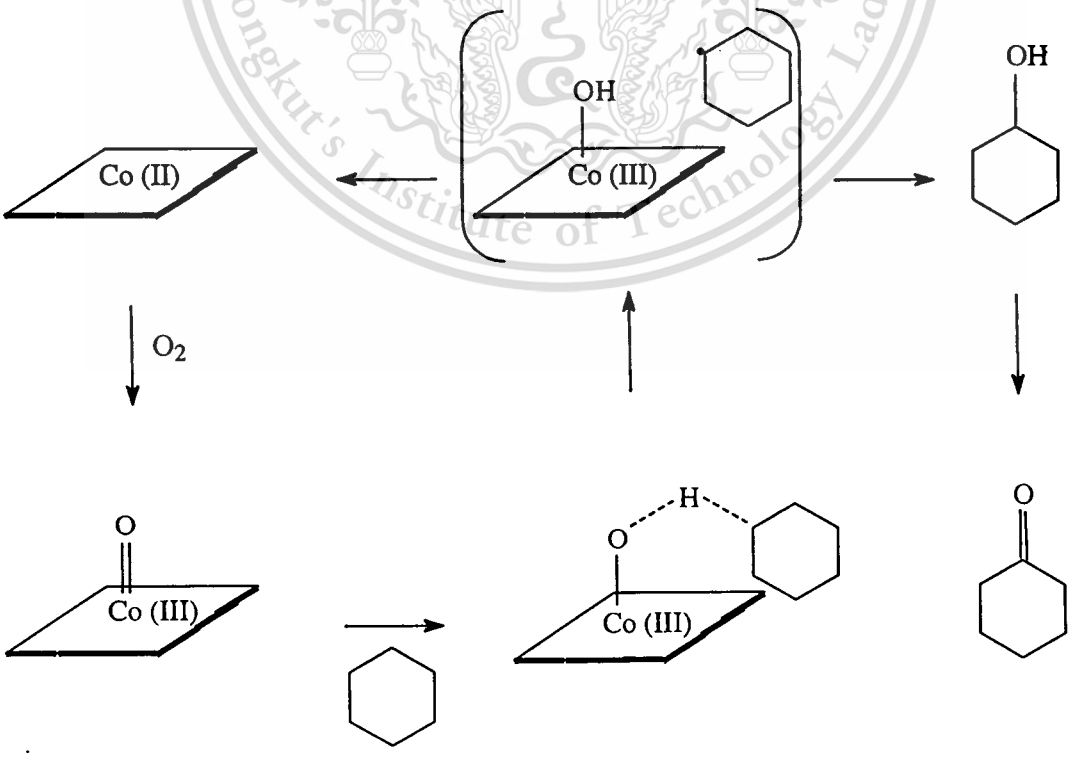

4.2.2.3 Effect of host material

Catalytic Activity

In this research cobalt phthalocyanine was immobilized in the cavities of two types of host material, zeolite EMT and zeolite BEA. Both of them are used as a catalyst in the oxidation of cyclohexane. The conversion of cyclohexane from the reaction using Ion-EMT-CoPc and Ion-BEA-CoPc as catalyst are shown in Figure 4.37.

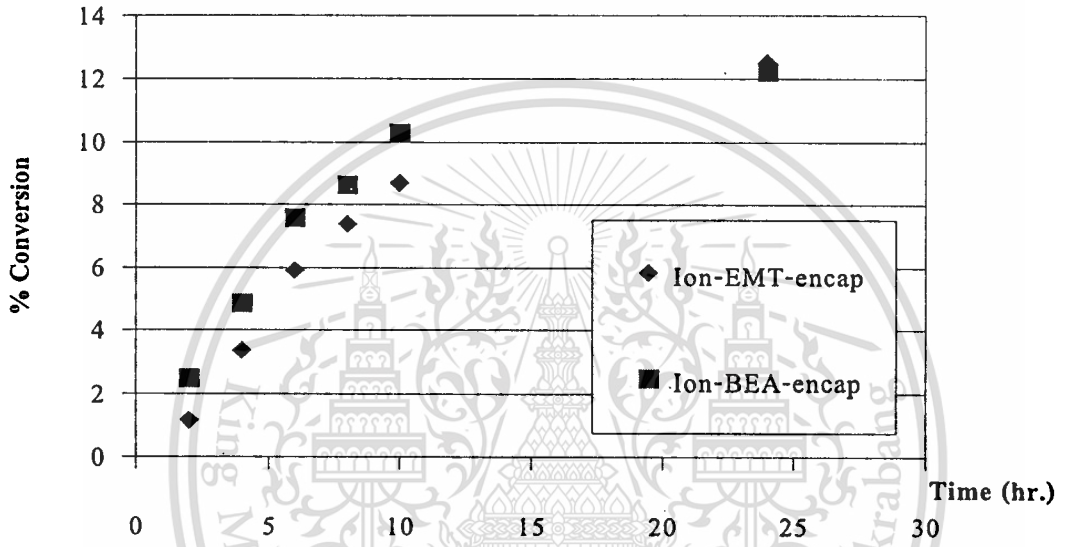

Figure 4.37 The conversion of cyclohexane; *cyclohexane = 12.25 g, catalyst weight = 0.375 g, reaction time = 8 hr, temperature = 343 K, solvent (acetic acid) = 22.25 g, oxygen 300 psi,* H_2O_2 *= 0.2 g.*

The higher rate of cyclohexane oxidation is observed when the catalyst used is Ion-BEA-CoPc. This can be explained that, generally, metal phthalocyanine is a relaxed planar conformation and it would be less active [20] as an oxidation catalyst than a metal phthalocyanine formed in constraint saddle conformation (as shown in section 4.1.6) when it is immobilized in some material such as zeolites. For the constraint saddle conformation, the metal site could be shifted out of the macrocycle and more accessible to coordinate the oxidizing agent. According to the part of characterization of catalyst, distort conformation of cobalt phthalocyanine could be observed in the cage of zeolite EMT and in the channel structure of zeolite BEA. However, it was found that more distort of cobalt phthalocyanine could be observed when it was immobilized in the channel structure of zeolite BEA. This is the result of a pore diameter limitation. The pore

diameter of zeolite EMT is 12 A that close to the diameter of cobalt phthalocyanine (ca. 13 A), while that of zeolite BEA is only 7 A. Consequently, cobalt phthalocyanine could be formed in the cage structure of zeolite EMT, while it could be formed around the pore intersection of zeolite BEA where possess 10 A of diameter. Hence, more distorted metal complexes located in the channel of zeolite BEA wold be more active than that located in the cavities of zeolite EMT. This fact is in accordance with these results. In the case of host material being zeolite BEA, the channel structure of zeolite BEA is about 7 A. Therefore, no complexes, diameter of 13 A, can form around here. It is suggested that the CoPc can form around the intersection of the channel where is more area as shown below

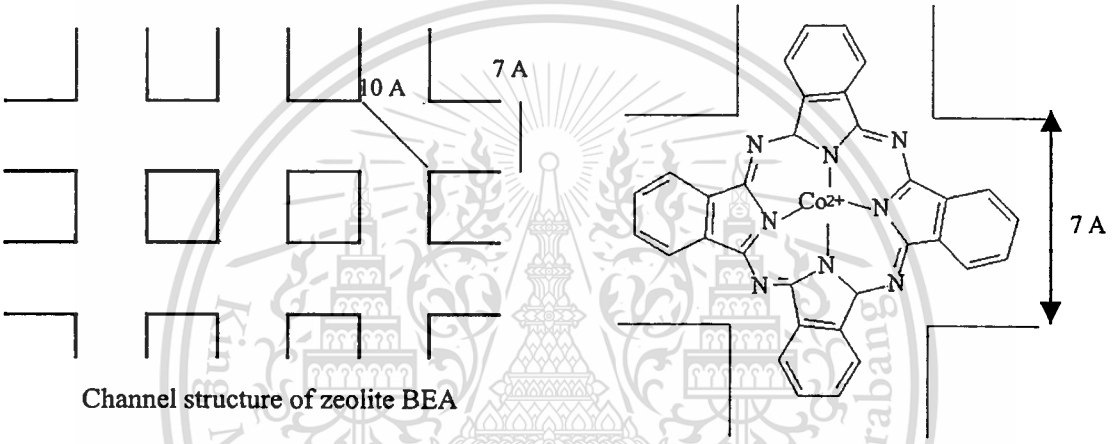

Channel structure of zeolite BEA

While, in the case of host material being zeolite EMT, pore diameter of the hyper-cage is around 12 A. Accordingly, cobalt phthalocyanine conformation in zeolite BEA should be more distort. In addition, the result from characterization synthesis catalysts by TGA could confirm this propose. The restricted intersection could make the complex appear to be distorted. This result in higher strain configuration of cobalt phthalocyanine encapsulated in the intersection of zeolite BEA. Generally, in the case of complex with strain configuration, electron cannot delocalize naturally. This lead the higher degree of coordinative unsaturaion would be obtained for the case of cobalt phthalocyanine encapsulated in zeolite BEA. These results can promote the formation of complexation with other ligands. Accordingly, this also facilitates the oxidative addition. Therefore, cobalt phthalocyanine encapsulated in the intersection of zeolite BEA would relatively more facilitate the oxidative addition of oxygen onto cobalt phthalocyanine complex. According to the purposed mechanism, it is found that the active oxidizing species would be generated via the oxidative addition of oxygen onto cobalt phthalocyanine complex. Hence, the active oxidizing

species would be formed easier for the case of complex encapsulated in zeolite BEA. This cause the higher amounts of products could be obtained when the used catalyst is Ion-BEA-CoPc.

Selectivity

The major products obtained from the reaction are typically cyclohexanol and cyclohexanone. However, after 8 hours reaction time, a trace of adipic acid was detected in the reaction. It is suggestion that a trace of adipic acid can be formed from a further oxidation of cyclohexanone. The reaction scheme for the oxidation of cyclohexane to adipic acid can be illustrated as follow;

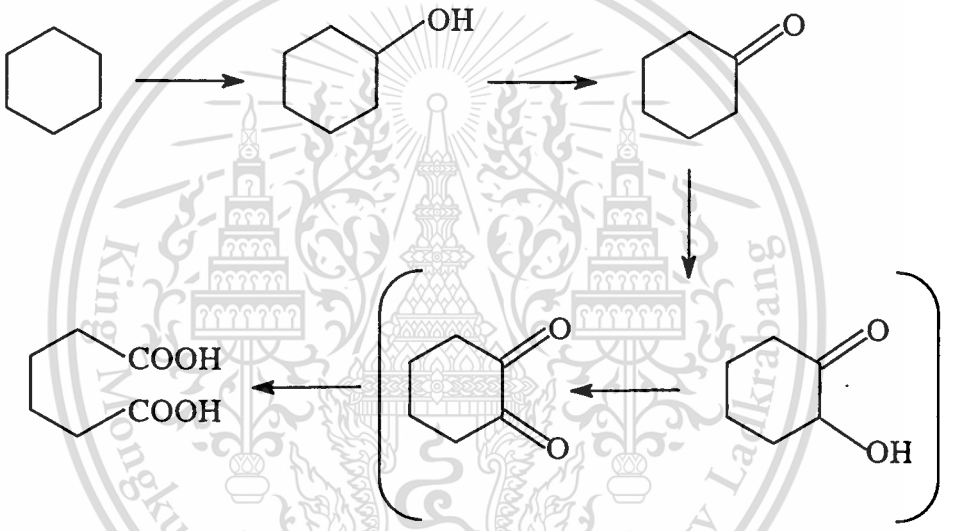

The selectivity of products and the selectivity of cyclohexanone obtained from the reaction using Ion-BEA-CoPc and Ion-EMT-CoPc as catalyst and the reaction without catalyst are revealed in Figure 4.38, 4.39 and 4.40.

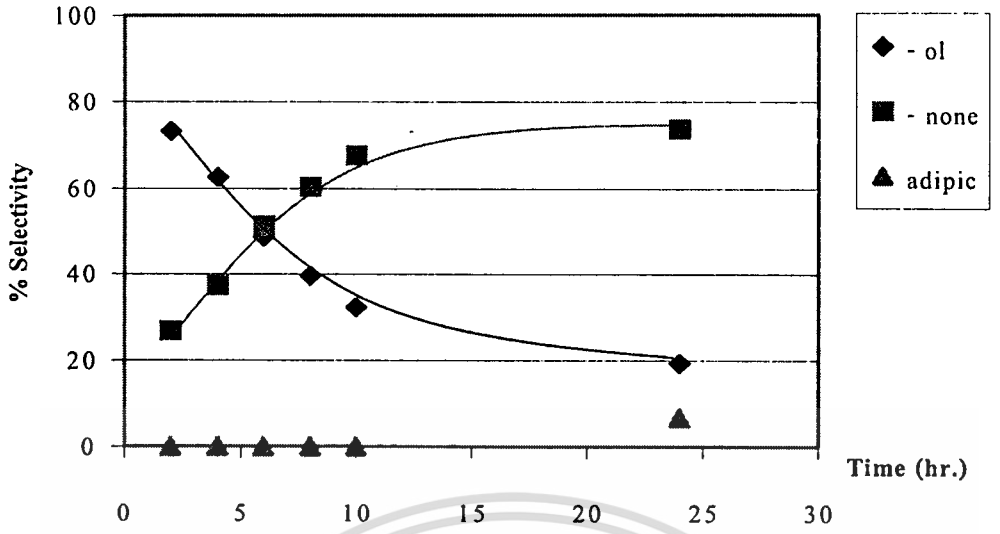

Figure 4.38 The selectivity of products obtained from the reaction using Ion-EMT-CoPc; *cyclohexane 12.25 g, catalyst weight = 0.375 g, reaction time = 24 hr. temperature = 343 K, solvent (acetic acid) = 22.25 g, oxygen 300 psi,* H_2O_2 *= 0.2 g.*

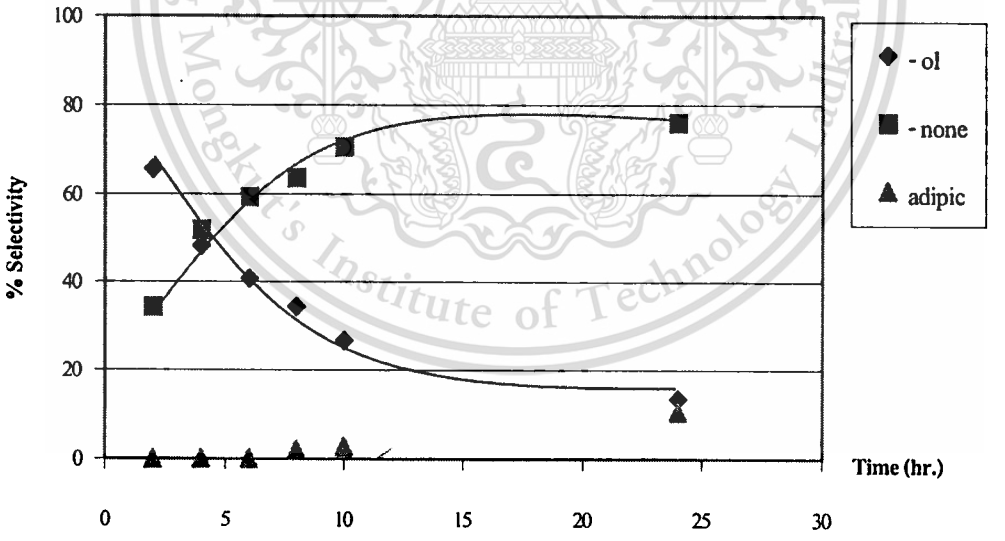

Figure 4.39 The selectivity of products obtained from the reaction using Ion-BEA-CoPc; *cyclohexane 12.25 g, catalyst weight = 0.375 g, reaction time = 24 hr. temperature = 343 K, solvent (acetic acid) = 22.25 g, oxygen 300 psi,* H_2O_2 *= 0.2 g.*

It can be seen that cyclohexanone increase with the increase in reaction time. This result supports the reaction pathway proposed earlier that the first product for the catalytic oxidation of

cyclohexane is cyclohexanol. It was then further oxidized to cyclohexanone. However, after a long reaction time, adipic acid was formed in the reaction with catalyst. It is suggested that some of cyclohexanone can be further oxidized to di-ketone and it cleaves to give adipic acid as shown below. The rate of di-ketone oxidation (k_2) seems to be so fast that this species cannot be observed in the reaction products.

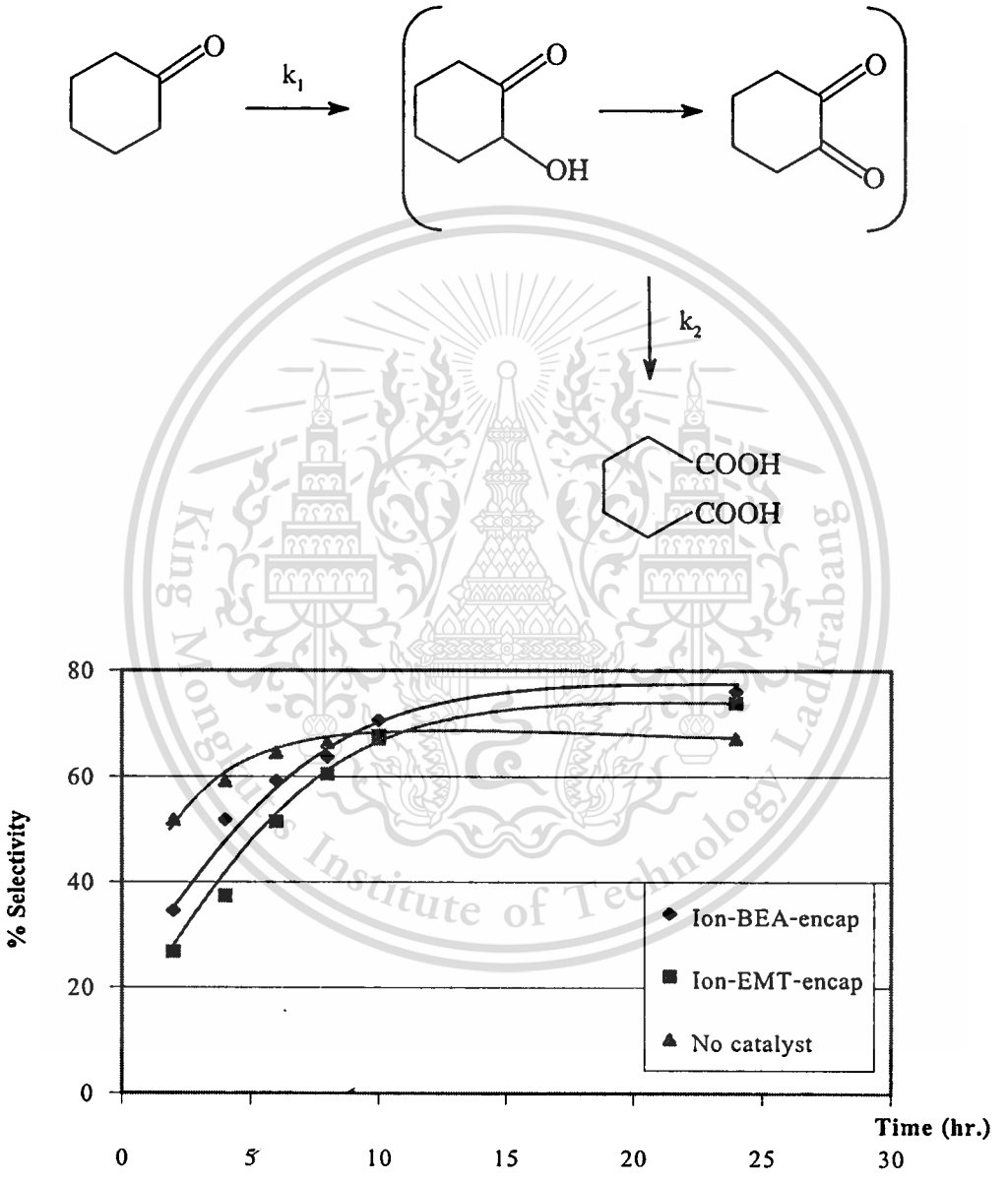

Figure 4.40 The selectivity of cyclohexanone in the reactions with Ion-BEA-CoPc, Ion-BEA-CoPc and without catalyst; *cyclohexane 12.25 g, catalyst weight = 0.375 g, reaction time = 24 hr. temperature = 343 K, solvent (acetic acid) = 22.25 g, oxygen 300 psi, H_2O_2 = 0.2 g.*

In addition, it was found that although, the reaction with catalyst produces higher amounts of products than that without catalyst, the selectivity of cyclohexanone at the initial time in the reaction with catalyst was lower than that in without catalyst. This is because the selective oxidation doesn't occur in the case of reaction without catalyst. Accordingly, cyclohexane (reactant) or cyclohexanol (the primary product) can be readily oxidized in such case. Consequently, at the beginning of the reaction, cyclohexanone (the secondary product) can be largely produced from cyclohexanol oxidation. In contrast, the selective oxidation cyclohexane can be highly promoted in the reaction with catalyst.

At the beginning of the reaction with catalyst, cyclohexanol is largely produced, while a relatively less amount of cyclohexanone can be generated from cyclohexanol. This is due to the competitive reaction of cyclohexane over cyclohexanol in the presence of selective catalyst. In other word, it is possible to suppose that in the case of the reaction with catalyst, the rate of cyclohexane oxidation is faster than that of cyclohexanol. Accordingly, at the initial time, a relatively lower selectivity of cyclohexanone was observed in the case of the reaction with catalyst, as compared to that without catalyst.

However, after a long reaction time, the selectivity of cyclohexanone in the reaction with catalyst turns to be higher, while, the selectivity of cyclohexanone in the reaction without catalyst is almost the same. This is because, at the higher reaction time, a large amount of cyclohexane was oxidized to cyclohexanol. Thus the effect of the competitive reaction of cyclohexane over cyclohexanol become less important as compared to that observed at the beginning of the reaction. Cyclohexanol can be further oxidized to cyclohexanone. This results in a relatively larger amount of cyclohexanone. Consequently, at the long reaction time, the relatively higher selectivity of cyclohexanone was observed in the case of the reaction with catalyst.

It is also found that the selectivity of cyclohexanone obtained from the reaction using Ion-BEA-CoPc is higher than that from the reaction using Ion-EMT-CoPc. This is because of the higher activity presented in the reaction with Ion-BEA-CoPc. Accordingly, cyclohexanol, primary product, obtained from the oxidation of cyclohexane was oxidized to produce cyclohexanone, secondary product, with higher reaction rate. This lead the selectivity of cyclohexanone obtained from the reaction using Ion-BEA-CoPc is higher than that from the reaction using Ion-EMT-CoPc.

Furthermore, the physical property could be the other important thing that lead the selectivity of cyclohexanone obtained from the reaction using Ion-BEA-CoPc is higher than that

from the reaction using Ion-EMT-CoPc. The advantage in structure of zeolite BEA, as compared to that of zeolite EMT. Zeolite BEA is a channel structure zeolite, while zeolite EMT possess a cage structure. The structure of both zeolite are shown in Figure 4.21. It was found that zeolite BEA possess open dimension system. This feature could result in a better accessibility of encapsulated complexes for reactant molecule. Hence, at the same time, more reactant molecules can reach to the active site loaded in the cavities of zeolite BEA. Moreover, according to the better accessibility of zeolite BEA, the product form the oxidation of cyclohexane can diffuse out of the cavities zeolite easily. These results in higher selectivity of cyclohexanone can be observed when the used catalyst is Ion-BEA-CoPc.

4.2.2.4 Effect of hydrogenperoxide (H_2O_2)

As discussed earlier, it was found that the product can be generated by free radical mechanism. Accordingly, adding hydrogenperoxide in the reaction could effect to the conversion of cyclohexane. In this section, the reaction using Ion-BEA-CoPc as catalyst with and without hydrogenperoxide was inspected. The conversion of cyclohexane from the reaction using Ion-BEA-CoPc as a catalyst with and without hydrogenperoxide are shown in Figure 4.41.

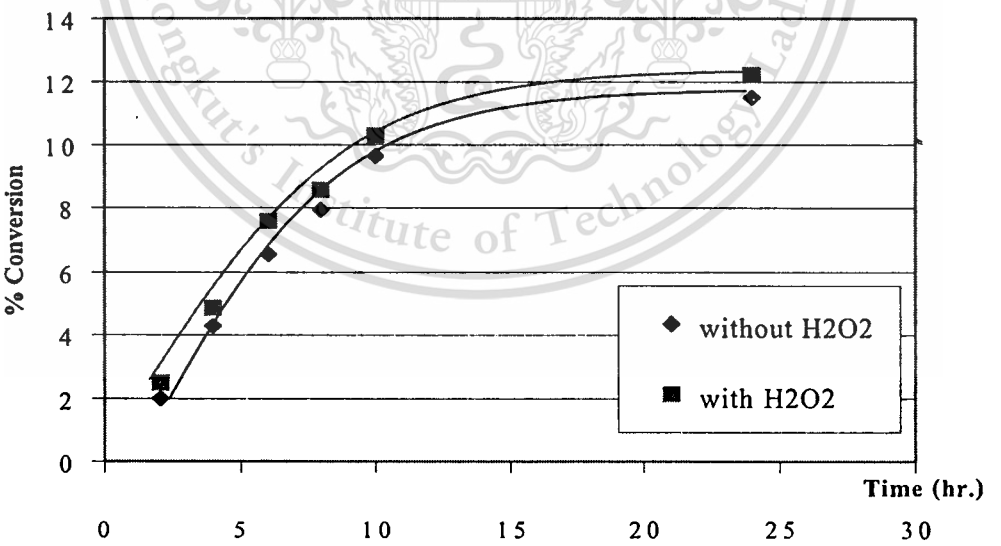

Figure 4.41 The conversion of reaction with hydrogenperoxide and without hydrogenperoxide; *cyclohexane = 12.25 g, catalyst weight = 0.375 g, reaction time = 8 hr. temperature = 343 K, solvent (acetic acid) = 22.25 g, oxygen 300 psi, H_2O_2 = 0.2 g.*

A slightly higher conversion of cyclohexane was observed when hydrogenperoxide was available in the reaction mixture. According to the mechanism of cytochrome P-450 described earlier, it was found that, generally, peroxides can directly interact with iron porphyrin complexes to generate active oxidizing species. In addition, peroxide can directly interact with other metal phthaloicyanine to generate oxo-peroxy complex [38]. Accordingly, it is reasonable to assume that cobalt phthalocyanine would be able to react with hydrogenperoxide to generate oxo-peroxy complex which further become active oxidizing species as shown below. The fact that no significant enhancement of the activity was observed indicating that oxygen can directly interact with the active site without the aid of other oxidizing species, under the experimental conditions.

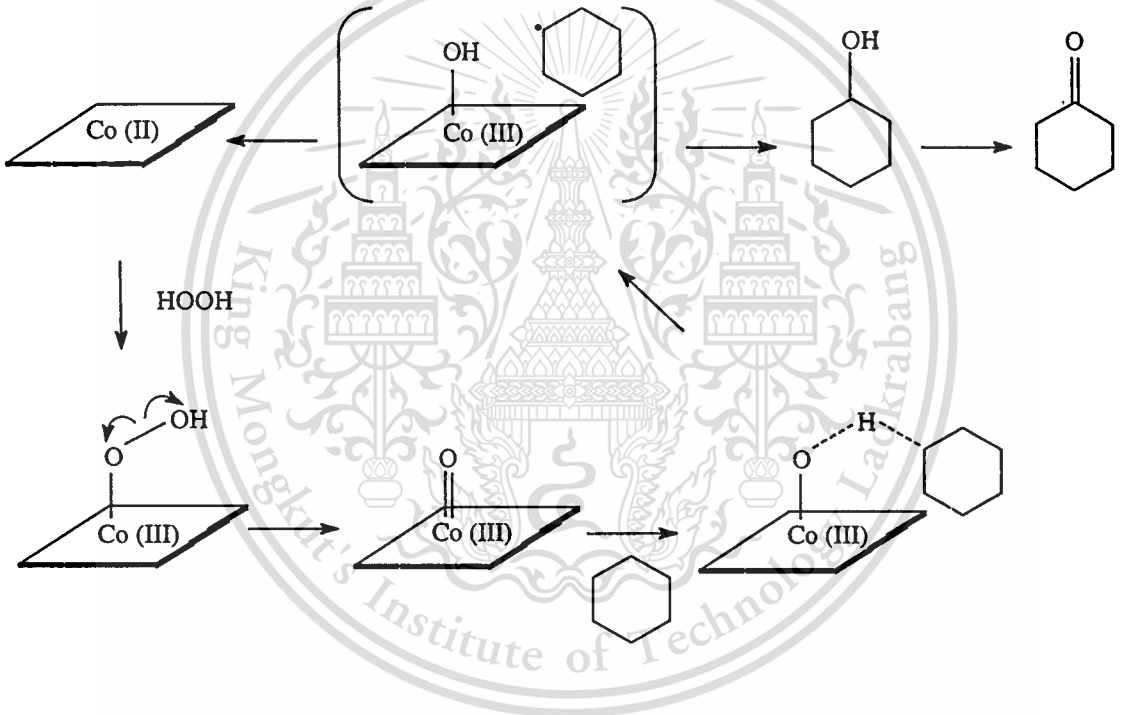

Consequently, a slightly higher conversion of cyclohexane could be observed when hydrogenperoxide is present in the reaction mixture.

4.2.2.5 Effect of oxygen partial pressure

The source of oxygen atom donor used in the oxidation reaction should be the major factor for the conversion of cyclohexane. Therefore, in this research, the catalyst (Ion-BEA-CoPc) was tested under the pressure of air compared with the reaction under the pressure of pure oxygen under the same experimental conditions. The conversion of cyclohexane under pressure of oxygen and air are shown in Figure 4.42

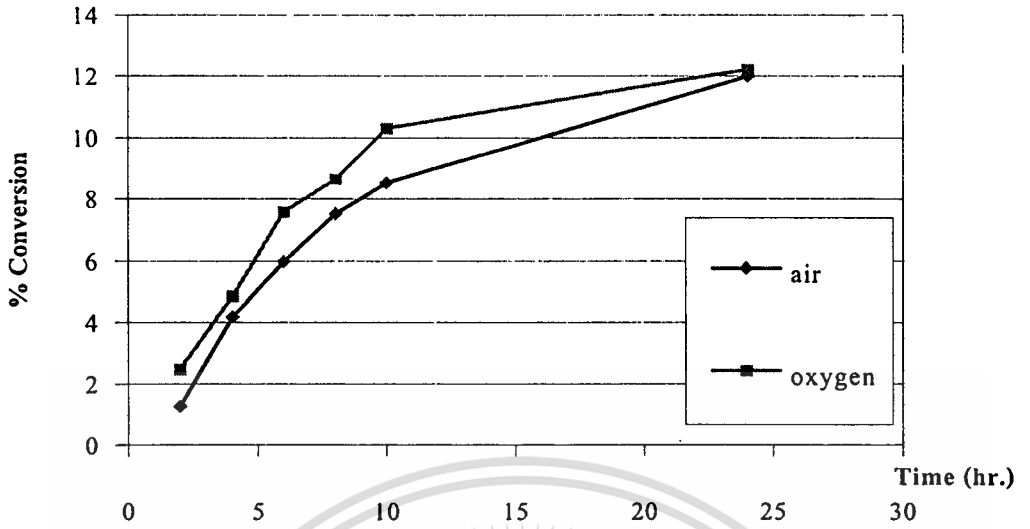

Figure 4.42 The conversion of the reaction under pressure of oxygen gas and air; *cyclohexane = 12.25 g, catalyst weight = 0.375 g, reaction time = 24 hr. temperature = 343 K, solvent (acetic acid) = 22.25 g, pressure = 300 psi,* H_2O_2 *= 0.2 g.*

It can be seen that higher conversion could be observed when pure oxygen gas was used instead of air. This can be suggested that oxygen plays the major role in the reaction, as presented in section 4.2.2.2. As higher conversion of oxygen was used (pure oxygen), there is more opportunity of oxygen molecules to react with the metal phthalocyanine complex. The reaction between substrate and active species can be reactively enhanced. As a result, more yields of products were formed when the reaction operates under the pressure of oxygen.

4.2.2.6 Effect of solvent

In the cyclohexane oxidation, the polarity of reactant and products are largely different. As the zeolite used in this research possess hydrophilic nature, comparative adsorption of reactant and product should be considered. It is anticipated that polar reactants will be preferentially adsorbed. As a result, it can be proposed that solvent, which mediates between reactants and active sites, is one factor for the oxidation of cyclohexane. Therefore, for comparison, three solvents including acetic acid, chloroform and dimethylformamide (DMF) are selected to be used as solvent in this research. The conversion of the reaction using acetic aicd, chloroform and DMF as solvent is illustrated in Figure 4.43.

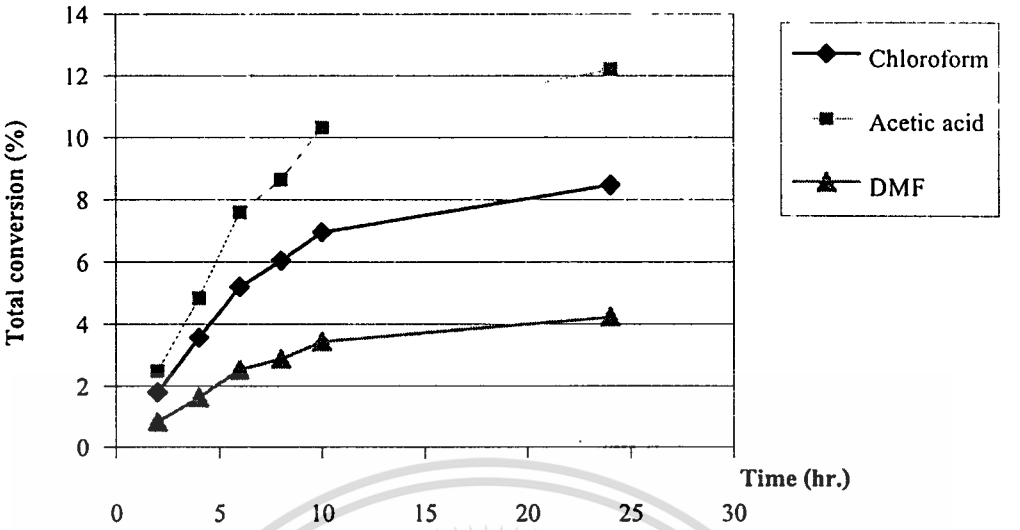

Figure 4.43 The conversion of reaction using acetic aicd, chloroform and DMF as solvent; *cyclohexane = 12.25 g, catalyst (Ion-BEA-CoPc) weight = 0.375 g, reaction time = 8 hr. temperature = 343 K, solvent = 22.25 g, oxygen 300 psi, H_2O_2 = 0.2 g.*

The study on effect of solvent shows that the higher conversion can be obtained from the reaction using acetic acid as solvent. This result could be explained by the polarity of the host material, solvent, reactant and product. In the reaction using chloroform, a relatively low polar solvent, cyclohexane can mediate in the bulk solution and diffuse to react with the catalyst to form primary product, alcohol. Such product is relatively high polar and tend to interact strongly with the active site located in the host material. This causes some difficulties for cyclohexane to interact with the active site and it is likely to diffuse out into the bulk solution. Accordingly, relatively low conversion is observed when chloroform is used as solvent.

In the reaction using acetic acid, a relatively high polar-protic solvent, cyclohexane can also mediate in the solution and diffuse into the cavities of host material. However, a preferential adsorption of cyclohexane is expected as compared to its partition the protic-media, acetic acid. Hence, cyclohexane can readily interact with the active site. Although, the product from the reaction possess higher polarity as compared to cyclohexane, they can readily partition in acetic acid and diffuse out of the cavities of host material leaving vacant sites for further adsorption and oxidizidation of cyclohexane.

In addition, in the reaction using acetic acid, peracetic acid can be generated. Acetic acid can readily react with hydrogenperoxide to form peracetic acid. This has been previously reported in the oxidation of cyclohexane using Ti-Zeolite as catalyst [42].

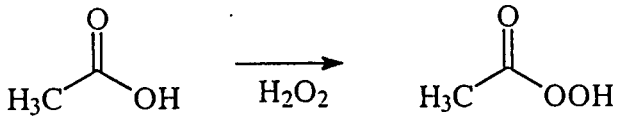

As discussed earlier in section 4.2.2.4, peroxides can directly interact with iron porphyrin complexes to generate active oxidizing species. In addition, peroxide can directly interact with other metal phthaloicyanine to generate oxo-peroxy complex [38]. Accordingly, it is reasonable to assume that cobalt phthalocyanine would be able to react with peracetic to generate oxo-peroxy complex which further become active oxidizing species as shown below.

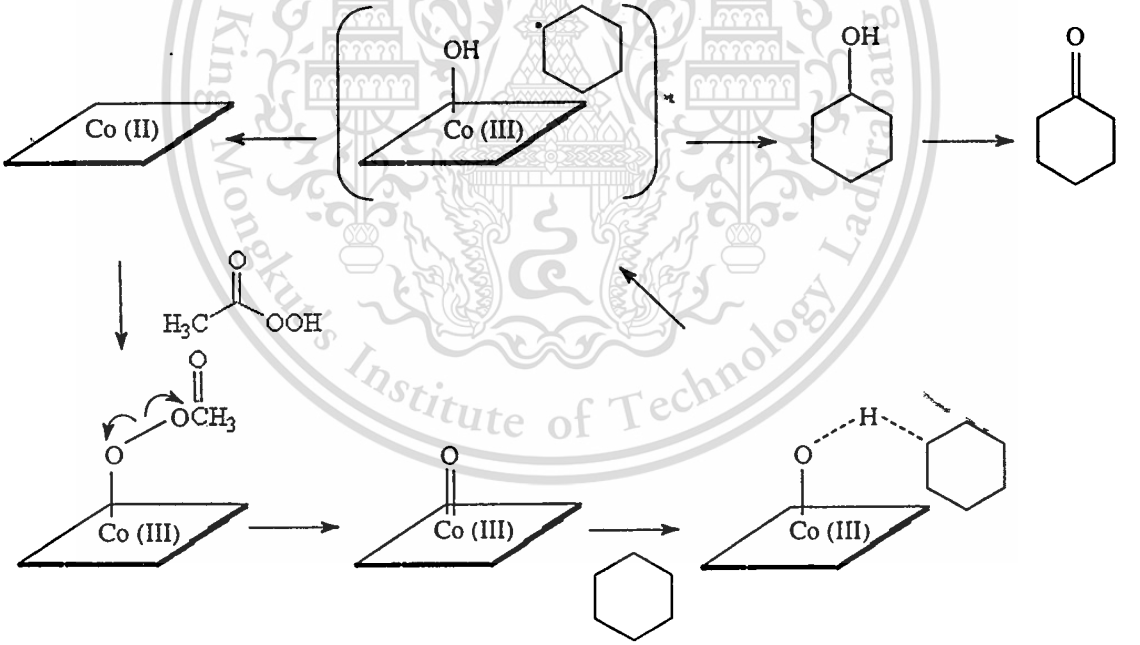

In the case of DMF, it was found that the lowest conversion was obtained which is not expected for high polar solvent. This can be explained that DMF probably act as strong ligand, due to its high affinity to lewis acid center. Accordingly, it can interfere either the formation of active species or interaction of active sites with cyclohexane. This leads to low conversion as seen when using DMF as solvent. It can be seen that solvent can be influence in the oxidation of

cyclohexane through competitive sorption / desorption in the zeolite cavities where active site is located.

From the results of the oxidation of cyclohexane, it was found that higher conversion could be obtained in the reaction under pressure. This is because more oxygen in gaseous phase can distribute into the liquid phase of the reaction mixture and the reaction under pressure could provide a high concentration of the reactants around the active sites. In the study of reaction pathway, it can be concluded that the mechanism for the catalytic oxidation by cobalt phthalocyanine encapsulated in the cavities of zeolite proceed via oxidative addition of oxygen onto the cobalt phthalocyanine encapsulated in the cavities of zeolite forming active species. Afterthat, the products could be obtained from the reaction between substrate and the generated active species. In addition, it was found that there are free radical species involved in this step of the proposed mechanism. This can be confirmed by the result from the reaction adding ethylenediamine and the reaction adding hydroquinone. The purposed mechanism is shown below.

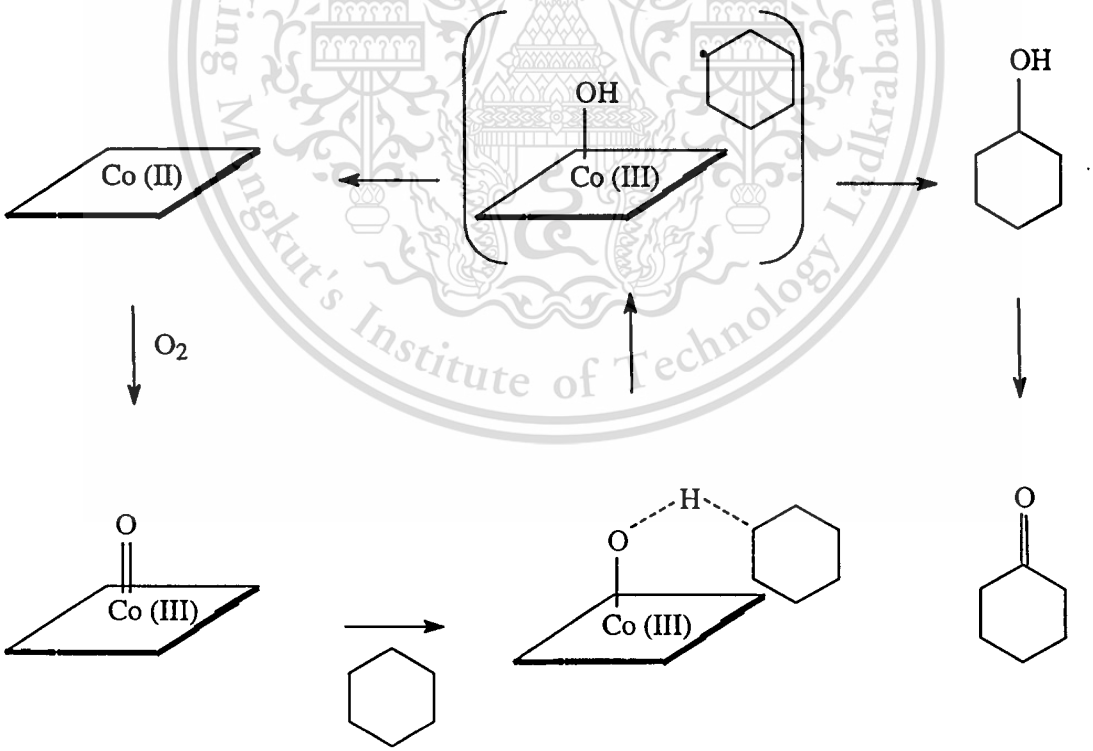

Furthermore, I can be seen that the higher rate of cyclohexane oxidation is observed when the catalyst used is Ion-BEA-CoPc. This could be explained like the oxidation of ethylbenzene in the earlier section. It was found that cyclohexanol is the primary product while

cyclohexanone is the secondary product. Moreover, a trace of adipic acid, the product from the further oxidation cyclohexanone, could be detected. According to study of the effect of hydrogenperoxide section, the slightly higher conversion of cyclohexane could be observed in the oxidation of cyclohexane in the present of hydrogenperoxide. From this result, it can be explained that cobalt phthalocyanine would be able to react with hydrogenperoxide to generate oxo-peroxy complex which further become active oxidizing species as discussed earlier. Furthermore, it can be seen that it can be seen that higher conversion of cyclohexane could be observed when pure oxygen gas was used instead of air. This can be suggested that oxygen play the major role in the reaction, as presented in section 4.2.2.2. In the study of the effect of solvent, it was found that solvent, which mediates between reactants and active sites, is one factor for the oxidation of cyclohexane. The highest conversion of cyclohexane cound be observed when solvent used in the reaction is acetic acid

Chapter 5

Conclusion and Suggestion

5.1 Conclusion

It can be concluded that cobalt phthalocyanine is indeed immobilized in the cavities of zeolite BEA and zeolite EMT. It was found that there is relatively more complexes formed in the cavities of zeolite EMT. Although, there is no solid evidence for the exact location of cobalt phthalocyanine in the zeolite cavities, it is suggested that in this study, that in the case of zeolite EMT, the complexes is likely to immobilize in the hypercage, while the complexes seem to be encapsulated in the intersection void in the case of zeolite BEA. As a result, the complexes formed in zeolite BEA may well be distorted.

In the catalytic activity study, the catalytic cycle of substrate oxidation by synthesis cobalt phthalocyanine involves the transfer of an oxygen atom, either directly from molecular oxygen or from other oxygen atom donors such as H_2O_2. This should lead to the formation of the active species, metal-oxo complex. The reaction with ethylenediamine show that the interaction of oxidizing species with metal phthalocyanine play important role in the formation of such active species. The interaction of active species with substrate results in hydrogen abstraction and the formation of radical intermediate that can be inhibited by hydroquinone that described earlier in section 4.2.2.2. The reverse transfer of the OH to the carbon radical before diffusing out from the cage, is known as the *oxygen rebound mechanism*, yielding the alcohol product that is further oxidized to ketone. In rare cases, some of ketone can also undergo destructive oxidation to carboxylic acid.

From the mechanistic study, it can be concluded that oxygen concentration play the major role in the reaction with metal phthalocyanine. This can be confirmed by the result from the effect of oxygen flow rate in the oxidation of ethylbenzene (4.2.1.5) and the effect of partial pressure of oxygen in the oxidation of cyclohexane (4.2.2.5). Furthermore, in the study of the effect of host material, it was found that more activity and higher conversion can be observed when zeolite BEA was used as host material for cobalt phthalocyanine. This is presumably due to distort conformation of metal phthalocyanine complex within the intersection of zeolite BEA 's channel. However, at the long reaction time, the reduced activity can be seen in the reaction using metal phthalocyanine immobilized in zeolite BEA as catalyst. It can be described that the

deactivation of catalyst may well occur due to oxidative destruction of cobalt phthalocyanine encapsulated particular in zeolite BEA due to its relative unstable conformation as explained in section 4.2.1.2. This suggestion can be confirmed by the result obtained from the reaction using regenerated catalyst in section 4.2.1.2. It can be clearly seen that a similar activity of the fresh counterpart is observed for the regenerated Ion-EMT-encap. While a lower activity was obtained when the Ion-BEA-encap was reused. This supports the suggestion that the deactivation of the Ion-BEA-encap occur at long reaction time while this was not the case for Ion-EMT-encap.

In addition, the higher conversion was observed when impregnation was used for cobalt loading method in both zeolite EMT and zeolite BEA. This method provides the higher amounts of metal complexes in the cavities of zeolite, which can be confirmed by Thermogravimetric Analysis and Surface Area Analysis (section 4.1.6 and 4.1.7, respectively). However, a reduced activity was observed at a long reaction time over the catalyst with high metal complex loading. This is not due to the decomposition of cobalt phthalocyanine but is suggested to be a result of products accumulation in the internal pore which inhibit the diffusion of reactants into the active sites. While, there are lower metal complex loaded into the cavities of zeolite by ion exchange. Hence, substrate and products can access into the cavities of zeolite somewhat more easily even at a long reaction time.

Furthermore, it can be concluded that solvent also play one important role in the reaction. It was found that solvent influence on the competitive sorption / desorption of substrate or the generated products in the zeolite cavities where active site is located. In this research, it can be seen that the higher conversion could be obtained from the reaction used acetic acid as solvent.

5.2 Suggestion

In the oxidation of cyclohexane, the reaction was carried out at a relatively high temperature (70 °C). It is interesting to test the reaction at lower temperature i.e. room temperature. Beside the temperature, the effect of pressure of oxygen in the pressure reactor also should be studied to obtain the optimal reaction condition.

References

[1] Carl M.W. "What is zeolite" [Online]. Available : http://mchhpi.ch..man.ac.uk/~mbdtscw/zeolite.html. 2001.

[2] Dyer A. **An Introduction to Zeolite Molecular Sieves**. New York : Wiley. 1998.

[3] Weit K. J., Karge H. G., Pfeifer H. and Holderich W. **Zeolites and Related Microporous materials**. New York : State of Art. 1994.

[4] K. Suslik, B. Cook and M. Fox. J. Chem. Soc. Chem Commun. 1980. pp. 580.

[5] S. I. Murahashi and N. Komiya. "New Types of Catalytic Oxidations in Organic Synthesis. Catalysis Today." vol. 41. 1998. pp. 339-349.

[6] P. R. Orthiz de Montellano. **Cytochrome P-450, Structure, Mechanism and Biochemistry**. New York : Plenum Press. 1995. pp. 119-160.

[7] Donald W. B. **Zeolite Molecular Sieves Structure, Chemistry and Use**. Sydney : Wiley & Sons. 1974.

[8] Danly D. E. and Cambell C. R. **Kirk Othmer Encyclopedia of Chemical Technology**, 3rd Ed. New York : Wiley. 1979. pp. 510.

[9] Derek H. R. Barton, Jean Boivin, Michel Gastiger, Jacek Morzycki, Robyn S. Hay-Motherwell, William B. Motherwell, Nubar Ozbalik and Kathy M. Schwartzentruber. Functionalization of Saturated Hydrocarbons. "The Gif System for Selective Oxidation using Molecular Oxygen." J. Chem Soc. Perkin Trans. 1986. pp. 947-955.

[10] Rudy F. Parton, Gunter J. Peere, Patricia E. Neys, Peter A. Jacobs, Rudi Claessens and Gino V. Baron. "Cyclohexane Oxidation with Tertiary-Butylhydroperoxide Catalyzed by Iron-phthalocyanines Homogeneously and Occluded in Y Zeolite." Journal of Molecular Catalysis A. vol. 113. 1996. pp. 445-454.

[11] Romanovsky B. V. and Gabrielov A. G. "New Developments in Selective Oxidation by Heterogeneous Catalyst. Studies in Surface Science and Catalysis." Vol. 72, Elsevier, Amsterdam. 1992. pp 443-452.

[12] Ernst S., Traa Y. and Deeg U. "Preparation, Characterization and Catalytic Properties of Cobalt Phthalocyanine Encapsulated in Zeolite EMT. Zeolites and Related Microporous Material" State of the Art. 1994

[13] Edgado Paez-Mozo, Nyole Gabriunas, Fabio Lucaccioni, Dwidht D. Acosta, Pasquale

Patrono, Aldo La Ginestra, Patricio Ruiz and Bernard Delmon. "Cobalt Phthalocyanine Encapsulated in Y Zeolite: A Physicochemical Study." J. Phys. Chem. vol. 97. 1993. pp. 12819-12827.

[14] Balkus K. J., Gabriielov A. G. and Bell S. L. "Zeolite Encapsulated Cobalt (II) and Copper (II) Perfluorophthalocyanines: Synthesis and Characterization." Inorg. Chem. vol. 33. 1994. pp. 67-72.

[15] Ernst S. and Selle M. "Immobilization and Catalytic Properties of Perfluorinated Ruthenium Phthalocyanine Complexes in MCM-41-Type Molecular Sieves." Microporous and Mesoporous Material. vol. 27. 1999. pp. 355-363.

[16] Alexander B. S and Alain T. "Metallophthalocyanine Functionalized Silicas: Catalysts for The Selective Oxidation of Aromatic Compounds." Catalysis today. vol. 57. 2000. pp. 45-59.

[17] Shevade S. S., Raja R. and Kotashane A. N. "Copper (II) Phthalocyanines Entrapped in MFI Zeolite Catalysts and Their Application in Phenol Hydroxylation." Applied Catalysis A : General. vol. 178. 1999. pp. 243-249.

[18] Gedon A., Valeux M., Gruia M., Minghua G. and Fraissard J. "ZSM-5 Zeolite Synthesis in The Presence of A Copper –Phthalocyanine Complexes Characterization by ESR and ^{129}Xe NMR." Solid State Nuclear Magnetic Resonance. vol. 9. 1997. pp. 269-276.

[19] Raja R. and Ratanasamy P. "Oxidation of Cyclohexane over Copper Phthalocyanines Encapsulated in Zeolite." Catalysis Letters. vol. 48. 1997. pp. 1-10.

[20] Danly D. E. and Cambell C. R. **Kirk Othmer Encyclopedia of Chemical Technology** 3rd Ed. New York : Wiley. 1979. pp. 910.

[21] Cronstedt A. F. "Adsorption Equilibrium in Zeolite Molecular Sieves" [Online] Available : http://www.drjohn.demon.co.uk/adsorption.html. 2001

[22] Matar S. and Hatch L. F. **Chemistry of Petrochemical Processes.** Texas. Gulf Publishing Company. 1994. pp. 157-158.

[23] Barrer R. M. "Catalyst" [Online] Available : http://www.drjohn.demon.co.uk/catalyst.html. 2001

[24] Shriver D. F., Atkins P. W. and Langford C H. **Inorganic Chemistry.** Great Britain. ELBS. 1991.

[25] Meisel S. L. "Ion Exchange" [Online] Available : http://www.drjohn.demon.co.uk/ionexchange.html. 2001

[26] Donald W. B. **Zeolite Molecular Sieves Structure, Chemistry and Use**. Sydney. Wiley & Sons. 1974. pp. 529-537.

[27] Dent C. E. and Linstead R. P. J. Chem. Soc. 1936. pp. 1157-1163.

[28] Pratt L. S. **Organic Pigment**. New York. John Wiley & Sons. 1947.

[29] Roberton J. M. and Woodward I. J. Chem. Soc. 1940. pp. 36-48.

[30] Venkataraman K. **The chemistry of Synthetic Dyes**. New York. Academic Press. 1952. pp. 1118-1142.

[31] Garrett C. G. **Organic Semiconductors**. New York. Reinhold Publishing Corp. 1959. pp. 662-673.

[32] Nyberg S. C. **X-ray Analysis of Organic Structure**. New York. Academic Press. 1961.

[33] Heirich Z. **Color Chemistry, Synthesis, Properties and Application of Organic Dyes and Pigment**. New York. VCH Verlagsgesellschaft. 1987. pp. 74-82.

[34] Gordon P. F. and Gregory P. **Organic Chemistry in Color**. New York. Berlin Heidelberg. 1983. pp. 221-227.

[35] Murahashi S. I. and Naota T. **Comprehensive Organic Chemistry**. Oxford II. Pergamon. vol. 12. 1995. pp. 1177-1192.

[36] Olah G. A. and Molnar A. **Hydrocarbon Chemistry**. New York. John Wiley & Sons. 1995. pp. 291-372.

[37] Delprato F., Delmotte L., Guth J. L. and Huve L. "Synthesis of New Silica-Rich Cubic and Hexagonal Faujasites Using Crown-Ether-Based Supramolecules as Templates." Zeolites. vol. 10. 1991. pp. 546-552.

[38] Doungnier F., Patarin J. and Guth J. L. "Synthesis, Characterization, and Catalytic Properties of Silica-Rich Faujasites-Type Zeolite (FAU) nad its Hezagonal Analog (EMT) Prepared by Using Crown-Ethers as Templates." Zeolites. vol. 12. 1992. pp. 160-166.

[39] Borade R. B. and Clearfield A. "Synthesis of Beta Zeolite with high level of Tetrahedral Aluminium." Chem. Commun. 1996. pp. 625-626.

[40] Stephen G. D. **Oxford Chemistry Primers**. New York. Oxford University Press. 1997.

[41] Wade L. G. **Organic Chemistry.** New Jersy : Prentice-Hall, Inc. 1995

[42] Sooknoi T. and Limtrakul J. "Activity Enhancement by acetic acid in cyclohexane oxidation using Ti-Containing Zeolite Catalyst." Applied Catalysis A: General 233. 2002. pp. 227-237.

Appendices

Appendix A

A.1 Synthesis of zeolites

A.1.1 Zeolite Beta

The zeolite Beta employed in this thesis has been synthesized hydrothermally from an aluminosilicate gel with a nominal composition of

$$9SiO_2 : Al_2O_3 : Na_2O : 1.6TEAOH : 140H_2O$$

From this gel composition, the 35 grams of water is basis of calculation. Therefore, the mole composition is regulated to

$$0.1587SiO_2 : 0.0173Al_2O_3 : 0.0173Na_2O : 0.0277TEAOH : 1.0398H_2O$$

Therefore, the weight of materials is summarized in Table A.1.

Table A.1 Material weight of zeolite Beta (synthesis).

Materials	Mole composition	Weight (grams)
SiO_2	0.1587	9.539
Al_2O_3	0.0173	1.768
Na_2O	0.0173	1.074
TEAOH	0.0277	4.083
H_2O	1.0398	18.717

Calculation of SiO_2

SiO_2 9.539 grams prepared from 9.539 grams of fumed silica

Calculation of Al_2O_3 and Na_2O

$Na_2Al_2O_4$ consists of Na_2O = 37.57 % (w/w)

Al_2O_3 = 59.54 % (w/w)

Therefore,

Na_2O 37.57 grams prepared from $Na_2Al_2O_4$ 100 grams

Na_2O 1.074 grams prepared from $Na_2Al_2O_4$ (100/37.57)×1.074

= 2.8586 grams

$Na_2Al_2O_4$ 100 grams consists of Al_2O_3 59.54 grams

$Na_2Al_2O_4$ 2.8586 grams consists of Al_2O_3 (59.54/100)×2.8586

= 1.7020 grams

Thus, It required Al_2O_3 = 1.768-1.7020

= 0.065 grams = 6.375×10^{-4} mol

0.01134 mol of Al_2O_3 can prepared from $Al(OC_2H_5)_3$ that

$$2Al(OC_2H_5)_3 + 3H_2O \longrightarrow Al_2O_3 + 3C_2H_5OH$$

Al_2O_3 1 mol prepared from $Al(OC_2H_5)_3$ 2 mol

Al_2O_3 6.375×10^{-4} mol prepared from $Al(OC_2H_5)_3$ (2/1)× 6.375×10^{-4}

= 1.275×10^{-3} mol

= 0.2067 grams

Al_2O_3 1 mol prepared from H_2O 3 mol

Al_2O_3 6.375×10^{-4} mol prepared from H_2O (3/1)× 6.375×10^{-4}

= 1.888×10^{-3} mol

= 0.034 grams

Accordingly, water 0.034 grams was added into the gel composition.

Calculation of TEAOH

TEAOH (40%, w/w)

TEAOH 40 grams prepared from TEAOH solution 100 grams

TEAOH 4.083 grams prepared from TEAOH solution (100/40)×4.083

= 10.2075 grams

The TEAOH solution consists of water = 10.2075 – 4.083

= 6.1245 grams

Calculation of H_2O

The water is added = 18.717+0.034-6.1245

= 12.6265 grams

From above calculation, the materials required are summarized in Table A.2.

Table A.2 Summarized of required chemical reagents.

Material sources	SiO_2	Al_2O_3	Na_2O	TEAOH	Water
0.9947 g of $Na_2Al_2O_4$ (37.57% wt Na_2O, 59.54 % wt Al_2O_3)	-	0.5922	0.3737	-	-
0.2891 g of $Al(OC_2H_5)_3$	-	0.0909	-	-	-
30.1923 g of Ludox (40%SiO_2, w/w)	12.0769	-	-	-	18.1154
14.7998 g of TEAOH (40%, w/w)	-	-	-	5.9199	8.8799
8.0529 g of H_2O	-	-	-	-	8.0529
Total	12.0769	0.6831	0.3737	5.9199	35.0482

A.1.2 Zeolite EMT

The zeolite EMT employed in this thesis has been synthesized hydrothermally from an aluminosilicate gel with a nominal composition of

$10SiO_2 : Al_2O_3 : 2.4Na_2O : 0.7$ 18-Crown-6 $: 140H_2O$

From this gel composition, the 35 grams of water is basis of calculation. Therefore, the mole composition is regulated to

$0.0983SiO_2 : 0.0098Al_2O_3 : 0.0264Na_2O : 0.0068TPABr : 1.3778H_2O$

Therefore, the weight of materials is summerized in Table A.3.

Table A.3 Material weight of zeolite Beta (synthesis).

Materials	Mole composition	Weight (grams)
SiO_2	0.0983	5.9
Al_2O_3	9.8077×10^{-3}	1
Na_2O	0.0264	1.64
TPABr	6.8856×10^{-3}	1.82
H_2O	1.3778	24.8

Calculation of SiO_2

Ludox (40%SiO_2, w/w)

SiO_2 40 grams prepared from Ludox solution 100 grams

SiO_2 5.9 grams prepared from Ludox solution $(100/40) \times 5.9$

$= 14.75$ grams

Ludox solution 14.75 grams comprise of water $= 14.75-5.9$

$= 8.85$ grams

Calculation of Al_2O_3 and Na_2O

$Na_2Al_2O_4$ consists of Na_2O = 37.57 % (w/w)

Al_2O_3 = 59.54 % (w/w)

Therefore,

Al_2O_3 59.54 grams prepared from $Na_2Al_2O_4$ 100 grams

Al_2O_3	1	grams prepared from $Na_2Al_2O_4$	(100/59.54)×1		
			= 1.68	grams	
$Na_2Al_2O_4$	100	grams consists of Na_2O	37.37	grams	
$Na_2Al_2O_4$	1.68	grams consists of Na_2O	(37.37/100)×1.68		
			= 0.63	grams	

Thus, It required Na_2O = 1.64-0.63

= 1.01 grams = 0.0163 mol

0.0136 mol of sodium oxide can be prepared from

$$2NaOH \longrightarrow Na_2O + H_2O$$

Na_2O	1	mol prepared from NaOH	2	mol
Na_2O	0.0163	mol prepared from NaOH	(2/1)×0.0163	
			= 0.0326	mol
			= 1.304	grams
NaOH	2	mol produced H_2O	1	mol
NaOH	0.0326	mol produced H_2O	(1/2)×0.0326	
			= 0.0163	mol
			= 0.2934	grams

Calculation of H_2O

The water is added = 24.8-8.85-0.2934

= 15.6566 grams

From above calculation, the materials required are summarized in Table A.4.

Table A.4 Summarized of required chemical reagents.

Material sources	SiO_2	Al_2O_3	Na_2O	TPABr	Water
0.2773 g of $Na_2Al_2O_4$ (37.57% wt Na_2O, 59.54 % wt Al_2O_3)	-	0.1651	0.1042	-	-
0.3838 g of NaOH	-	-	0.2974	-	0.0864
9.7338 g of Ludox (40%SiO_2, w/w)	3.8935	-	-	-	5.8403
0.8622 g of TPABr	-	-	-	0.8622	-
29.0733 g of H_2O	-	-	-	-	29.0733
Total	3.8935	0.1651	0.4016	0.8622	35.0000

Appendix B

B.1 X-ray diffraction of standard pattern

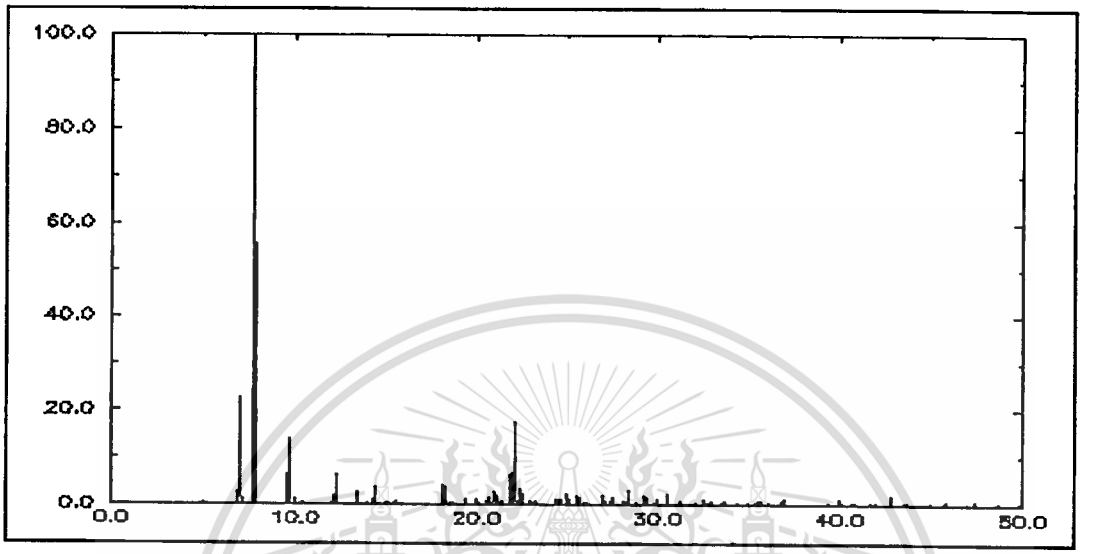

Figure B.1 X-ray diffraction pattern of standard Beta.

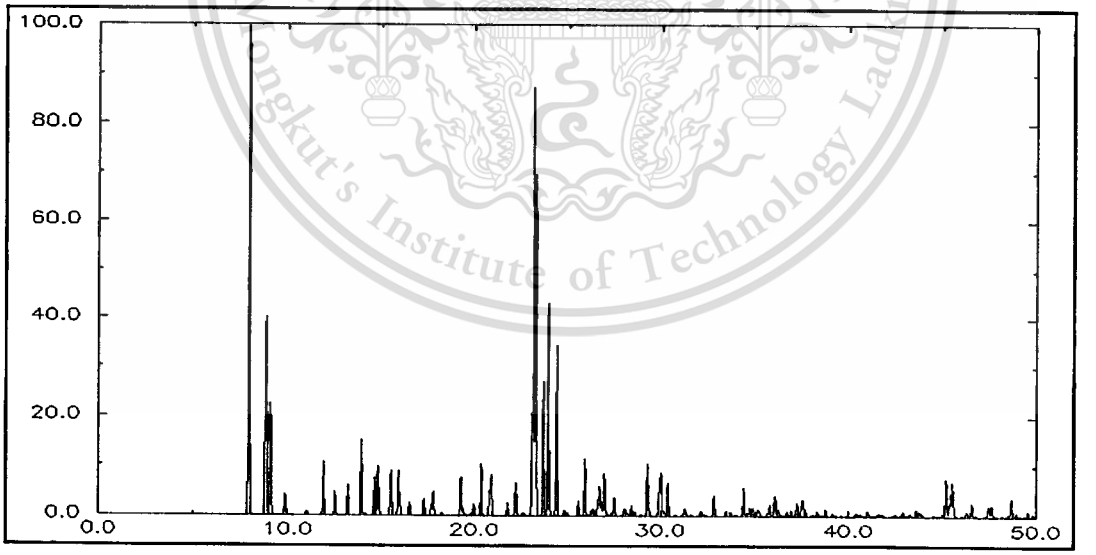

Figure B.2 X-ray diffraction pattern of standard EMT.

B.2 Determination of silicon/aluminium ratio of zeolites

B.2.1 Determination of silicon

The standard curve is plotted between concentration and absorbance as linear curve. The silicon concentration of zeolites can be calculated by comparing with the standard calibration curve. The concentration and absorbance of standard and sample are shown in Table B.1.

Table B.1 The concentration and absorbance of silicon determined by UV-Vis Spectrophotometry.

Material	Concentration	Absorbance (815 nm)
Standard of silicon	0.231	0.073
Standard of silicon	0.462	0.238
Standard of silicon	0.693	0.400
Standard of silicon	0.924	0.552
Zeolite EMT	-	0.349

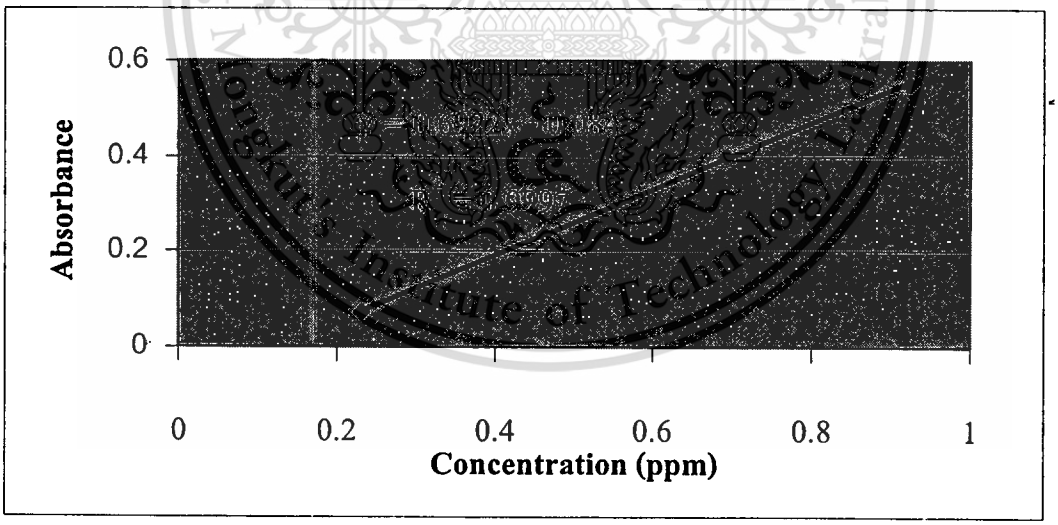

Figure B.3 Calibration curve and equation related between concentration and absorbance.

From the curve, relation between concentration and absorbance can be determined by;

$$Y = 0.6922\,[X] - 0.0840$$

Where, X = silicon concentration (ppm)

Y = absorbance

From the experiment, this sample solution is diluted 100 times as follows:

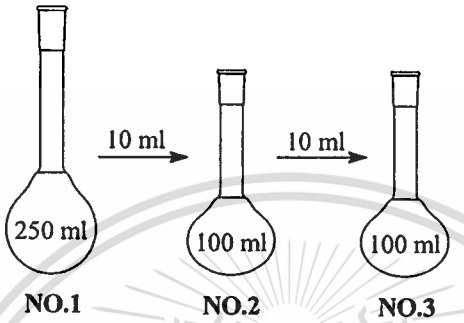

This equation is used for calculation silicon of zeolite sample. For example, the absorbance of zeolite BEA is 0.349 then;

$$Y = 0.6922[Si] - 0.0840$$

$$[Si] = 0.625541 \text{ ppm}$$

The accurate silicon concentration of the flask NO.1is 62.5541 ppm (or 15.6385 mg/250 ml). Therefore, the mole of silicon is 15.6385/28 = 0.5585.

B.2.2 Determination of aluminium

The standard curve is plotted between concentration and absorbance as linear curve. The aluminium concentration of zeolites can be calculated by comparing with the standard calibration curve. The concentration and absorbance of standard and sample are shown in Table B.2.

Table B.2 The concentration and absorbance of aluminium determined by UV-Vis Spectrophotometry.

Material	Concentration	Absorbance (410 nm)
Standard of aluminium	0.502	0.087
Standard of aluminium	1.004	0.209
Standard of aluminium	1.506	0.332
Standard of aluminium	2.008	0.456
Zeolite EMT	-	0.277

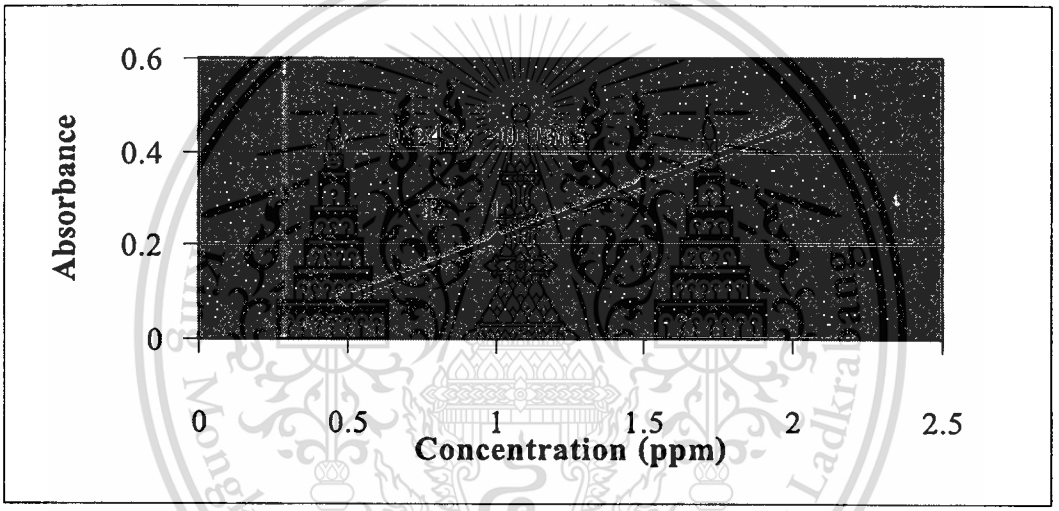

Figure B.4 Calibration curve and equation related between concentration and absorbance.

From the curve, relation between concentration and absorbance can be determined by;

$$Y = 0.2450[X] - 0.0365$$

Where, X = aluminium concentration (ppm)

Y = absorbance

From the experiment, this sample solution is diluted 10 times as follows:

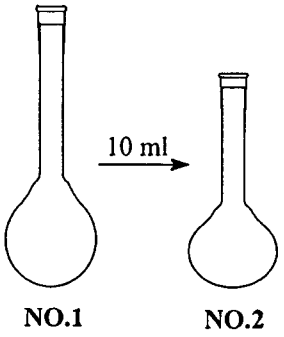

This equation is used for calculation aluminium of zeolite sample. For example, the absorbance of zeolite BEA is 0.277 then;

$$Y = 0.2450[Al] - 0.0365$$

$$[Al] = 1.2792 \text{ ppm}$$

The accurate aluminium concentration of the flask NO.1is 12.7923 ppm (or 3.1981 mg/250 ml). Therefore, the mole of aluminium is 3.1981/27 = 0.1184.

From the above results, the silicon/aluminium ratio is calculated as follows:

$$\frac{\text{Mol of silicon}}{\text{Mol of aluminium}} = \frac{[Si]}{[Al]}$$

Thus, Si/Al of zeolite EMT is 4.7153.

Table B.3 Elemental analysis of synthetic zeolite

Material	Silicon	Aluminium	Si/Al	SiO_2/Al_2O_3
Zeolite EMT	0.5585	0.1184	4.7153	4.7153
Zeolite BEA	0.6320	0.1282	4.9266	4.9266

B.3 Calculation of the cobalt that is exchangeable into the cavities of zeolite

B.3.1 Exchangeable cobalt in zeolite EMT

Unit cell of zeolite EMT comprise 384 of oxygen atom (O = 384) and 192 of silicon atom and aluminium atom

$$Si+Al = 192 \quad (1)$$

According to B.2, it is know that

$$Si/Al = 4.7 \quad (2)$$

From (1) and (2),

Si = 157 atom

Al = 35 atom

Thus, 1 unit cell of zeolite EMT can be exchanged with 17.5 ≈ 17 atom of cobalt (II) ion. Accordingly,

1 mol of CoEMT = Silicon + Aluminium + Cobalt + Oxygen

= (157×28) + (35×27) + (17×58.9) + (384×16)

= 12,486.3 grams

CoEMT	12,486.3	grams consists of Co	37.37	grams
CoEMT	1	grams consists of Co	0.0802	grams
			= 0.00136	mole

Accordingly, it can be concluded that 0.00136 mol of cobalt ion could be exchange with sodium ion in the zeolite framework (1 gram of zeolite).

B.3.2 Exchangeable cobalt in zeolite BEA

Unit cell of zeolite BEA comprise 128 of oxygen atom (O = 128) and 64 of silicon atom and aluminium atom

$$Si+Al = 64 \quad (1)$$

According to B.2, it is know that

$$Si/Al = 4.9 \quad (2)$$

From (1) and (2),

Si ≈ 53 atom

Al ≈ 11 atom

Thus, 1 unit cell of zeolite BEA can be exchanged with 5.5 ≈ 5 atom of cobalt (II) ion. Accordingly,

1 mol of CoBEA = Silicon + Aluminium + Cobalt + Oxygen

= (53×28) + (11×27) + (5×58.9) + (128×16)

= 4123.5 grams

CoBEA	4123.5	grams consists of Co	294.5	grams
CoBEA	1	grams consists of Co	0.0714	grams
			= 0.00121	mole

Accordingly, it can be concluded that 0.00121 mol of cobalt ion could be exchange with sodium ion in the zeolite framework (1 gram of zeolite).

B.4 Calculation the amount of cobalt nitrate ($Co(NO_3)_2.6H_2O$) using in impregnation.

B.4.1 Impregnation of cobalt nitrate in zeolite EMT.

From the calculation of the cobalt that is exchangeable into the cavities of zeolite discussed earlier, it was found that 0.00136 mol of cobalt ion could be exchanged with sodium ion in the zeolite framework (1 grams of zeolite). Therefore;

Zeolite EMT	1	grams can consist with Co	0.00136	mol
Zeolite EMT	2	grams can consist with Co	0.00272	mol

1 mol of cobalt nitrate ($Co(NO_3)_2.6H_2O$) = (1×58.9) + (2×14) + (12×16) + (12×1)

= 290.9 grams

Therefor;

Zeolite EMT 2 grams can be impregnated with 0.00272×290.9

= 0.79 grams

B.4.2 Impregnation of cobalt nitrate in zeolite BEA.

From the calculation of the cobalt that is exchangeable into the cavities of zeolite discussed earlier, it was found that 0.00121 mol of cobalt ion could be exchanged with sodium ion in the zeolite framework (1 grams of zeolite). Therefore;

Zeolite BEA	1	grams can consist with Co	0.00121	mol
Zeolite BEA	2	grams can consist with Co	0.00242	mol

1 mol of cobalt nitrate ($Co(NO_3)_2.6H_2O$) $= (1\times58.9) + (2\times14) + (12\times16) + (12\times1)$

$= 290.9$ grams

Therefor;

Zeolite BEA 2 grams can be impregnated with 0.00242×290.9

$= 0.71$ grams

Appendix C

Fourier Transform Infrared Spectrophotometry

Table C.1 Major absorption band from Fourier Transform Infrared Spectrophotometry

CoPc [14]	H2Pc [13]	Imp-EMT-encap	Ion-EMT-encap	Imp-BEA-encap	Ion-BEA-encap
1289	-	1286	1285	1288	1288
1332	1334	1330	1328	1332	1331
-	1384	-	-	-	-
1426	-	1425	1424	1427	1426
1448	-	1448	1445	1442	1446
1520	-	1519	1520	1516	1520
1610	-	1612	1615	1610	1612

Appendix D

UV/Visible Spectrophotometry

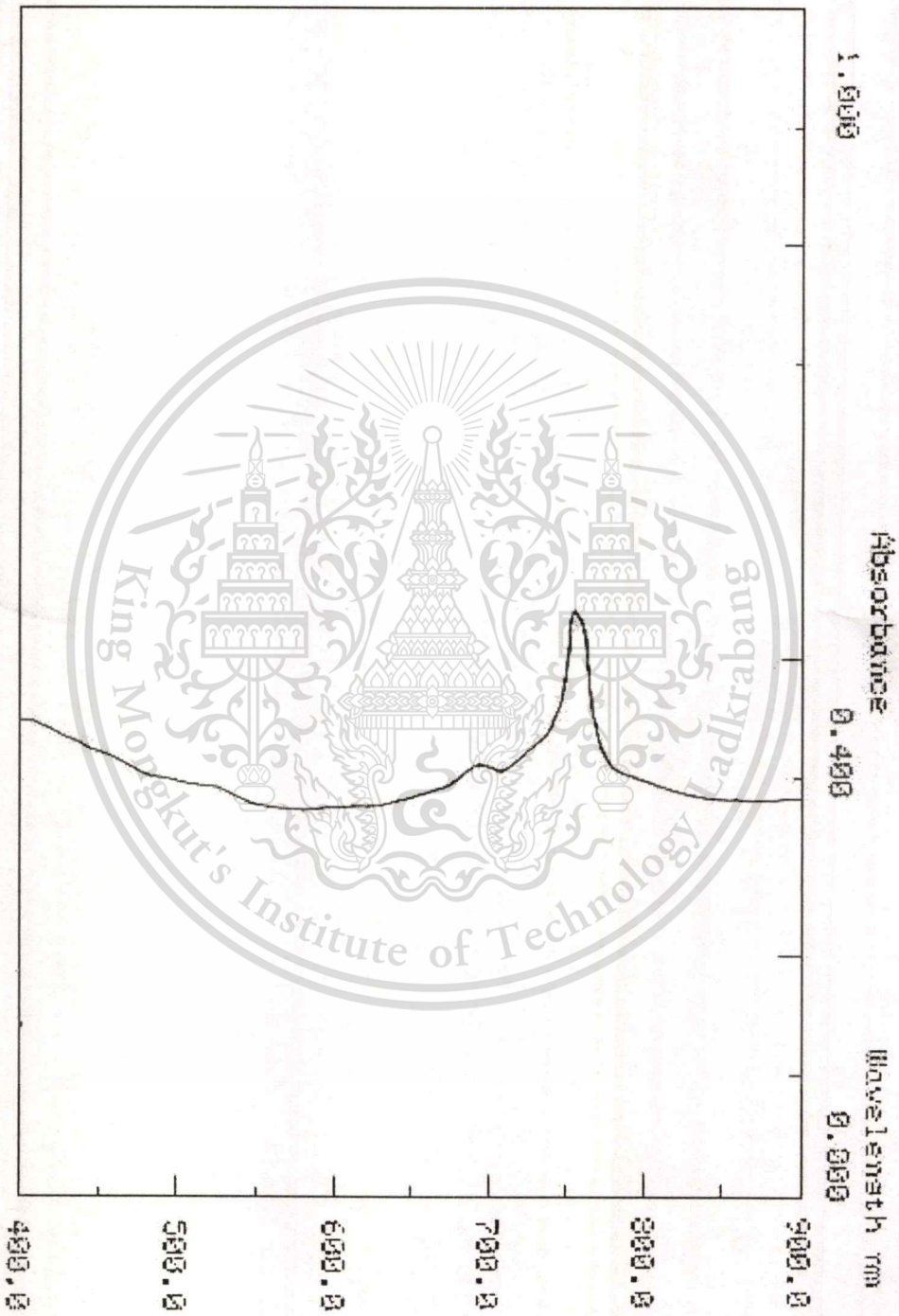

Figure D.1 UV/Vis absorption band of Ion-EMT-encap

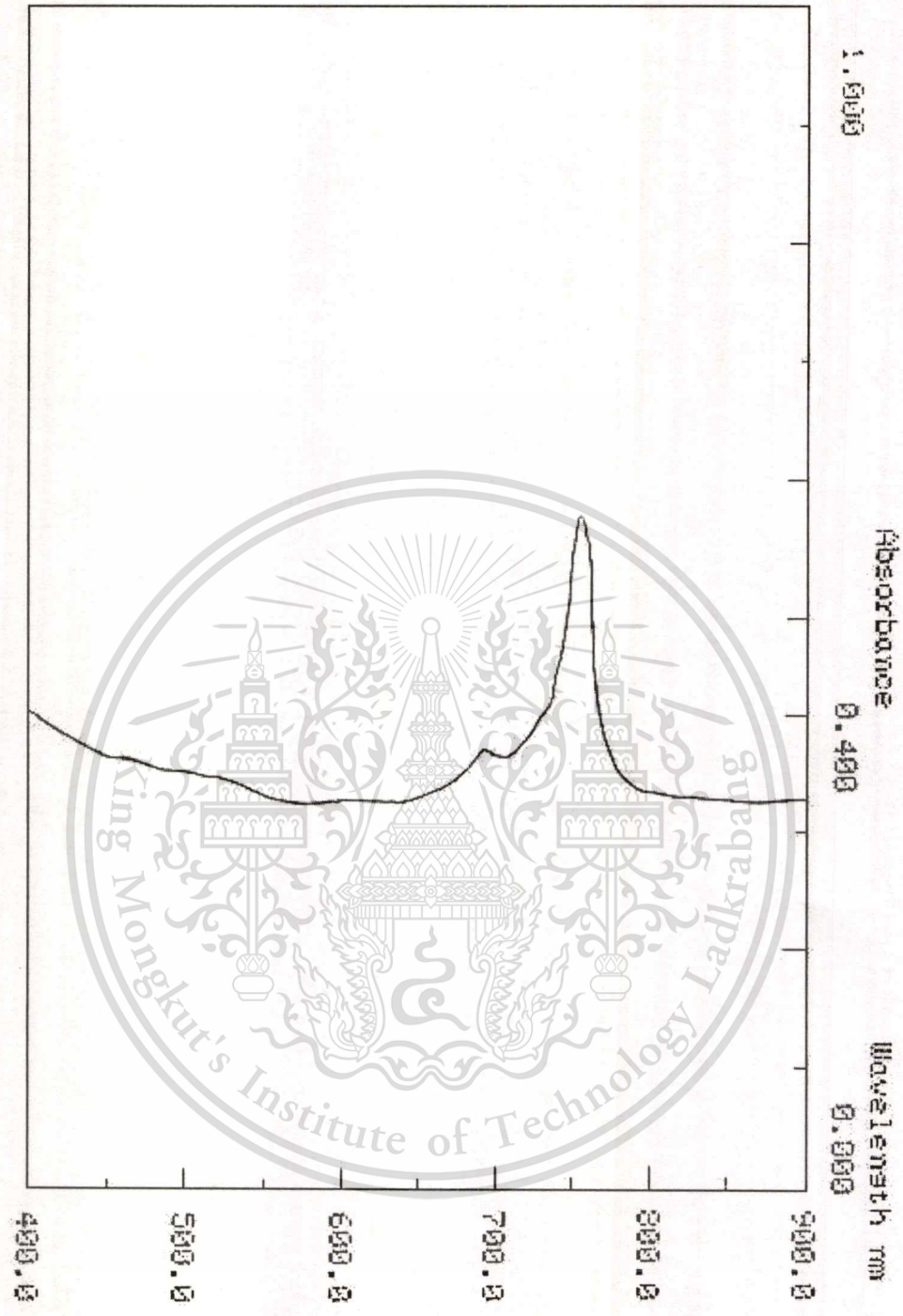

Figure D.2 UV/Vis absorption band of Imp-EMT-encap

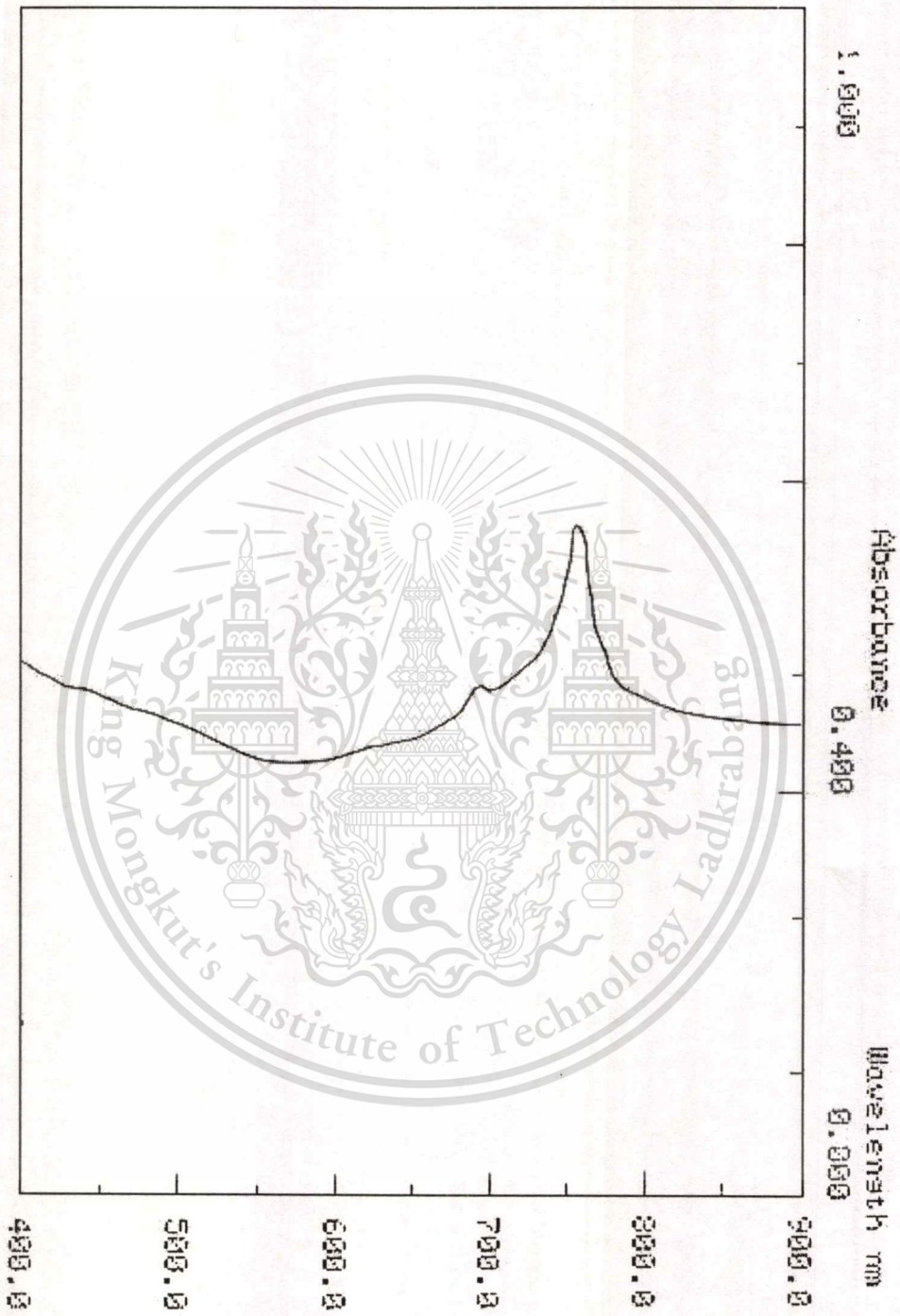

Figure D.3 UV/Vis absorption band of Ion-BEA-encap

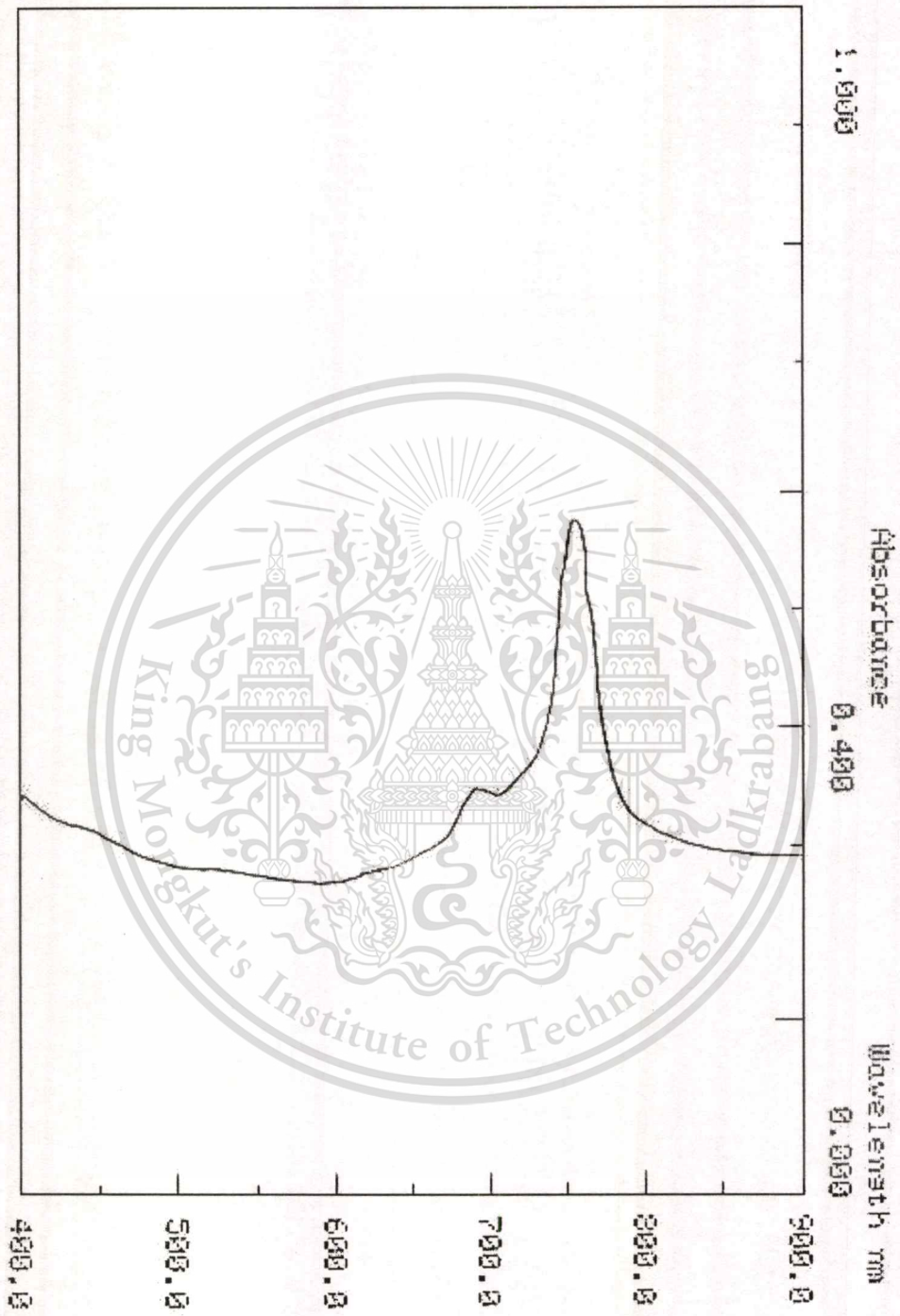

Figure D.4 UV/Vis absorption band of Ion-BEA-encap

Table D.1 Major Absorption Band from UV/Vis Spectroscopy

Synthetic zeolite	Absorption band (nm.)
Ion-EMT-encap	695 785
Imp-EMT-emcap	697 784
Ion-BEA-encap	691 780
Imp-BEA-encap	690 781
CoPc [14]	967 784

Appendix E

Thermogravimetric Analysis

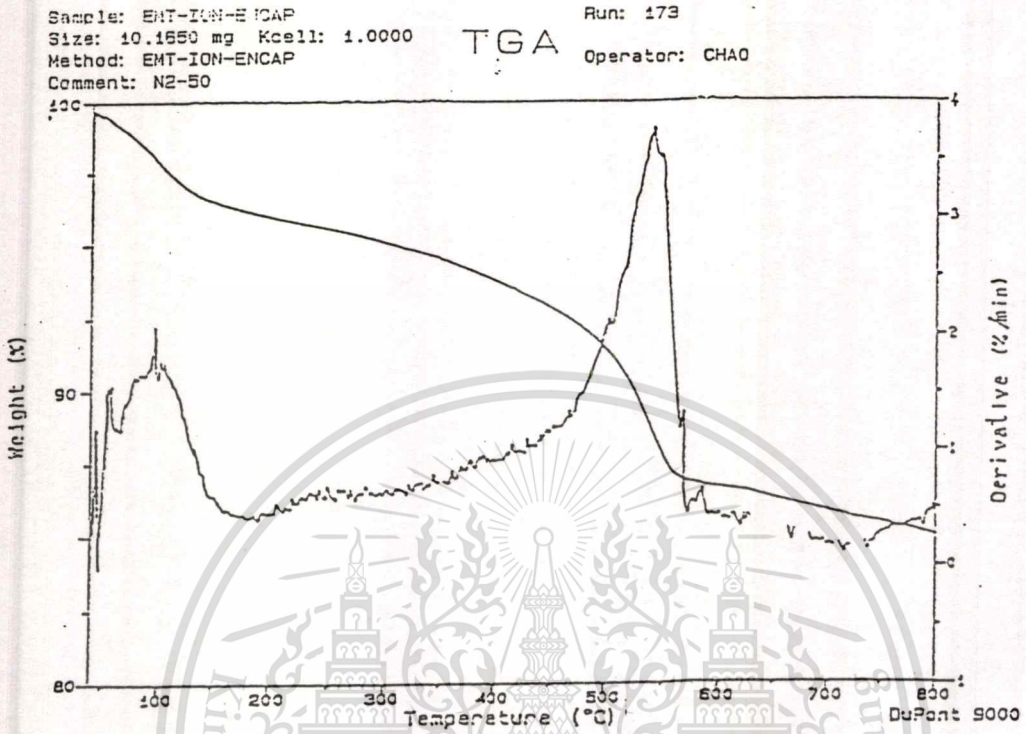

Figure E.1 Thermogram of Ion-EMT-encap

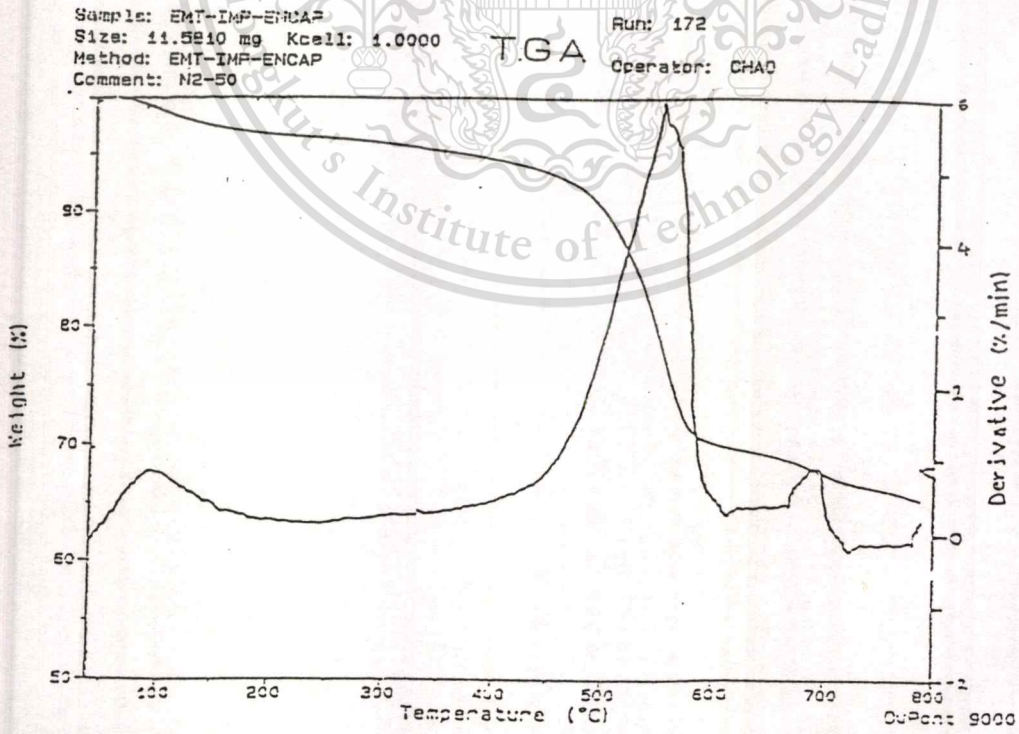

Figure E.2 Thermogram of Imp-EMT-encap

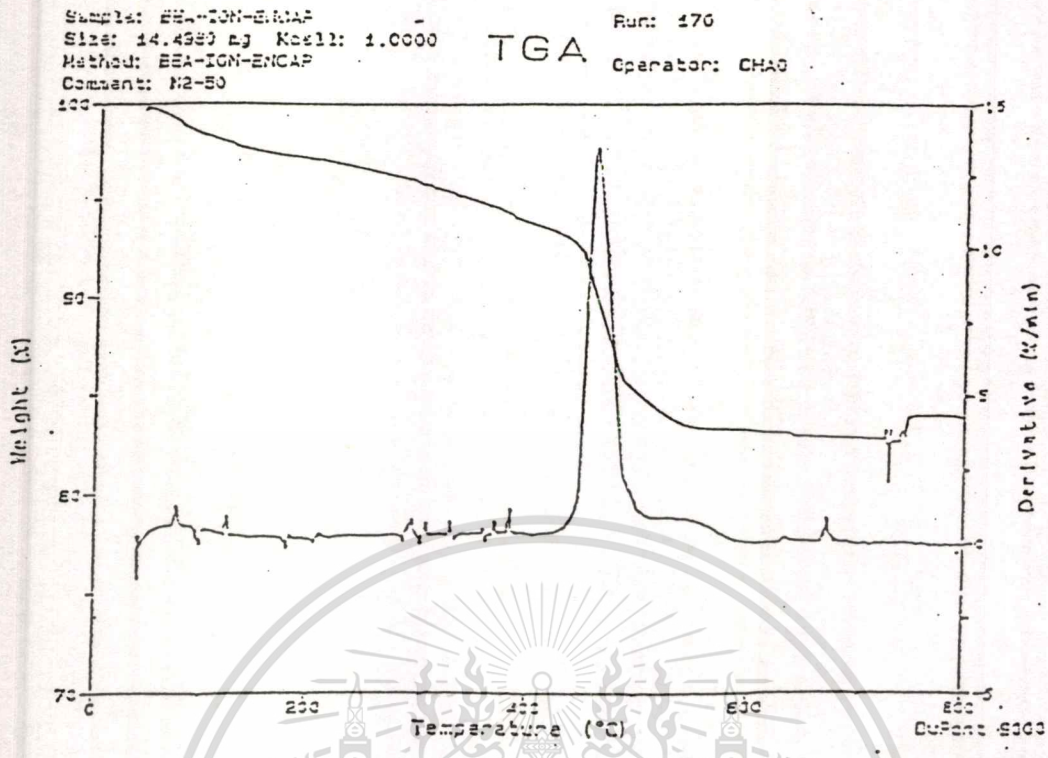

Figure E.3 Thermogram of Ion-BEA-encap

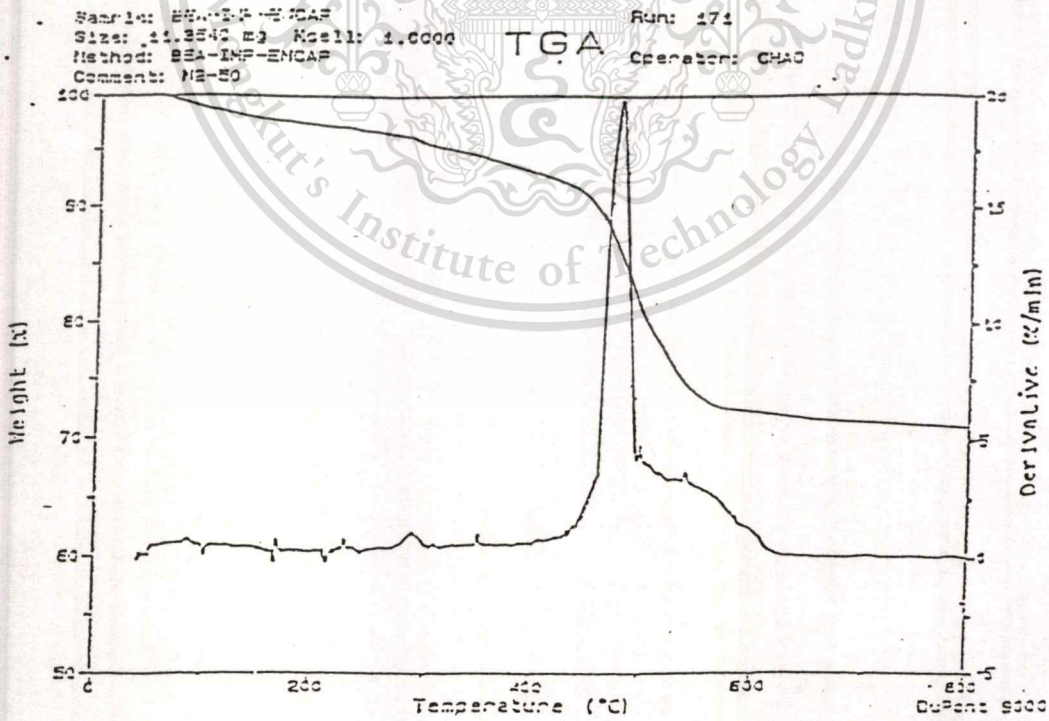

Figure E.4 Thermogram of Imp-BEA-encap

Table E.1 Decomposition Temperature

Synthetic zeolite	Decomposition temp.
Ion-EMT-encap	508
Imp-EMT-encap	510
Ion-BEA-encap	482
Imp-BEA-encap	480
CoPc [13]	500

Appendix F

Atomic Absorption Spectrometry

Table F.1 The amount of cobalt ion in the cavities of zeolite.

Synthetic zeolite	The amount of cobalt ion (10^{-4} mole/gram of zeolite)
Ion-EMT-encap	9.4
Imp-EMT-encap	13.3
Ion-BEA-encap	8.9
Imp-BEA-encap	12.6

Appendix G

Correction Factor Curve for Gas Chromatography Analysis and Product Calculation

Correction Factor Curve Preparation

The correction factor curve, a standard curve for correcting the area percentage from gas chromatography analysis to the relative molar concentration of sample, was prepared by analysis of the standard solution containing cyclohexanone and cyclohexanone oxime using gas chromatography. Standard concentration (the percentage that related to percent mole) was plotted with the area percentage of the sample.

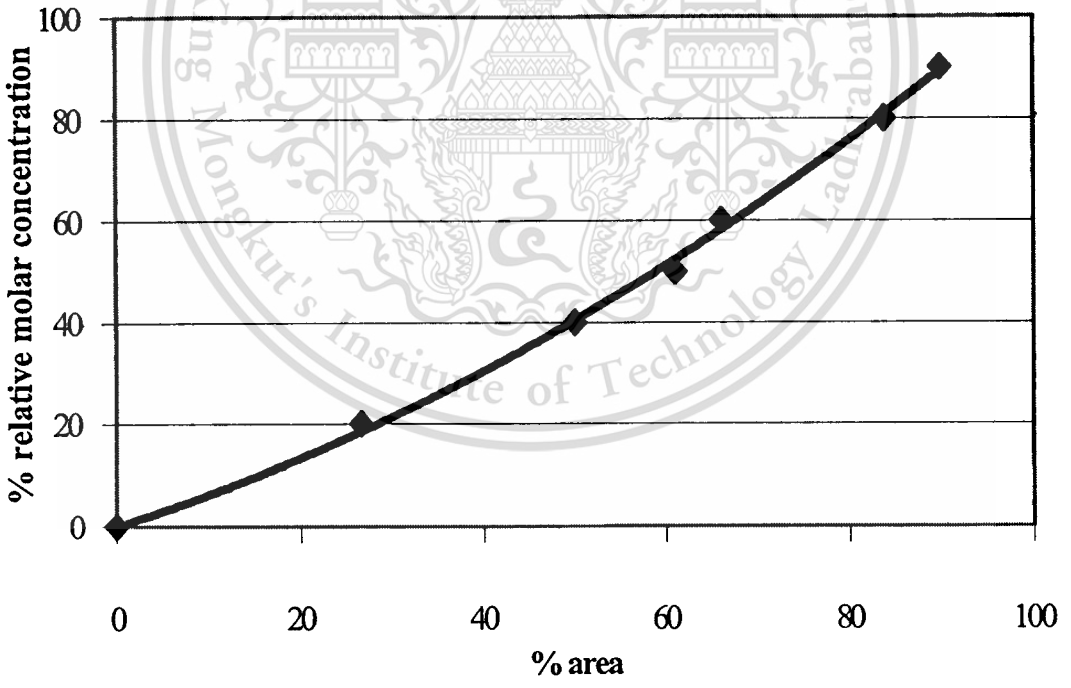

Figure G.1 Correction factor curve of cyclohexane

Equation fitted the correction factor curve of relative molar concentration of cyclohexane is shown below;

$$y = 0.0048x^2 + 0.5567x + 0.4906$$

- x is the area percentage of cyclohexane in sample
- y is the relative molar concentration of cyclohexane

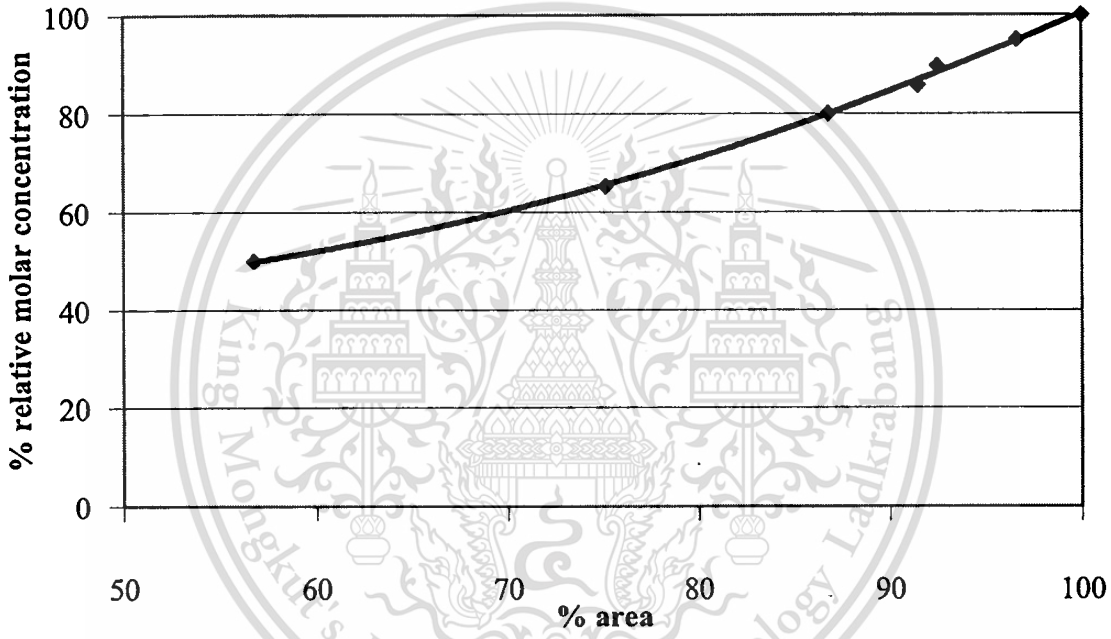

Figure G.2 Correction factor curve of cyclohexanone

Equation fitted the correction factor curve of relative molar concentration of cyclohexanone

$$y = 0.0065x^2 + 1.0198x + 0.1142$$

- x is the area percentage of cyclohexanone
- y is the relative molar concentration of cyclohexanone

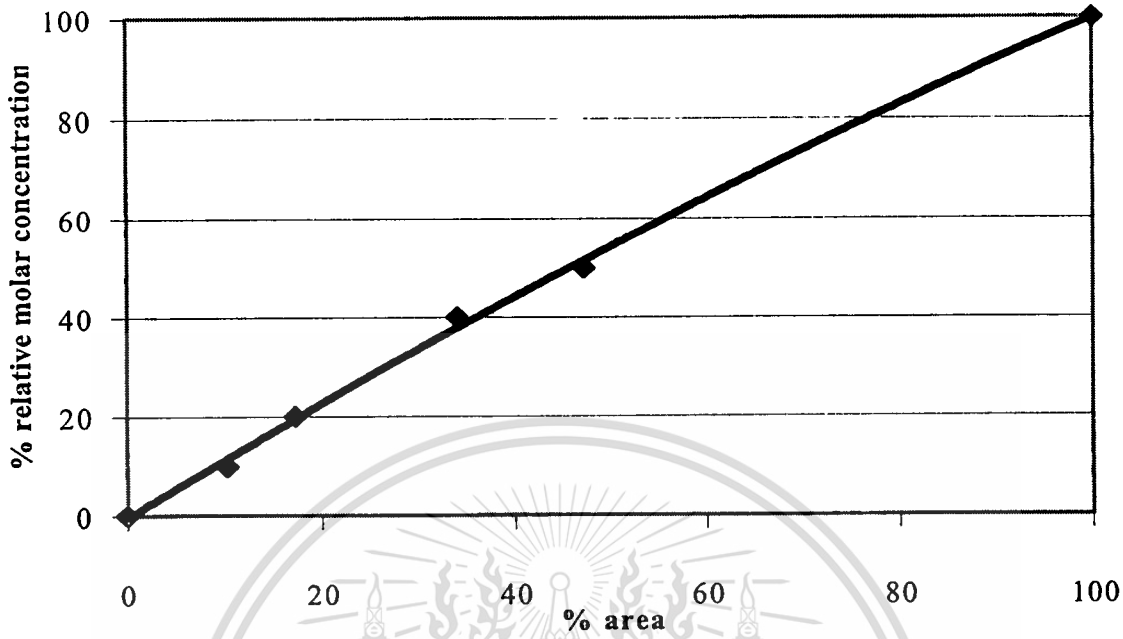

Figure G.3 Correction factor curve of cyclohexanol

Equation fitted the correction factor curve of relative molar concentration of cyclohexanol

$$y = -0.0019x^2 + 1.1886x - 0.4335$$

- x is the area percentage of cyclohexanol
- y is the relative molar concentration of cyclohexanol

After correcting the area percentage to relative molar concentration of sample, the mole percentage of sample was calculated by normalization.

Conversion

The conversion of cyclohexane can be calculated from the remaining cyclohexane in the reaction. It can be expressed as following.

% Conversion of cyclohexane = 100 – mole percent of remaining cyclohexane

Selectivity

The selectivity of cyclohexanone is the ratio of cyclohexane that converted to cyclohexanone over all cyclohexane that convert to all products. It can be expressed as following.

$$\% \text{ Selectivity of cyclohexanone} = \frac{\% \text{ Yield of cyclohexanone}}{\% \text{ Conversion of cyclohexane}} \times 100$$

Example

The product concentration was calculated from GC result. For example, the area percentage from the reaction using Ion-BEA-encap as a catalyst in acetic acid for 6 hours in the Parr reactor with oxygen 300 psi is shown in Figure I.3.

Peak No	Ret. Time (min)	Peak Name	Result ()	Area (counts)
1	1.47	cyclohexane	92.807	328554
2	3.05	cyclohexanone	4.319	15290
3	3.78	cyclohexanol	2.874	10175
		Totals	100	354019

Figure I.3 Area percentage of products remaining reaction from gas chromatography

The relative molar concentration of cyclohexane

The relative molar concentration of cyclohexane was calculated from equation fitted the correction factor curve of percent relate with mole of cyclohexane

$$y = 0.0048x^2 + 0.5567x + 0.4906$$

- x is the area percentage of cyclohexane
- y is the relative molar concentration of cyclohexane

$$\text{Relative molar concentration of cyclohexane} = 0.0048(92.807)^2 + 0.5567(92.807) + 0.4906$$
$$= 93.50$$

The relative molar concentration of cyclohexanol

The relative molar concentration of cyclohexanol can be calculated from the equation fitted the correction factor curve of relative molar concentration of cyclohexanol.

$$y = -0.0019x^2 + 1.1886x - 0.4335$$

- x is the area percentage of cyclohexanol
- y is the relative molar concentration of cyclohexanol

Relative molar concentration of cyclohexanol $= -0.0019(2.874)^2 + 1.1886(2.874) - 0.4335$

$= 2.97$

The relative molar concentration of cyclohexanone

The relative molar concentration of cyclohexanone can be calculated from the equation fitted the correction factor curve of relative molar concentration of cyclohexanone.

$$y = 0.0065x^2 + 1.0198x + 0.1142$$

- x is the area percentage of cyclohexanone
- y is the relative molar concentration of cyclohexanone

Relative molar concentration of cyclohexanone $= 0.0065(4.319)^2 + 1.0198(4.319) + 0.1142$

$= 4.64$

Normalization

Normalization all of product would lead to yield of product, conversion and selectivity.

Total relative molar concentration of sample = 93.50 + 2.97 + 4.64

= 101.11

Normalized to 100 percent

Mole percentage of cyclohexane = (93.50 × 100)/101.11

= 92.48 %

Mole percentage of cyclohexanol = (2.97 × 100)/101.11

= 2.93 %

Mole percentage of cyclohexanone = (4.64 × 100)/101.11

= 4.59 %

Conversion of cyclohexanone

The conversion of cyclohexane was calculated by equation as following.

% Conversion of cyclohexane = 100 – mole percent of remaining cyclohexanone

= 100 – 92.48

= 7.52 %

Selectivity of cyclohexanone

The selectivity of cyclohexanone was calculated by equation as following.

$$\% \text{ Selectivity of cyclohexanone} = \frac{\% \text{ Yield of cyclohexanone}}{\% \text{ Conversion of cyclohexane}} \times 100$$

$$= (4.59/7.52) \times 100$$

$$= 61.00\ \%$$

Appendix H

Surface Analysis

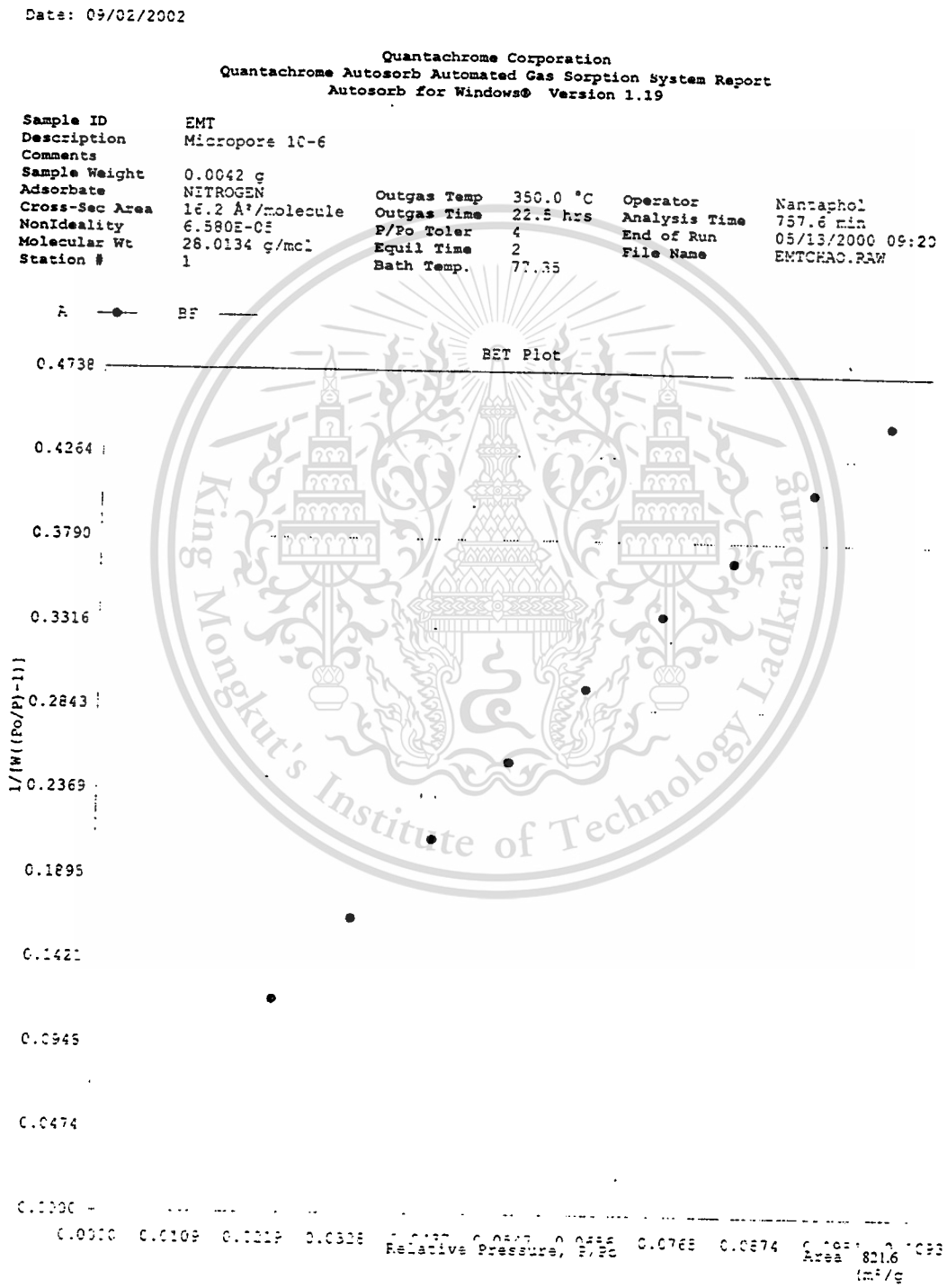

Figure H.1 BET surface area of zeolite EMT

Date: 09/02/2002

Quantachrome Corporation
Quantachrome Autosorb Automated Gas Sorption System Report
Autosorb for Windows® Version 1.19

Sample ID	Beta 5				
Description	Micropore 10-6				
Comments					
Sample Weight	0.0012 g				
Adsorbate	NITROGEN	Outgas Temp	350.0 °C	Operator	Nantaphol
Cross-Sec Area	16.2 Å²/molecule	Outgas Time	22.5 hrs	Analysis Time	397.0 min
NonIdeality	6.580E-05	P/Po Toler	4	End of Run	05/14/2000 12:35
Molecular Wt	28.0134 g/mol	Equil Time	2	File Name	BEACHAO.RAW
Station #	1	Bath Temp.	77.35		

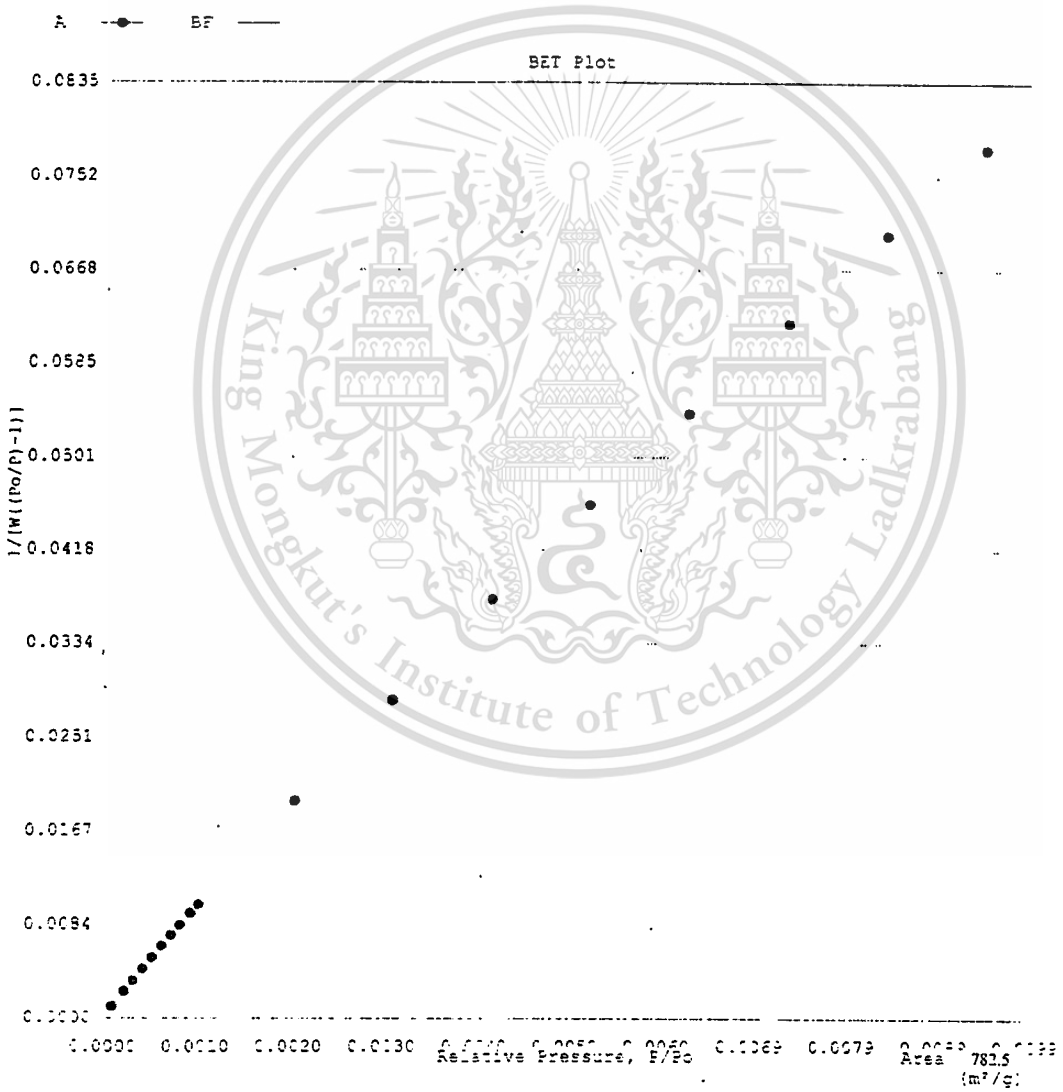

Figure H.2 BET surface area of zeolite BEA

Date: 09/02/2002

Quantachrome Corporation
Quantachrome Autosorb Automated Gas Sorption System Report
Autosorb for Windows® Version 1.19

Sample ID	emt_ion				
Description	Micropore 10-6				
Comments					
Sample Weight	0.0020 g				
Adsorbate	NITROGEN	Outgas Temp	350.0 °C	Operator	Nantaphol
Cross-Sec Area	16.2 Å²/molecule	Outgas Time	22.5 hrs	Analysis Time	573.4 min
NonIdeality	6.560E-05	P/Po Toler	4	End of Run	05/20/2009 12:32
Molecular Wt	28.0134 g/mol	Equil Time	2	File Name	EMTCHAOI.RAW
Station #	1	Bath Temp.	77.35		

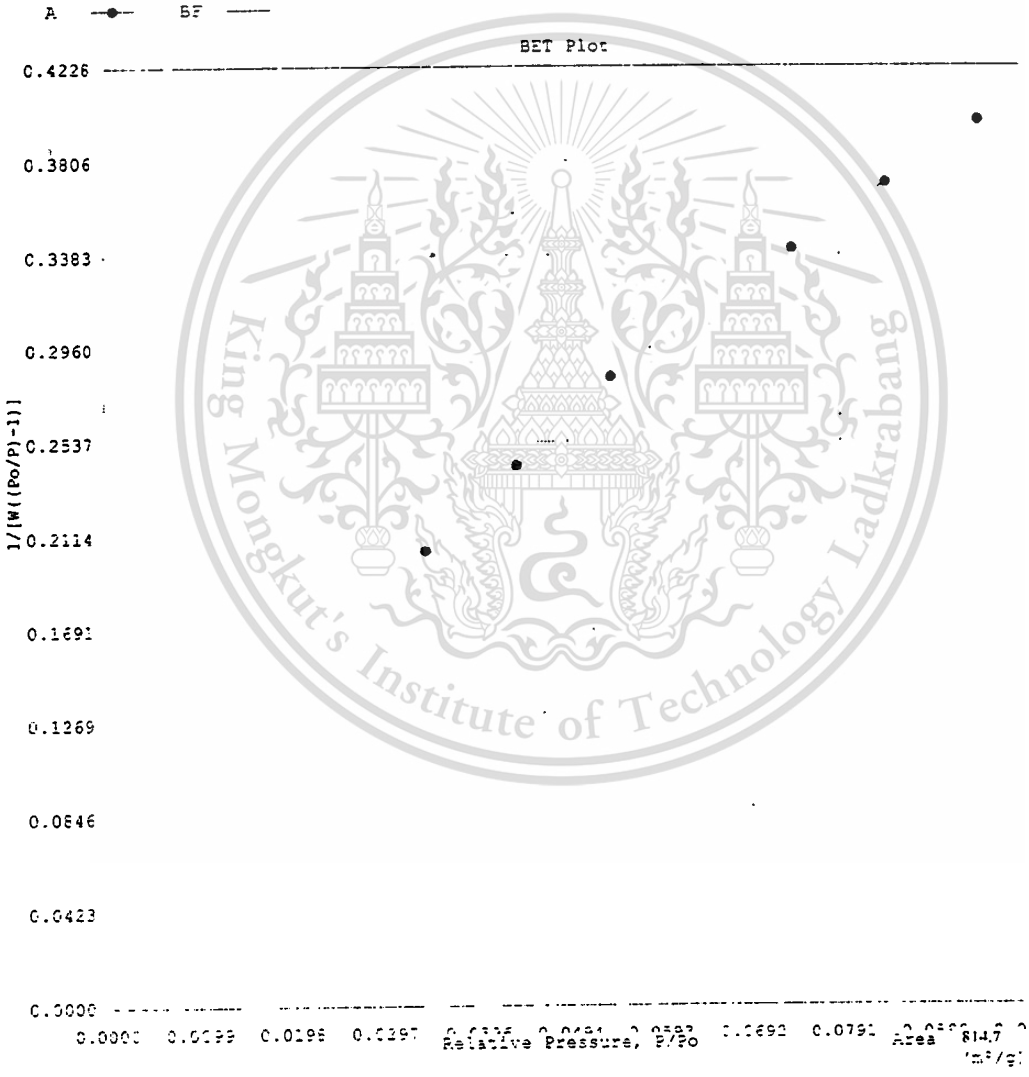

Figure H.3 BET surface area of Ion-EMT

Date: 09/02/2002

Quantachrome Corporation
Quantachrome Autosorb Automated Gas Sorption System Report
Autosorb for Windows® Version 1.19

Sample ID	beaion				
Description	Micropore 10-6				
Comments					
Sample Weight	0.0012 g				
Adsorbate	NITROGEN	Outgas Temp	350.0 °C	Operator	Nantaphol
Cross-Sec Area	16.2 Å²/molecule	Outgas Time	22.5 hrs	Analysis Time	397.0 min
NonIdeality	6.580E-05	P/Po Toler	4	End of Run	05/14/2000 12:35
Molecular Wt	28.0134 g/mol	Equil Time	2	File Name	BEACHAO.RAW
Station #	1	Bath Temp.	77.35		

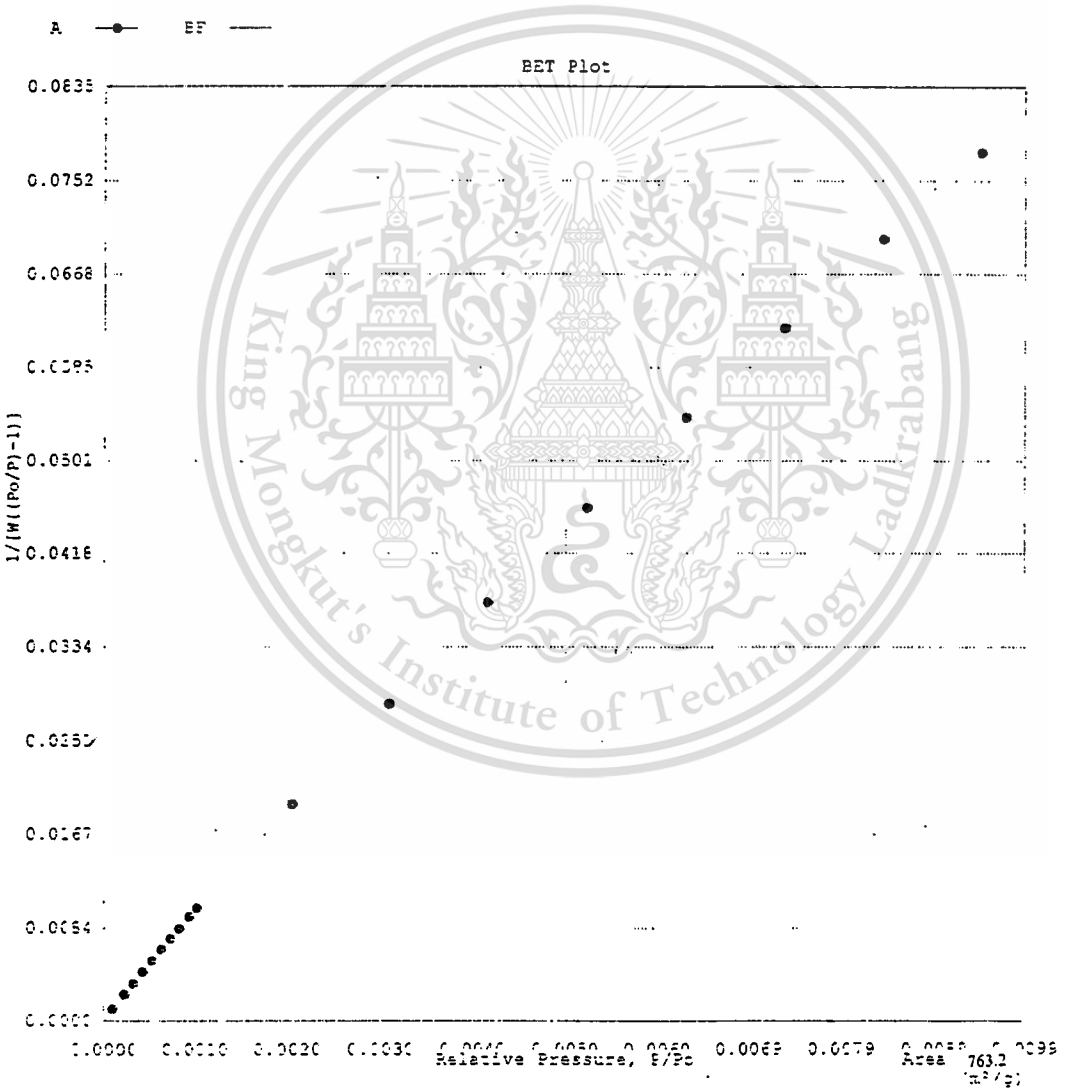

Figure H.4 BET surface area of Ion-BEA

Date: 09/02/2002

Quantachrome Corporation
Quantachrome Autosorb Automated Gas Sorption System Report
Autosorb for Windows® Version 1.19

Sample ID	emt-imp				
Description	Micropore 10-6				
Comments					
Sample Weight	0.0042 g				
Adsorbate	NITROGEN	Outgas Temp	350.0 °C	Operator	Nantaphol
Cross-Sec Area	16.2 Å²/molecule	Outgas Time	22.5 hrs	Analysis Time	787.6 min
NonIdeality	6.580E-05	P/Po Toler	4	End of Run	05/13/2000 09:20
Molecular Wt	28.0134 g/mol	Equil Time	2	File Name	EMTCHAC.RAW
Station #	1	Bath Temp.	77.35		

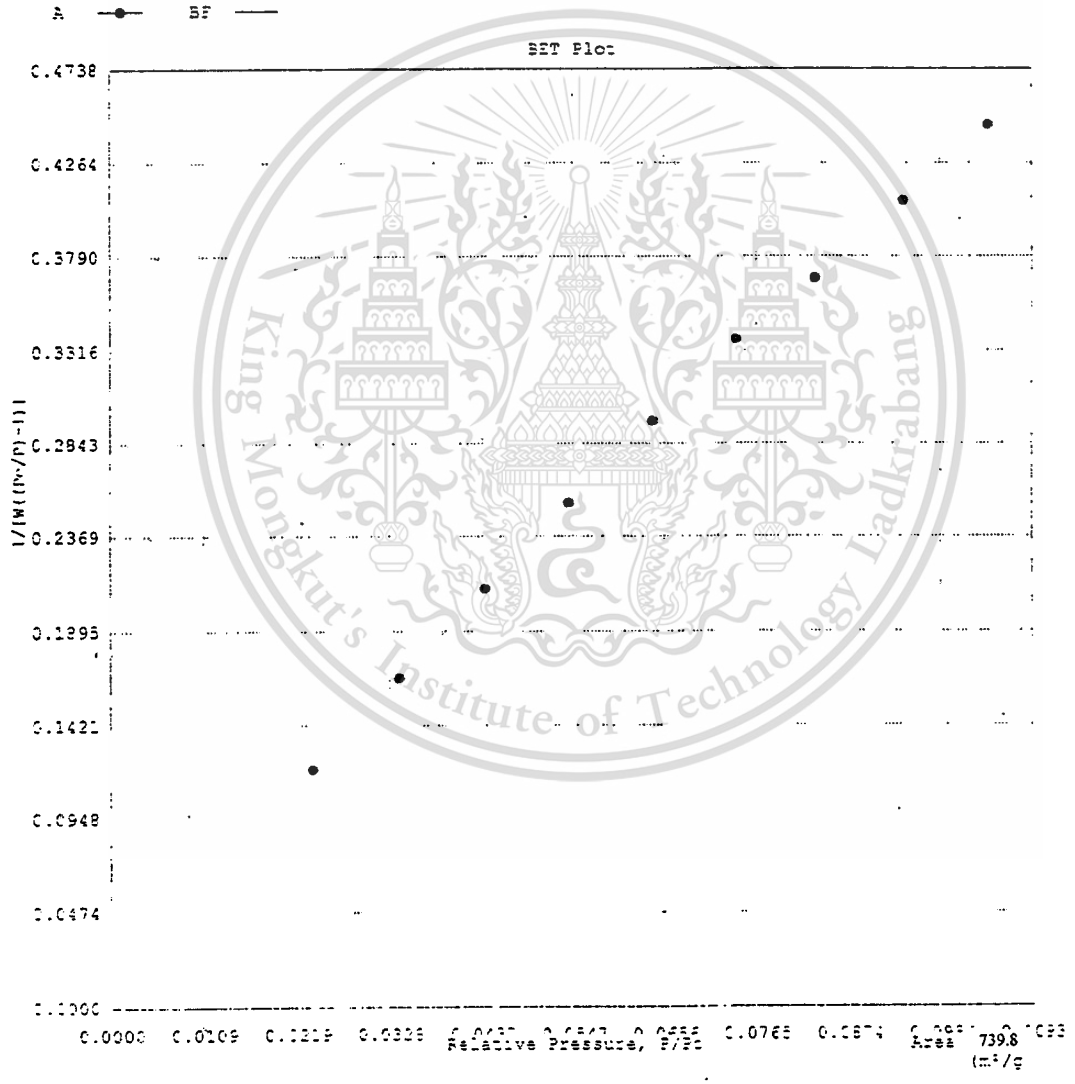

Figure H.5 BET surface area of Imp-EMT

Date: 09/02/2002

Quantachrome Corporation
Quantachrome Autosorb Automated Gas Sorption System Report
Autosorb for Windows® Version 1.19

Sample ID	bea_impregnate with Co2+				
Description	Micropore 10-6				
Comments					
Sample Weight	0.0028 g				
Adsorbate	NITROGEN	Outgas Temp	350.0 °C	Operator	Nantaphol
Cross-Sec Area	16.2 Å²/molecule	Outgas Time	22.5 hrs	Analysis Time	476.2 min
NonIdeality	6.580E-05	P/Po Toler	4	End of Run	05/23/2000 15:21
Molecular Wt	28.0134 g/mol	Equil Time	2	File Name	BEAJAOIM.RAW
Station #	1	Bath Temp.	77.35		

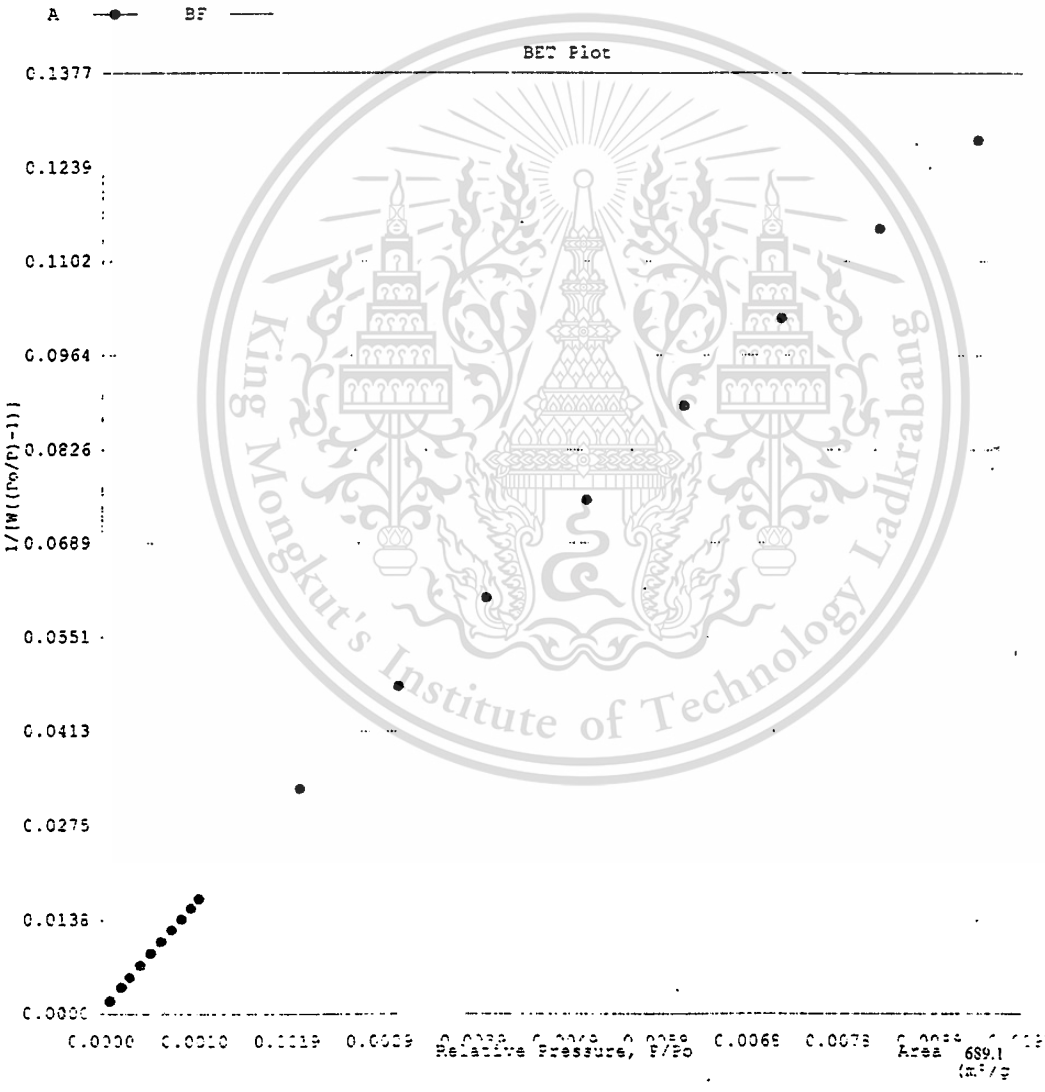

Figure H.6 BET surface area of Imp-BEA

Date: 09/02/2002

Quantachrome Corporation
Quantachrome Autosorb Automated Gas Sorption System Report
Autosorb for Windows® Version 1.19

Sample ID	Ion-EMT-encap				
Description	Micropore 10-6				
Comments					
Sample Weight	0.1020 g				
Adsorbate	NITROGEN	Outgas Temp	350.0 °C	Operator	Nantaphol
Cross-Sec Area	16.2 Å²/molecule	Outgas Time	22.5 hrs	Analysis Time	572.4 min
NonIdeality	6.880E-05	P/Po Toler	4	End of Run	05/20/2001 12:30
Molecular Wt	28.0134 g/mol	Equil Time	2	File Name	EMTCHA01.RAW
Station #	1	Bath Temp.	77.35		

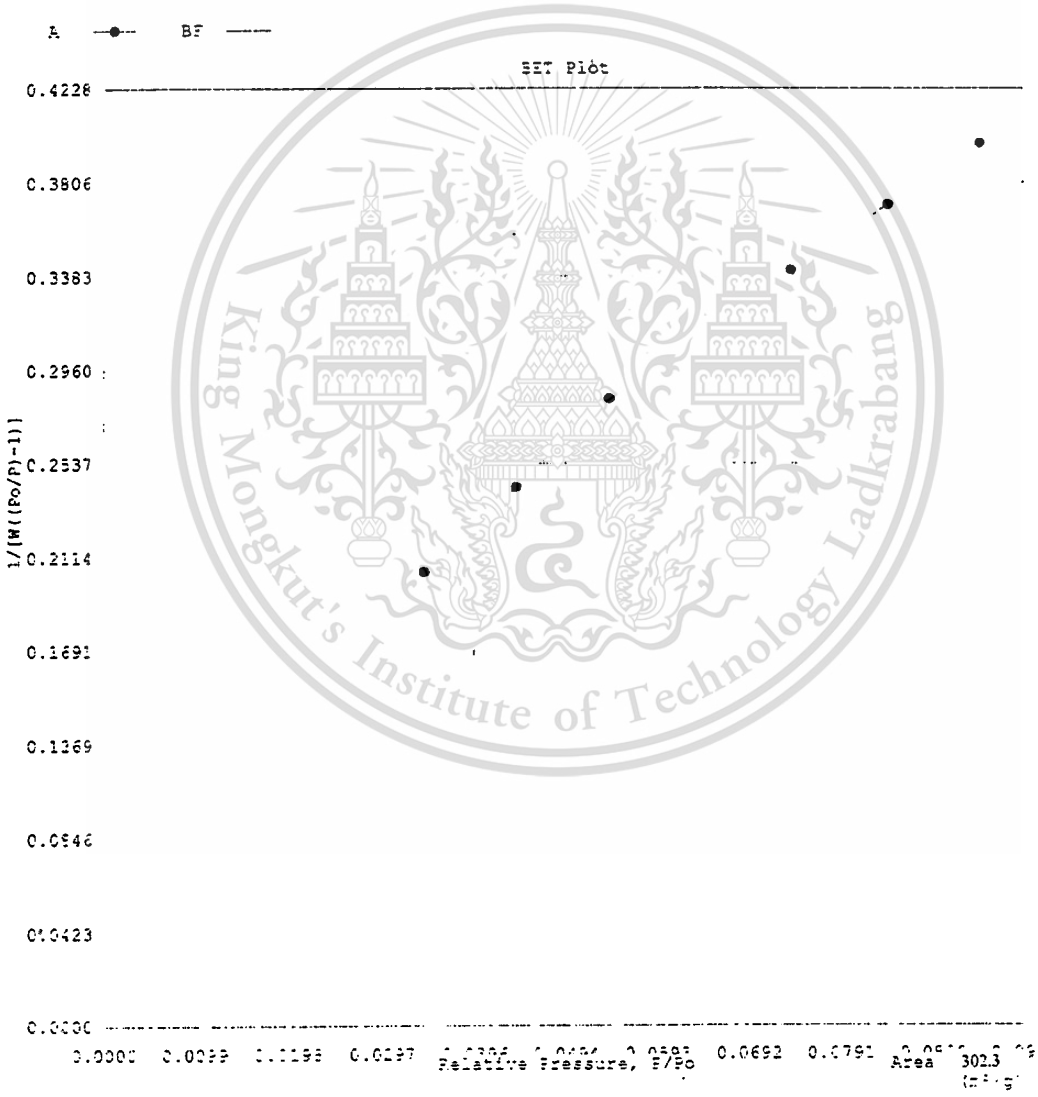

Figure H.7 BET surface area of Ion-EMT-encap

Date: 05/02/2002

Quantachrome Corporation
Quantachrome Autosorb Automated Gas Sorption System Report
Autosorb for Windows® Version 1.19

Sample ID	bea_ion_encap				
Description	Micropore 10-6				
Comments					
Sample Weight	0.0020 g				
Adsorbate	NITROGEN	Outgas Temp	350.0 °C	Operator	Nantaphol
Cross-Sec Area	16.2 Å²/molecule	Outgas Time	22.0 hrs	Analysis Time	358.2 min
NonIdeality	6.580E-05	P/Po Toler	4	End of Run	05/22/2001 01:50
Molecular Wt	28.0134 g/mol	Equil Time	2	File Name	BEACHADE.RAW
Station #	1	Bath Temp.	77.35		

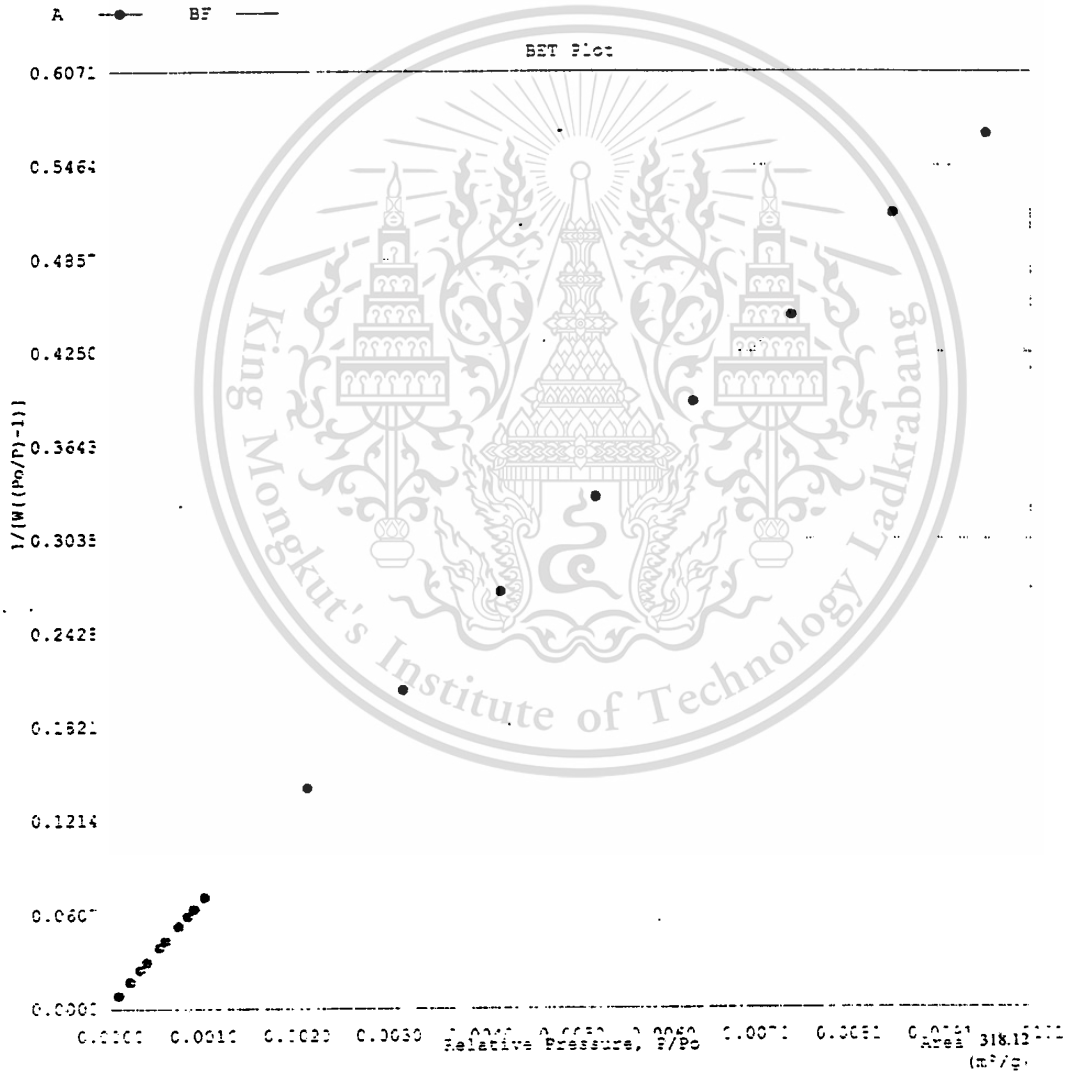

Figure H.8 BET surface area of Ion-BEA-encap

Date: 09/02/2002

Quantachrome Corporation
Quantachrome Autosorb Automated Gas Sorption System Report
Autosorb for Windows® Version 1.19

Sample ID	Imp-EMT-encap				
Description	Micropore 10-6				
Comments					
Sample Weight	0.0026 g				
Adsorbate	NITROGEN	Outgas Temp	350.0 °C	Operator	Nantaphol
Cross-Sec Area	16.2 Å²/molecule	Outgas Time	22.5 hrs	Analysis Time	476.2 min
NonIdeality	6.580E-03	P/Po Toler	4	End of Run	05/23/2000 15:21
Molecular Wt	28.0134 g/mol	Equil Time	2	File Name	BEAJAOIM.RAW
Station #	1	Bath Temp.	77.35		

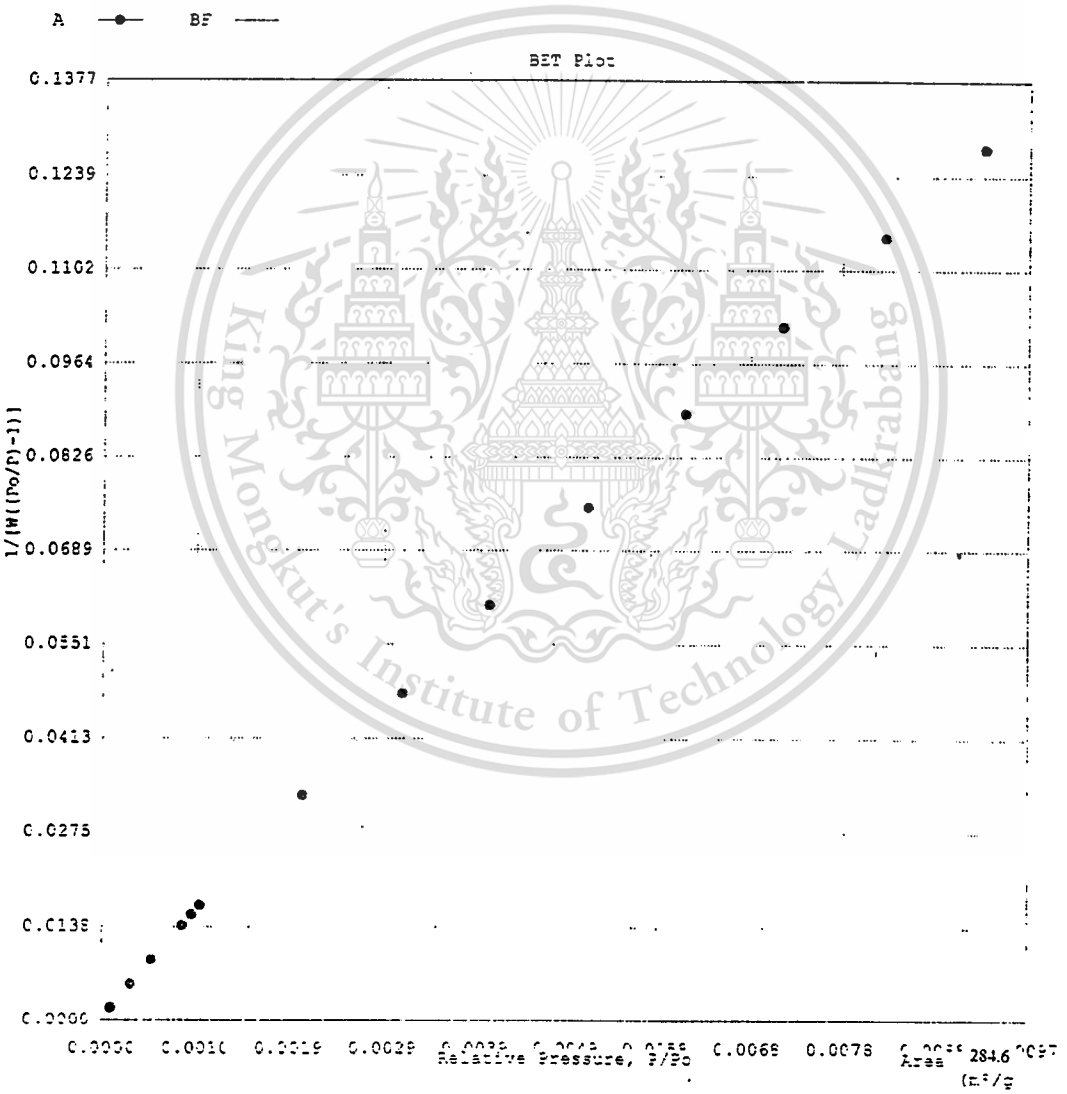

Figure H.9 BET surface area of Imp-EMT-encap

Date: 09/02/2002

Quantachrome Corporation
Quantachrome Autosorb Automated Gas Sorption System Report
Autosorb for Windows® Version 1.19

Sample ID	Imp-BEA-encap				
Description	Micropore 10-6				
Comments					
Sample Weight	0.0020 g				
Adsorbate	NITROGEN	Outgas Temp	350.0 °C	Operator	Nantaphol
Cross-Sec Area	16.2 Å²/molecule	Outgas Time	22.5 hrs	Analysis Time	358.2 min
NonIdeality	6.590E-03	P/Po Toler	4	End of Run	09/23/2000 01:50
Molecular Wt	28.0134 g/mol	Equil Time	2	File Name	BEACHAOE.RAW
Station #	1	Bath Temp.	77.35		

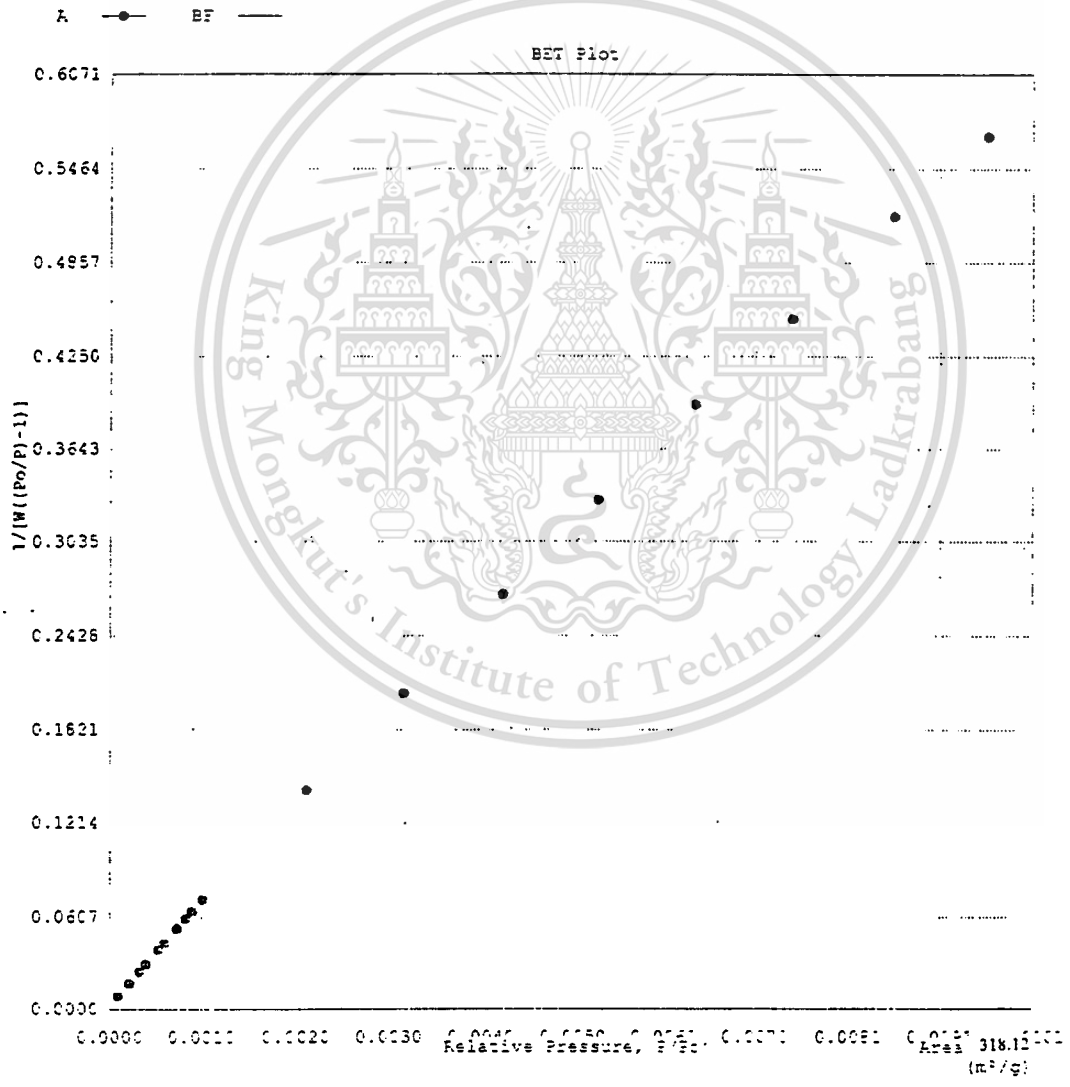

Figure H.10 BET surface area of Imp-EMT-encap

Table H.1 BET surface area of zeolite and modified zeolite

Synthetic zeolite	BET surface area (m^2/g)
Zeolite EMT	821.6
Zeolite BEA	782.5
Ion-EMT	814.7
Imp-EMT	739.8
Ion-BEA	763.2
Imp-BEA	689.1
Ion-EMT-encap	302.3
Imp-EMT-encap	284.6
Ion-BEA-encap	318.12
Imp-BEA-encap	297.9

Appendix I

Results from the Oxidation of Ethylbenzene

Table I.1 Results from the oxidation of ethylbenzene using Ion-EMT-encap, Ion-BEA-encap and without catalyst

time (hour)	% conversion of ethylbenzene using Ion-EMT-encap as catalyst	% conversion of ethylbenzene using Ion-BEA-encap as catalyst	% conversion of ethylbenzene without catalyst
0	-	-	-
2	2.36	4.20	0.48
4	4.07	5.50	0.88
6	5.03	7.14	1.12
8	6.10	9.23	1.40
10	7.72	10.87	2.17
12	8.18	12.65	3.98
16	9.72	15.76	4.64
24	14.66	19.60	5.85

Reaction condition : ethylbenzene 45 g, catalyst weight 0.15 g, reaction time 24 hr. temperature 138 ^{o}C and oxygen flow rate 40 ml/min

Table I.2 Results from the oxidation of ethylbenzene using Ion-BEA-encap as catalyst

time (hour)	% conversion of ethylbenzene	% yield of acetophenone	% selectivity of acetophenone
0	-	-	-
2	4.20	3.15	75.05
4	5.50	4.19	76.16
6	7.14	5.62	78.67
8	9.23	7.41	80.26
10	11.37	9.32	81.95
12	12.65	10.43	82.51
16	14.76	12.50	84.67
24	19.60	16.99	86.67
50	32.10	29.59	92.20
60	33.21	31.01	93.38
70	33.61	32.28	96.04
72	33.80	32.50	96.16

Reaction condition : ethylbenzene 45 g, catalyst weight 0.15 g, reaction time 72 hr. temperature 138 ^{o}C and oxygen flow rate 40 ml/min

Table I.3 Results from the oxidation of ethylbenzene using Ion-EMT-encap as catalyst

time (hour)	% conversion of ethylbenzene	% yield of acetophenone	% selectivity of acetophenone
0	-	-	-
2	2.36	1.73	73.05
4	4.67	3.47	74.35
6	5.03	3.81	75.82
8	6.10	4.64	76.05
10	7.72	6.00	77.65
12	8.18	6.45	78.88
16	9.72	7.98	82.15
24	14.66	12.35	84.29
50	35.11	31.80	90.57
60	39.77	36.85	92.67
70	43.23	41.28	95.49
72	43.89	42.03	95.76

Reaction condition : ethylbenzene 45 g, catalyst weight 0.15 g, reaction time 72 hr. temperature 138 ^{o}C and oxygen flow rate 40 ml/min

Table I.4 Results from the oxidation of ethylbenzene using regenerated Ion-EMT-encap as catalyst

time (hour)	% conversion of ethylbenzene	% yield of acetophenone	% selectivity of acetophenone
0	-	-	-
2	1.96	1.42	72.32
4	3.97	2.98	75.09
6	4.51	3.42	75.74
8	6.70	5.04	75.29
10	7.41	5.64	76.10
12	8.80	7.08	80.46
16	10.13	8.32	82.15
24	14.35	12.10	84.29

Reaction condition : ethylbenzene 45 g, catalyst weight 0.15 g, reaction time 24 hr. temperature 138 °C and oxygen flow rate 40 ml/min

Table I.5 Results from the oxidation of ethylbenzene using regenerated Ion-BEA-encap as catalyst

time (hour)	% conversion of ethylbenzene	% yield of acetophenone	% selectivity of acetophenone
0	-	-	-
2	3.31	2.47	74.55
4	4.66	3.54	75.98
6	5.42	4.23	78.02
8	7.63	6.12	80.16
10	8.41	6.85	81.45
12	10.89	8.98	82.50
16	12.93	10.91	84.37
24	16.83	14.47	85.97

Reaction condition : ethylbenzene 45 g, catalyst weight 0.15 g, reaction time 24 hr. temperature 138 oC and oxygen flow rate 40 ml/min

Table I.6 Results from the oxidation of ethylbenzene using Imp-EMT-encap as catalyst

time (hour)	% conversion of ethylbenzene	% yield of acetophenone	% selectivity of acetophenone
0	-	-	-
2	3.05	2.24	73.43
4	4.65	3.46	74.46
6	5.40	4.17	77.24
8	6.91	5.45	78.96
10	8.25	6.66	80.64
12	9.71	7.99	82.34
16	11.41	9.58	84.02
24	15.91	13.68	85.94
50	33.86	30.48	90.01
60	37.46	34.60	92.36
70	39.99	38.17	95.46
72	40.13	38.41	95.72

Reaction condition : ethylbenzene 45 g, catalyst weight 0.15 g, reaction time 72 hr. temperature 138 oC and oxygen flow rate 40 ml/min

Table I.7 Results from the oxidation of ethylbenzene using Imp-BEA-encap as catalyst

time (hour)	% conversion of ethylbenzene	% yield of acetophenone	% selectivity of acetophenone
0	-	-	-
2	4.42	3.29	74.98
4	6.01	4.57	76.06
6	7.90	6.17	78.73
8	10.12	8.11	80.01
10	13.33	10.85	81.70
12	15.16	12.51	82.84
16	17.97	15.16	84.67
24	21.86	18.79	86.63
50	29.56	27.04	91.45
60	30.19	28.14	93.22
70	30.81	29.57	95.97
72	30.91	29.73	96.21

Reaction condition : ethylbenzene 45 g, catalyst weight 0.15 g, reaction time 24 hr. temperature 138 oC and oxygen flow rate 40 ml/min

Table I.8 Results from the oxidation of ethylbenzene using regenerated Imp-EMT-encap as catalyst

time (hour)	% conversion of ethylbenzene	% yield of acetophenone	% selectivity of acetophenone
0	-	-	-
2	2.46	1.84	74.55
4	4.27	3.24	75.98
6	5.63	4.39	78.02
8	6.10	4.89	80.16
10	7.52	6.13	81.45
12	10.08	8.31	82.50
16	10.72	9.04	84.37
24	15.56	13.37	85.97

Reaction condition : ethylbenzene 45 g, catalyst weight 0.15 g, reaction time 24 hr. temperature 138 oC and oxygen flow rate 40 ml/min

Table I.9 Results from the oxidation of ethylbenzene using regenerated Imp-BEA-encap as catalyst

time (hour)	% conversion of ethylbenzene	% yield of acetophenone	% selectivity of acetophenone
0	-	-	-
2	2.51	1.87	74.55
4	3.45	2.62	75.98
6	5.81	4.53	78.02
8	8.30	6.66	80.16
10	9.58	7.80	81.45
12	11.99	9.89	82.50
16	13.98	11.80	84.37
24	19.25	16.55	85.97

Reaction condition : ethylbenzene 45 g, catalyst weight 0.15 g, reaction time 24 hr. temperature 138 oC and oxygen flow rate 40 ml/min

Table I.10 Results from the oxidation of ethylbenzene using Ion-EMT-encap as catalyst, with oxygen flow rate 20 ml/min

time (hour)	% conversion of ethylbenzene	% yield of acetophenone	% selectivity of acetophenone
0	-	-	-
2	1.05	0.78	0.72
4	1.96	1.49	1.37
6	2.64	2.06	1.90
8	3.37	2.70	2.48
10	4.12	3.55	3.27
12	5.55	4.58	4.21
16	6.85	5.78	5.32
24	10.99	9.44	8.68
50	33.02	27.51	83.32
60	36.54	31.15	85.26
70	39.95	35.10	87.85
72	40.05	35.29	88.10

Reaction condition : ethylbenzene 45 g, catalyst weight 0.15 g, reaction time 72 hr. temperature 138 oC and oxygen flow rate 20 ml/min

Table I.11 Results from the oxidation of ethylbenzene using Ion-EMT-encap as catalyst; with oxygen flow rate 80 ml/min

time (hour)	% conversion of ethylbenzene	% yield of acetophenone	% selectivity of acetophenone
0	-	-	-
2	3.55	2.62	73.78
4	5.33	4.00	75.09
6	6.29	4.82	76.58
8	7.32	5.62	76.81
10	9.01	7.07	78.43
12	9.81	7.80	79.47
16	11.66	9.67	82.97
24	9.01	7.66	85.03
50	9.81	8.73	88.94
60	38.07	34.63	90.96
70	41.09	38.08	92.67
72	41.51	38.57	92.92

Reaction condition : ethylbenzene 45 g, catalyst weight 0.15 g, reaction time 72 hr. temperature 138 °C and oxygen flow rate 80 ml/min

Table I.12 Results from the oxidation of ethylbenzene using regenerated Ion-EMT-CoPc obtained from the reaction using 80 ml/in oxygen flow rate

time (hour)	% conversion of ethylbenzene	% yield of acetophenone	% selectivity of acetophenone
0	-	-	-
2	1.50	1.05	69.67
4	2.86	2.03	70.89
6	3.64	2.63	72.27
8	4.73	3.43	72.59
10	5.92	4.38	74.01
12	6.86	5.16	75.15
16	8.18	6.40	78.22
24	11.86	9.47	79.86

Reaction condition : ethylbenzene 45 g, catalyst weight 0.15 g, reaction time 24 hr. temperature 138 $^{\circ}$C and oxygen flow rate 80 ml/min

Appendix J

Results from the Oxidation of Cyclohexane

Table J.1 Results from the oxidation of cyclohexane using Ion-BEA-CoPc as a catalyst at atmospheric pressure

time (hour)	% conversion of ethylbenzene	% yield of acetophenone	% selectivity of acetophenone
0	-	-	-
2	0.27	0.06	22.40
4	0.35	0.09	25.49
6	0.42	0.12	28.32
8	0.50	0.16	31.44
10	0.53	0.19	36.35
24	0.60	0.23	38.06

Reaction condition cyclohexane = 12.25 g, catalyst (Ion-BEA-CoPc) weight = 0.375 g, reaction time = 8 hr. temperature = 343 K, solvent (acetic acid) = 22.25 g with oxygen flow rate 40 ml/min

Table J.2 Results from the oxidation of cyclohexane using Ion-BEA-CoPc as a catalyst under pressure of oxygen

time (hour)	% conversion of ethylbenzene	% yield of acetophenone	% selectivity of acetophenone
0	-	-	-
2	2.48	0.85	34.27
4	4.85	2.51	51.75
6	7.58	4.48	59.10
8	8.63	5.59	64.77
10	10.30	7.27	70.58
24	12.22	9.30	76.09

Reaction condition cyclohexane = 12.25 g, catalyst (Ion-BEA-CoPc) weight = 0.375 g, reaction time = 8 hr. temperature = 343 K, solvent (acetic acid) = 22.25 g, oxygen 300 psi, H_2O_2 = 0.2 g

Table J.3 Results from the oxidation of cyclohexane without catalyst under pressure

time (hour)	% conversion of ethylbenzene	% yield of acetophenone	% selectivity of acetophenone
0	-	-	-
2	0.07	0.02	26.27
4	0.15	0.05	30.50
6	0.22	0.08	37.84
8	0.30	0.13	43.23
10	0.34	0.16	48.25
24	0.40	0.21	53.08

Reaction condition cyclohexane = 12.25 g, reaction time = 8 hr. temperature = 343 K, solvent (acetic acid) = 22.25 g, oxygen 300 psi, H2O2 = 0.2 g

Table J.4 Results from the oxidation of cyclohexane using Ion-BEA-CoPc under pressure with ethylenediamine

time (hour)	% conversion of ethylbenzene	% yield of acetophenone	% selectivity of acetophenone
0	-	-	-
2	0.11	0.02	18.98
4	0.35	0.07	20.50
6	0.41	0.09	22.03
8	0.51	0.12	24.18
10	0.54	0.14	26.22
24	0.58	0.16	27.41

Reaction condition cyclohexane = 12.25 g, catalyst (Ion-BEA-CoPc) weight = 0.375 g, reaction time = 8 hr. temperature = 343 K, solvent (acetic acid) = 22.25 g, oxygen 300 psi, H_2O_2 = 0.2 g (with 0.23 g of ethylenediamine)

Table J.5 Results from the oxidation of cyclohexane using Ion-BEA-CoPc under pressure with hydroquinone

time (hour)	% conversion of ethylbenzene	% yield of acetophenone	% selectivity of acetophenone
0	-	-	-
2	-	-	-
4	0.10	0.01	11.14
6	0.17	0.02	12.49
8	0.22	0.03	14.61
10	0.24	0.04	16.28
24	0.28	0.05	16.97

Reaction condition cyclohexane = 12.25 g, catalyst (Ion-BEA-CoPc) weight = 0.375 g, reaction time = 8 hr. temperature = 343 K, solvent (acetic acid) = 22.25 g, oxygen 300 psi, H_2O_2 = 0.2 g (with 0.23 g of hydroquinone)

Table J.6 Results from the oxidation of cyclohexane using Ion-EMT-CoPc under pressure

time (hour)	% conversion of ethylbenzene	% yield of acetophenone	% selectivity of acetophenone
0	-	-	-
2	1.15	0.23	19.88
4	3.37	1.26	37.39
6	5.90	3.13	53.05
8	7.39	4.57	61.84
10	8.69	5.88	67.66
24	12.51	9.54	76.26

Reaction condition cyclohexane = 12.25 g, catalyst (Ion-EMT-CoPc) weight = 0.375 g, reaction time = 8 hr. temperature = 343 K, solvent (acetic acid) = 22.25 g, oxygen 300 psi, H_2O_2 = 0.2 g

Table J.7 Results from the oxidation of cyclohexane using Ion-BEA-CoPc under pressure without hydrogenperoxide

time (hour)	% conversion of ethylbenzene	% yield of acetophenone	% selectivity of acetophenone
0	-	-	-
2	2.01	0.23	11.39
4	4.26	1.26	29.48
6	6.55	3.03	46.31
8	7.97	4.57	57.35
10	9.66	5.88	60.85
24	11.49	8.67	75.46

Reaction condition cyclohexane = 12.25 g, catalyst (Ion-BEA-CoPc) weight = 0.375 g, reaction time = 8 hr. temperature = 343 K, solvent (acetic acid) = 22.25 g, oxygen 300 psi

Table J.8 Results from the oxidation of cyclohexane using Ion-BEA-CoPc under pressure of air

time (hour)	% conversion of ethylbenzene	% yield of acetophenone	% selectivity of acetophenone
0	-	-	-
2	1.25	0.32	25.66
4	4.18	1.91	45.57
6	5.98	3.00	50.14
8	7.52	4.52	60.10
10	8.52	6.03	70.73
24	11.98	8.87	74.02

Reaction condition cyclohexane = 12.25 g, catalyst (Ion-EMT-CoPc) weight = 0.375 g, reaction time = 8 hr. temperature = 343 K, solvent (acetic acid) = 22.25 g, air 300 psi, H_2O_2 = 0.2 g

Table J.9 Results from the oxidation of cyclohexane using Ion-BEA-CoPc under pressure using 3 kind of solvent

time (hour)	% conversion of ethylbenzene		
	using acetic acid as solvent	using chloroform as solvent	using dimethylformamide as solvent
0	-	-	-
2	2.48	1.78	0.83
4	4.85	3.56	1.62
6	7.58	5.21	2.53
8	8.63	6.05	2.88
10	10.30	7.01	3.43
24	12.22	8.45	4.23

Reaction condition cyclohexane = 12.25 g, catalyst (Ion-BEA-CoPc) weight = 0.375 g, reaction time = 8 hr. temperature = 343 K, solvent = 22.25 g, oxygen 300 psi, H_2O_2 = 0.2 g

AUTHOR BIOGRAPHY

Mr. Nantaphol Klansorn was born on November 15, 1977 in Bangkok. He received a Bachelor Degree in Industrial Chemistry from the Department of Chemistry, Faculty of Science, King Mongkut's Institute of Technology Ladkrabang in 1998. He has been a graduated student of the Program of Petrochemical and Hydrocarbon Chemistry, Graduate School, King Mongkut's Institute of Technology Ladkrabang, since 1999.